National Nanotechnology Coordinated Infrastructure (NNCI)

Research and Education Highlights

Year 8 (October 2022 – September 2023)

National Nanotechnology Coordinated Infrastructure

NSF

Table of Contents

National Nanotechnology Coordinated Infrastructure

Center for Nanoscale Systems (CNS)

National Nanotechnology Coordinated Infrastructure

Laser writing of spin defects in nanophotonic cavities

High-yield engineering and characterization of cavity-emitter coupling is an outstanding challenge in developing scalable quantum network nodes. Ex situ defect formation systems prevent real-time analysis, and previous in situ methods are limited to bulk substrates or require further processing to improve the emitter properties(1-6). Here we demonstrate the direct laser writing of cavity-integrated spin defects using a nanosecond pulsed above-bandgap laser. Photonic crystal cavities in 4H-silicon carbide serve as a nanoscope monitoring silicon-monovacancy defect formation within the approximately 200 nm(3) cavity-mode volume. We observe spin resonance, cavity-integrated photoluminescence and excited-state lifetimes consistent with conventional defect formation methods, without the need for post-irradiation thermal annealing. We further find an exponential reduction in excited-state lifetime at fluences approaching the cavity amorphization threshold and show the single-shot annealing of intrinsic background defects at silicon-monovacancy formation sites. This real-time in situ method of localized defect formation, paired with cavity-integrated defect spins, is necessary towards engineering cavity-emitter coupling for quantum networking.

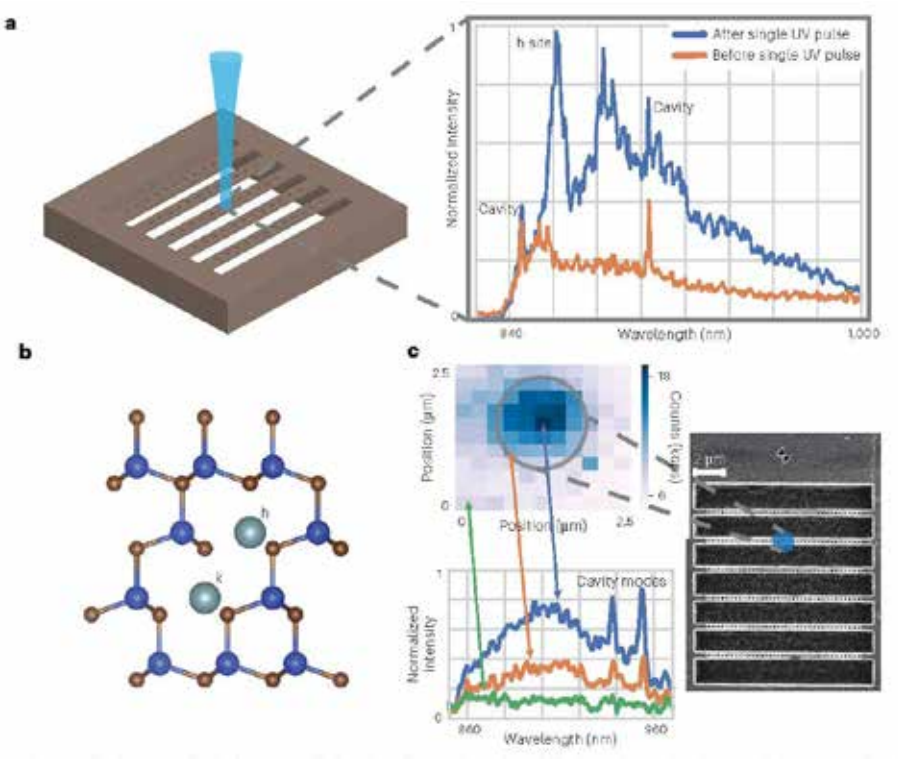

Day, Aaron M. [1] ; Sutula, Madison [2]; Hu, Evelyn L. [1] ; [1] Harvard Univ, John A Paulson School of Engineering & Appl Sci,, [2] Harvard Univ, Dept Phys. Work performed at Harvard CNS.

This work was supported by NSF DMR-1231319, the Harvard University Center for Nanoscale Systems (CNS), NSF RAISE-TAQS Award 1839164. *Nat. Mater.* ***22****, 696–702 (2023).*

National Research Priority: NSF–Quantum Leap

National Nanotechnology Coordinated Infrastructure

Center for Nanoscale Systems Harvard University FAS • SEAS

Superconductivity and strong interactions in a tunable moire quasicrystal

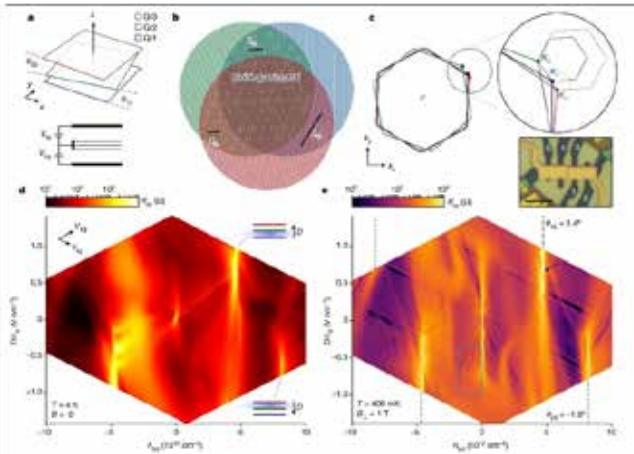

Electronic states in quasicrystals generally preclude a Bloch description(1), rendering them fascinating and enigmatic. Owing to their complexity and scarcity, quasicrystals are underexplored relative to periodic and amorphous structures. Here we introduce a new type of highly tunable quasicrystal easily assembled from periodic components. By twisting three layers of graphene with two different twist angles, we form two mutually incommensurate moire patterns. In contrast to many common atomic-scale quasicrystals(2,3), the quasiperiodicity in our system is defined on moire length scales of several nanometres. This 'moire quasicrystal' allows us to tune the chemical potential and thus the electronic system between a periodic-like regime at low energies and a strongly quasiperiodic regime at higher energies, the latter hosting a large density of weakly dispersing states. Notably, in the quasiperiodic regime, we observe superconductivity near a flavour-symmetry-breaking phase transition(4,5), the latter indicative of the important role that electronic interactions play in that regime. The prevalence of interacting phenomena in future systems with in situ tunability is not only useful for the study of quasiperiodic systems but may also provide insights into electronic ordering in related periodic moire crystals(6-12). We anticipate that extending this platform to engineer quasicrystals by varying the number of layers and twist angles, and by using different two-dimensional components, will lead to a new family of quantum materials to investigate the properties of strongly interacting quasicrystals.

Uri, Aviram [1] ; Rodan-Legrain, Daniel [1] ; Devakul, Trithep [1] ; ; Watanabe, Kenji [2] ; Taniguchi, Takashi [3] ; Lifshitz, Ron [4]; Ashoori, Raymond C. [1] ; Jarillo-Herrero, Pablo [1], [1] MIT, Dept. Physics; [2] Natl Inst Mat Sci, Res Ctr Funct Mat, Tsukuba, Japan; [3] Natl Inst Mat Sci, Int Ctr Mat Nanoarchitecton, Tsukuba, Japan, [4] Tel Aviv Univ, Raymond & Beverly Sackler Sch Phys & Astron. Work performed at Harvard CNS.

This work was supported by NSF Award DMR-1809802 and DMR-1231319. *Nature* ***620****, 762–767 (2023).*

National Research Priority: NSF–Quantum Leap

National Nanotechnology Coordinated Infrastructure

Center for Nanoscale Systems
Harvard University
FAS • SEAS

3D-printed machines that manipulate microscopic objects using capillary forces

Objects that deform a liquid interface are subject to capillary forces, which can be harnessed to assemble the objects(1-4). Once assembled, such structures are generally static. Here we dynamically modulate these forces to move objects in programmable two-dimensional patterns. We 3D-print devices containing channels that trap floating objects using repulsive capillary forces(5,6), then move these devices vertically in a water bath. Because the channel cross-sections vary with height, the trapped objects can be steered in two dimensions. The device and interface therefore constitute a simple machine that converts vertical to lateral motion. We design machines that translate, rotate and separate multiple floating objects and that do work on submerged objects through cyclic vertical motion. We combine these elementary machines to make centimetre-scale compound machines that braid micrometre-scale filaments into prescribed topologies, including non-repeating braids. Capillary machines are distinct from mechanical, optical or fluidic micromanipulators in that a meniscus links the object to the machine. Therefore, the channel shapes need only be controlled on the scale of the capillary length (a few millimetres), even when the objects are microscopic. Consequently, such machines can be built quickly and inexpensively. This approach could be used to manipulate micrometre-scale particles or to braid microwires for high-frequency electronics.

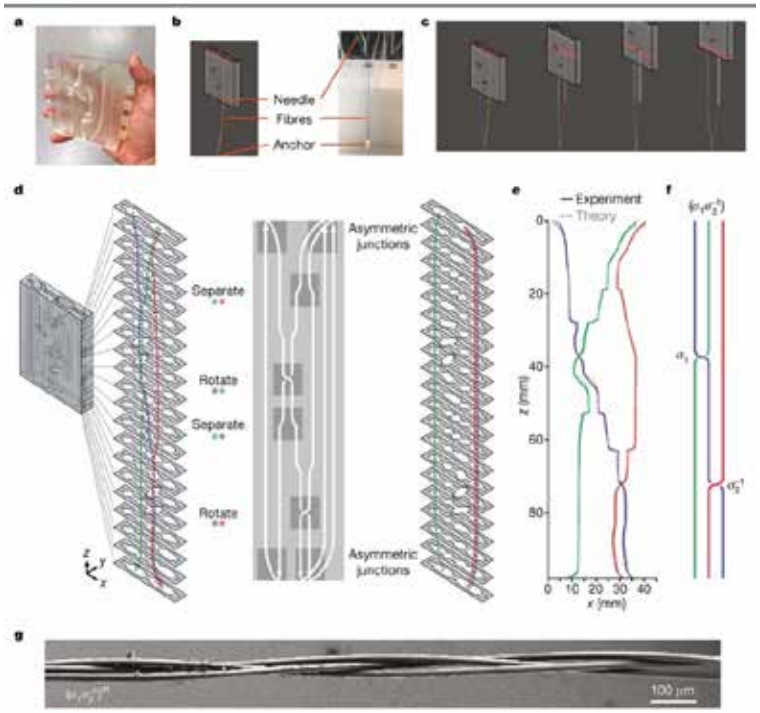

Manoharan, Vinothan N., Harvard John A Paulson Sch Engn & Appl Sci. Work performed at Harvard CNS.

This work was supported by DARPA contract FA8650-15-C-7543, by NSF through grant DMR-2011754. Additional support was provided by NSF through grant NNCI ECCS-1541959; *Nature* ***611****, 68–73 (2022).*

National Research Priority: NSF–Growing Convergence Research

National Nanotechnology Coordinated Infrastructure

Center for Nanoscale Systems
Harvard University
FAS • SEAS

Ultra-flexible endovascular probes for brain recording through micrometer-scale vasculature

Implantable neuroelectronic interfaces have enabled advances in both fundamental research and treatment of neurological diseases but traditional intracranial depth electrodes require invasive surgery to place and can disrupt neural networks during implantation. We developed an ultrasmall and flexible endovascular neural probe that can be implanted into sub-100-micrometer-scale blood vessels in the brains of rodents without damaging the brain or vasculature. In vivo electrophysiology recording of local field potentials and single-unit spikes have been selectively achieved in the cortex and olfactory bulb. Histology analysis of the tissue interface showed minimal immune response and long-term stability. This platform technology can be readily extended as both research tools and medical devices for the detection and intervention of neurological diseases.

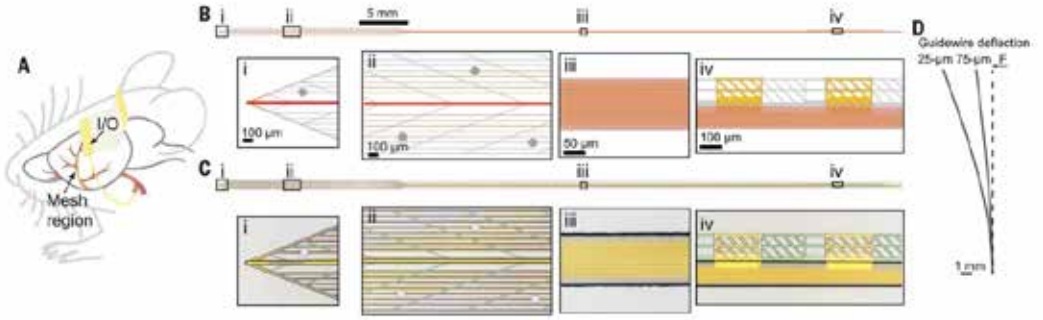

Fig. 1. Endovascular implantation and overview of the MEV probe. (**A**) Schematic showing an MEV probe (yellow) implanted into a rat brain through the blood vessels in the neck. The mesh region with electrodes is implanted in deep cerebrovasculature whereas the input/output (I/O) region remains exteriorized for subsequent connection and measurement. (**B**) Schematic of the MEV probe with the ultraflexible mesh region at left tapering into the stem and I/O region at right. The middle line in red is the thick SU-8 guidewire layer. Insets provide magnified views of (i) probe tip containing the 25-μm wide guidewire (red) and ultraflexible SU-8 mesh region (light gray); (ii) Pt recording electrodes (gray circles); (iii) SU-8 stem containing independent interconnects for each electrode; and (iv) the I/O pads consisting of a gold region (yellow) connected by SU-8. (**C**) Tiled brightfield images of the MEV probe with a 25-μm wide guidewire. The overview and insets are the same size as the schematic regions in (B). The cross-section surface profiles of the probe are shown in fig. S2. (**D**) Side view of the calculated bending of the 18-mm-long guidewire in the device region under the same applied force (F = 10 nN). Deflection of the tip of the 25-μm guidewire probe is 3 times that of the 75-μm guidewire probe (Supplementary Text, fig. S4).

Zhang, Anqi [1],[2],[3] ; Mandeville, Emiri T. [4],[5] ; Xu, Lijun [6] ; Lieber, Charles M. [3], [1] Stanford Univ, Dept Chem Engn,; [2] Stanford Univ, Dept Bioengn,; [3] Harvard Univ, Dept Chem & Chem Biol.; [4] Massachusetts Gen Hosp, Dept Radiol & Neurol, Neuroprotect Res Lab; [5] Harvard Med Sch; [6] Stanford Univ, Dept Anesthesiol Perioperat Pain Med, Sch Med. Work performed at Harvard CNS>

Supported by Air Force Office of Scientific Research (FA9550-18-1-0469, FA9550-19-1- 0246), NIH (R01NS099620, R01NS107445), and American Heart Association (23POST1018301). *Science 20 Jul 2023 Vol 381, Issue 6655 pp. 306-312.*

National Research Priority: NSF–Understanding the Rules of Life

National Nanotechnology Coordinated Infrastructure

Center for Nanoscale Systems
Harvard University
FAS • SEAS

Topologically protected optical polarization singularities in four-dimensional space

Optical singularities play a major role in modern optics and are frequently deployed in structured light, superresolution microscopy, and holography. While phase singularities are uniquely defined as locations of undefined phase, polarization singularities studied thus far are either partial, i.e., bright points of well-defined polarization, or are unstable for small field perturbations. We demonstrate a complete, topologically protected polarization singularity; it is located in the four-dimensional space spanned by the three spatial dimensions and the wavelength and is created in the focus of a cascaded metasurface-lens system. The field Jacobian plays a key role in the design of such higher-dimensional singularities, which can be extended to multidimensional wave phenomena, and pave the way for unconventional applications in topological photonics and precision sensing.

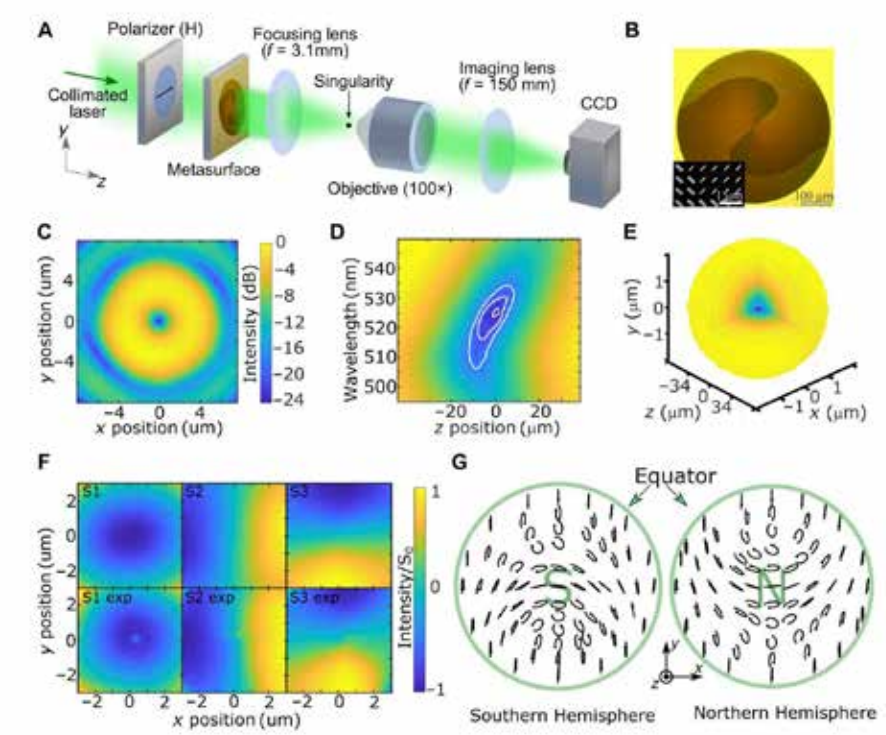

Spaegele, Christina M. [1] ; Tamagnone, Michele [1] , [2] ; Capasso, Federico [1] [1] Harvard Univ, Harvard John A Paulson Sch Engn & Appl Sci; [2] Fdn Ist Italiano Tecnol, Genoa, Italy. Work performed at Harvard CNS>

This work was supported by Air Force Office of Scientific Research FA9550-22-1-0243 and FA9550-21-1-0312 and European Research Council (ERC grant no. 948250). *Science Advances 16 Jun 2023 Vol 9, Issue 24*

National Research Priority: NSF–Quantum Leap

National Nanotechnology Coordinated Infrastructure

Center for Nanoscale Systems
Harvard University
FAS • SEAS

All-Optical Tunability of Metalenses Permeated with Liquid Crystals

Metasurfaces have been extensively engineered to produce a wide range of optical phenomena, allowing exceptional control over the propagation of light. However, they are generally designed as single-purpose devices without a modifiable postfabrica-tion optical response, which can be a limitation to real-world applications. In this work, we report a nanostructured planar-fused silica metalens permeated with a nematic liquid crystal (NLC) and gold nanoparticle solution. The physical properties of embedded NLCs can be manipulated with the application of external stimuli, enabling reconfigurable optical metasurfaces. We report the all-optical, dynamic control of the metalens optical response resulting from thermoplasmonic-induced changes of the NLC solution associated with the nematic-isotropic phase transition. A continuous and reversible tuning of the metalens focal length is experimentally demonstrated, with a variation of 80 mu m (0.16% of the 5 cm nominal focal length) along the optical axis. This is achieved without direct mechanical or electrical manipulation of the device. The reconfigurable properties are compared with corroborating numerical simulations of the focal length shift and exhibit close correspondence.

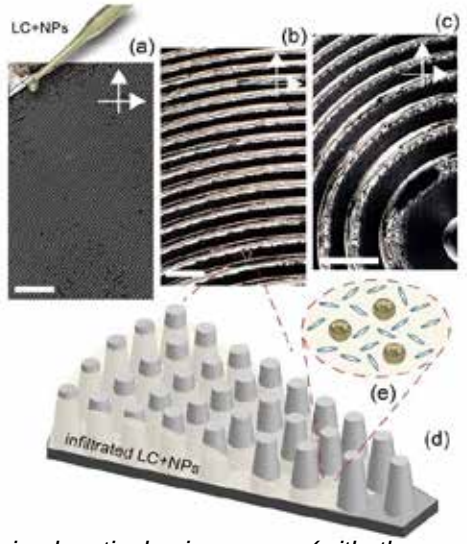

Figure 1. Polarized optical microscopy (with the metalens between crossed polarizers (90 °), shown as perpendicular arrows) image of 6CB+AuNPs filled metalens along the (a) far edge, (b) inner, and (c) central region; scale bar: 200 μm. The pipet in (a) illustrates a droplet of LC placed at the edge of the lens during the infiltration procedure. (d) Illustration of a pillars region of the metalens infiltrated with the 6CB+AuNPs mixture (e).

Palermo, Giovanna [1] ; Lininger, Andrew [3] ; Ricciardi, Loredana [2] ; Park, Joon-Suh) [4] , [5] ; Capasso, Federico [4] ; Strangi, Giuseppe [1] , [2] , [3] [1] Univ Calabria, Dept Phys, NLHT Lab; [2] CNR NANOTEC Ist Nanotecnol.; [3] Case Western Reserve Univ, Dept Phys. [4] Harvard John A Paulson Sch Engn & Appl Sci.; [5] Korea Inst Sci & Technol, Nanophoton Res Ctr. Work performed at Harvard CNS.

This work was supported by NSF Award # 1904592; *ACS Nano* ***2022*** *16 (10), 16539-1654*

National Research Priority: NSF–Quantum Leap

National Nanotechnology Coordinated Infrastructure

Center for Nanoscale Systems
Harvard University
FAS • SEAS

Nonspherical ultrasound microbubbles

Surface tension provides microbubbles (MB) with a perfect spherical shape. Here, we demonstrate that MB can be engineered to be nonspherical, endowing them with unique features for biomedical applications. Anisotropic MB were generated via one-dimensionally stretching spherical poly(butyl cyanoacrylate) MB above their glass transition temperature. Compared to their spherical counterparts, nonspherical polymeric MB displayed superior performance in multiple ways, including i) increased margination behavior in blood vessel-like flow chambers, ii) reduced macrophage uptake in vitro, iii) prolonged circulation time in vivo, and iv) enhanced blood-brain barrier (BBB) permeation in vivo upon combination with transcranial focused ultrasound (FUS). Our studies identify shape as a design parameter in the MB landscape, and they provide a rational and robust framework for further exploring the application of anisotropic MB for ultrasound-enhanced drug delivery and imaging applications.

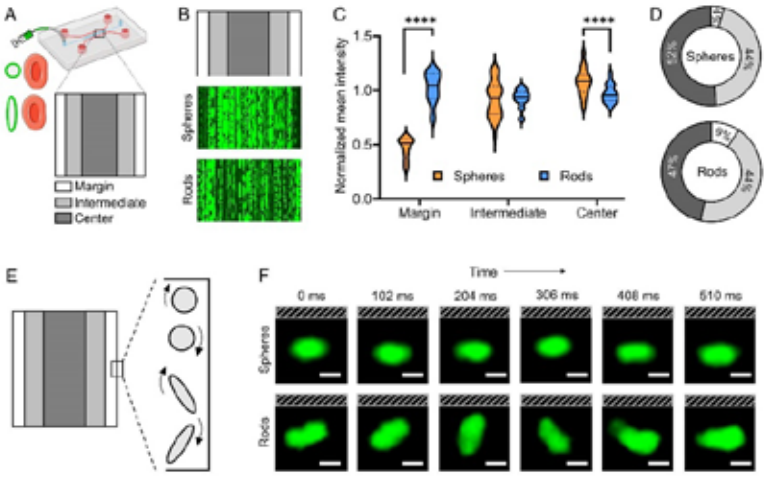

Dasgupta, Anshuman [1] , [2] , [3] , [6] ; Weiler, Marek) [1] , [6] ; Motta, Alessandro [1] , [6] ; Porte, Celine [1] , [6] ; ; Graham, Adam) [2] , [6] ; Mitragotri, Samir) [2] , [3] , [6]; [1] Rhein Westfal TH Aachen Univ, Inst Expt Mol Imaging, Med Fac,; [2] Harvard Univ, John A Paulson Sch Engn & Appl Sci.; [3] Harvard Univ, Wyss Inst Biolog Inspired Engn.; [4] Harvard Med Sch, Brigham & Womens Hosp, Dept Radiol, Focused Ultrasound Lab.; [5] Ist Italiano Tecnol, Lab Nanotechnol Precis Med.; [6] Rhein Westfal TH Aachen Univ, Leibniz Inst Interact Mat.; [7] Rhein Westfal TH Univ Aachen, Inst Tech & Macromol Chem, Polymer Biomat.; [8] Rhein Westfal TH Aachen Univ, Med Fac, Dept Obstet & Gynecol.; [9] Rhein Westfal TH Aachen Univ, Inst Appl Med Engn, Med Fac, Adv Mat Biomed. Work performed at Harvard CNS.

This work was supported by European Research Council (ERC-CoG 864121: Meta-Targeting), German Research Foundation [Deutsche Forschungsgemeinschaft: GRK/RTG2375 (grant #331065168) and SFB 1066], and NIH (R01 EB033307). *PNAS*, March 20, 2023; 120 (13) e2218847120.

National Research Priority: NSF–Understanding the Rules of Life

National Nanotechnology Coordinated Infrastructure

Center for Nanoscale Systems
Harvard University
FAS • SEAS

Fibre-infused gel scaffolds guide cardiomyocyte alignment in 3D-printed ventricles

Hydrogels are attractive materials for tissue engineering, but efforts to date have shown limited ability to produce the microstructural features necessary to promote cellular self-organization into hierarchical three-dimensional (3D) organ models. Here we develop a hydrogel ink containing prefabricated gelatin fibres to print 3D organ-level scaffolds that recapitulate the intra- and intercellular organization of the heart. The addition of prefabricated gelatin fibres to hydrogels enables the tailoring of the ink rheology, allowing for a controlled sol-gel transition to achieve precise printing of free-standing 3D structures without additional supporting materials. Shear-induced alignment of fibres during ink extrusion provides microscale geometric cues that promote the self-organization of cultured human cardiomyocytes into anisotropic muscular tissues in vitro. The resulting 3D-printed ventricle in vitro model exhibited biomimetic anisotropic electrophysiological and contractile properties.

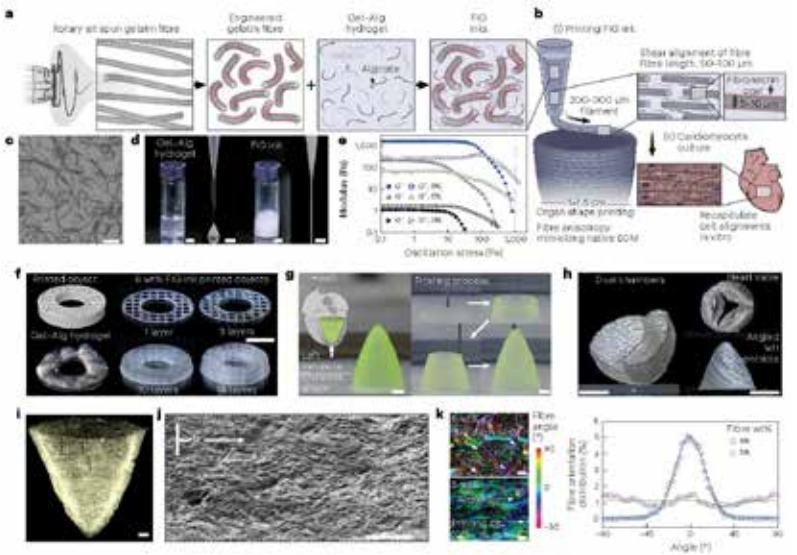

Choi, Suji [1] ; Lee, Keel Yong [1] , [2] ; Ardona, Herdeline Ann M.) [1] , [3] ; Liu, Xujie [4] , [5] ; Heiler, Ann-Caroline [6] , [7] , [8] ; Parker, Kevin Kit [1] , [9] , [11] ; [1] Harvard Univ, John A Paulson Sch Engn & Appl Sci, Dis Biophys Grp; [2] Sejong Univ, Dept Integrat Biosci & Biotechnol; [3] Univ Calif Irvine, Samueli Sch Engn, Dept Chem & Biomol Engn; [4] Boston Childrens Hosp, Dept Cardiol; [5] Chinese Acad Med Sci, Fuwai Hosp; [6] Tech Univ Munich, TUM Sch Nat Sci, Dept Biosci; [7] Tech Univ Munich, Ctr Funct Prot Assemblies; [8] Tech Univ Munich, Ctr Organoid Syst COS; [9] Harvard Stem Cell Inst; [10] Max Planck Sch Matter Life, Max Planck Sch; [11] Harvard Univ, Wyss Inst Biolog Inspired Engn. Work performed at Harvard CNS.

Supported by the NSF Harvard MRSEC (DMR-1420570, DMR-2011754, NIH and National Center for Advancing Translational Sciences (UH3HL141798 and UG3TR003279), and National Research Foundation of Korea (NRF) RS-2023-00248477, 2022R1A2C2012738. *Nat. Mater*. 22, 1039–1046 (2023).

National Research Priority: NSF–Understanding the Rules of Life

National Nanotechnology Coordinated Infrastructure

Center for Nanoscale Systems
Harvard University
FAS • SEAS

Cornell Nanoscale Science and Engineering Facility (CNF)

National Nanotechnology Coordinated Infrastructure

Widely Tunable and Narrow-Linewidth Chip-Scale Laser From Near-Ultraviolet to Near-Infrared Wavelengths

Researchers from Columbia University used CNF to fabricate photonic devices, demonstrating a chip-scale visible laser platform that enables tunable and narrow-linewidth lasers from near-ultraviolet to near-infrared wavelengths. Such integrated photonic platforms are critical for applications such as quantum optics, optical clocks, and fundamental studies of atomic and molecular physics.

The on-chip lasers were achieved by using micrometer-scale silicon nitride resonators with high quality factor and commercial Fabry-Pérot laser diodes. The tunable and narrow-linewidth lasing was achieved by designing a broadband and low-loss optical-feedback scheme based on ring resonators.

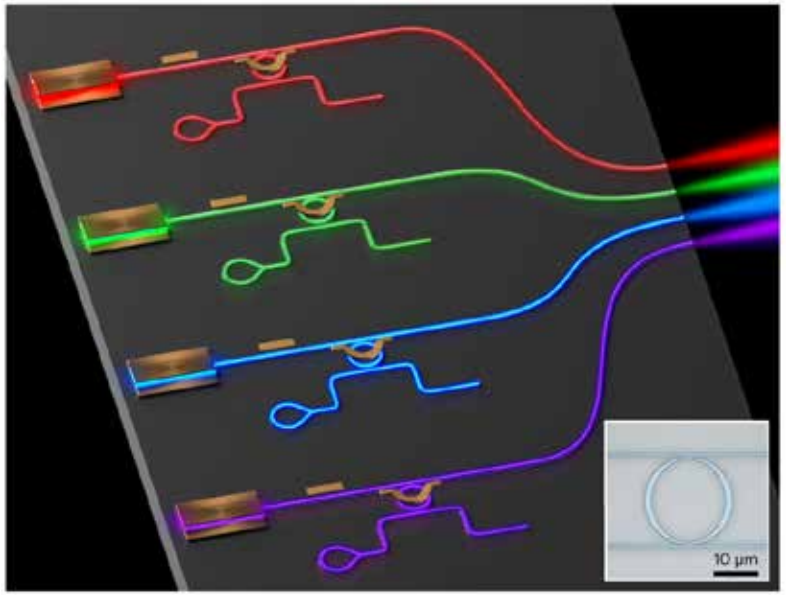

Schematic vision of integrated platform, where a single chip generates narrow-linewidth and tunable visible light of all colors. Inset: Microscope image of ring resonator.

M. Corato-Zanarella, A. Gil-Molina, X. Ji, M. C. Shin, A. Mohanty, and M. Lipson, Dept. of Electrical Engineering, Columbia University. This work was performed in part at Cornell NanoScale Facility (CNS).

This work was supported by the Army Research Office under award no. W911NF2110286. *Nature Photonics 17, 157-164 (2023).*

National Research Priority: Advanced Photonics

National Nanotechnology Coordinated Infrastructure

CNF Cornell NanoScale Science and Technology Facility

Real-Space Imaging of Periodic Nanotextures in Thin Films via Phasing of Diffraction Data

Researchers at Cornell University broadened the capability of coherent X-ray diffractive imaging (CXDI) by imaging strained structural motifs in periodic nanotextured epitaxial thin films with unprecedented nanoscale resolution, exploiting the diffuse scattering pattern from a conventional synchrotron beam.

The developed non-destructive technique was used to discover a previously unknown periodic nanotexture, comprised of nanoscale metallic-structure wires separated by nanoscale Mott-insulating-structure walls, in a Mott insulator epitaxial thin film of Ca_2RuO_4. The observed nanotexture in Ca_2RuO_4 films has not been reported in bulk crystals. The demonstrated nanoscale, real-space CXDI imaging opens a powerful avenue for visualizing and quantifying periodic modulations in quantum and energy materials.

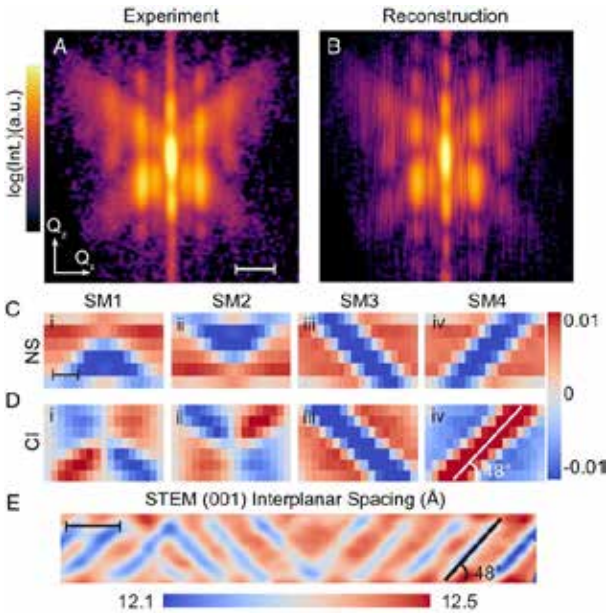

Real-space imaging of nanotextures in thin film Ca_2RuO_4. ***(A, B)*** *Measured and reconstructed diffraction pattern near the 008 peak of Ca_2RuO_4 at 7 K.* ***(C, D)*** *Real-space images of normal strain (NS) and crystal-plane inclination (CI) in the corresponding structural motifs (SM1-4).* ***(E)*** *A map of the interplanar spacing along [001] extracted from HAADF-STEM images of the cross-section of a ~34-nm-thick Ca_2RuO_4 film at ~100 K on the $[110]_{LAO}$ zone axis.*

Z. Shao, N. Schnitzer, J. Ruf, … D. G. Schlom, K. M. Shen, L. F. Kourkoutis, A. Singer, Dept. of Materials Science and Engineering, Cornell University. This work was performed in part at Cornell NanoScale Facility (CNS).

This work was supported by DOE BES no. DE-SC0019414.
PNAS 120 (28) e2303312120.

National Research Priority: DOE–Advanced and Sustainable Energy

National Nanotechnology Coordinated Infrastructure

CNF Cornell NanoScale Science and Technology Facility

Thermodynamic Evidence of Fractional Chern Insulator in Moiré $MoTe_2$

Chern insulators are the lattice analogues of the quantum Hall states and can manifest high-temperature topological orders at zero magnetic field, enabling next-generation topological quantum devices.

Researchers at Cornell University used CNF to fabricate twisted bilayer $MoTe_2$ devices and observed thermodynamic evidence of integer and fractional Chern insulators at zero magnetic field. The Cornell team further demonstrated electric-field-tuned topological phase transitions, paving the way for the demonstration of quantized fractional Hall conductance and anionic excitation and braiding in semiconductor moiré materials. Their work is the first realization of such systems in zero magnetic field.

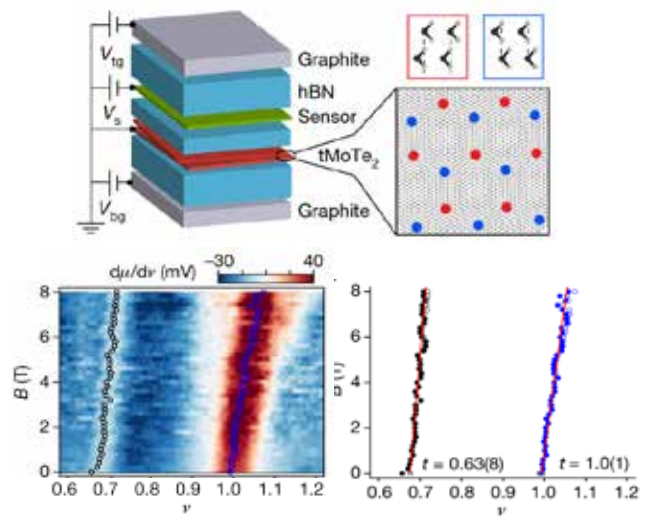

(Top) *Dual-gated twisted $MoTe_2$ with WSe_2 sensor for electronic compressibility measurements. The schematic on the right shows the Moiré pattern of the $MoTe_2$ stack.* ***(Bottom)*** *Electronic incom-pressibility as a function of hole filling factor (ν) and perpendi-cular magnetic field (B) near zero interlayer potential difference. Two incompressible states are observed at ν = 1 and 2/3.*

Y. Zhen, Z. Xia, K. Kang, J. Zhu, P. Knüppel, C. Vaswani, K. Watanabe, T. Taniquhci, K. F. Mak, and J. Shan, Dept. of Physics and School of Applied and Engineering Physics, Cornell University. This work was performed in part at Cornell NanoScale Facility (CNS).

This work was supported by DOE DE-SC0019481, AFOSR FA9550-20-1-0219, and NSF DMR-1719875. *Nature 622, 69-73 (2023).*

National Research Priority: NSF–Quantum Leap

Chip-Scale Simulations in a Quantum-Correlated Synthetic Space

Researchers at the University of Rochester used CNF to fabricate an on-chip quantum-correlated synthetic crystal. The demonstrated system shows a massive, nearly 400 x 400 synthetic lattice with electrically controlled tunability, opening an avenue towards chip-scale implementation of large-scale analogue quantum simulation and computation in the time-frequency domain.

The quantum-correlated synthetic crystal was realized by using a coherently controlled quantum optical frequency comb, composed of ~ 800 single-photon comb modes that were produced inside of dynamically modulated thin-film lithium niobate micro-resonators. The researchers successfully demonstrated two-particle quantum random walks and simulated Block oscillations of an electron in a crystal lattice.

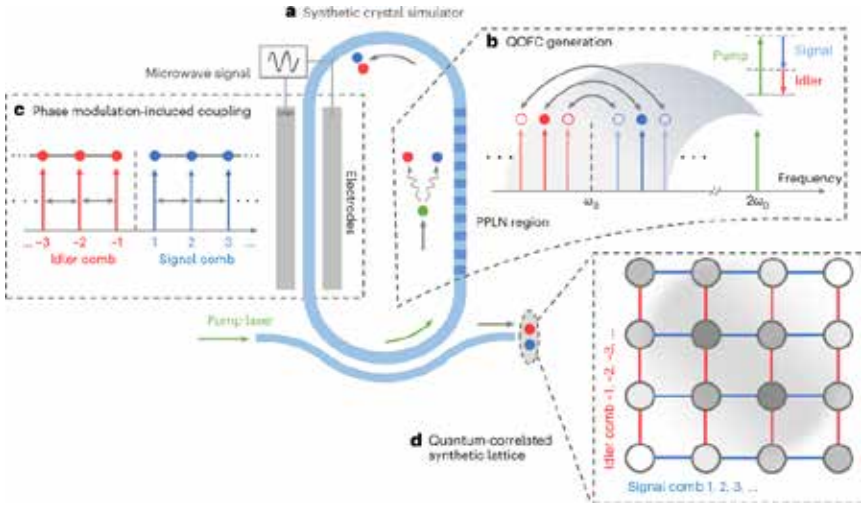

***(a)** Nanophotonic lithium niobate racetrack resonator. Periodically poled region in the resonator generates pairs of time–frequency entangled photons within a frequency comb, creating the nodes of the synthetic lattice (**b**). Electro-optic modulator embedded inside the resonator creates coupling within the comb lines forming a tight-binding lattice for each photon (**c**). Combining the two effects creates a 2D quantum-correlated synthetic lattice (**d**).*

U. A. Javid, R. Lopez-Rios, J. Ling, A. Graf, J. Staffa, and Q. Lin, Dept. of Electrical and Computer Engineering, University of Rochester. This work was performed in part at Cornell NanoScale Facility (CNS).

This work was supported by NSF OMA-2138174 and ECCS-2231036, DARPA QuICC program FA8650-23-C-7312 and LUMOS program HR001-20-2-0044. *Nature Photonics, 17, 883-890 (2023)*

National Research Priority: NSF–Quantum Leap

National Nanotechnology Coordinated Infrastructure

CNF Cornell NanoScale Science and Technology Facility

Bone-Matrix Mineralization Dampens Integrin-Mediated Mechanosignalling and Metastatic Progression in Breast Cancer

In patients with breast cancer, lower bone mineral density increases the risk of bone metastasis. By using collagen-based matrices with adjustable infrafibrillar mineralization, researchers at Cornell University show that matrix mineralization dampens integrin-mediated mechanosignalling and induces a less proliferative stem-cell-like phenotype in breast cancer cells. In mice with xenografted decellularized physiological bone matrices seeded with human breast tumor cells, the presence of bone mineral reduced tumor growth. Their findings suggest that bone-matrix changes in osteogenic niches regulate metastatic progression in breast cancer.

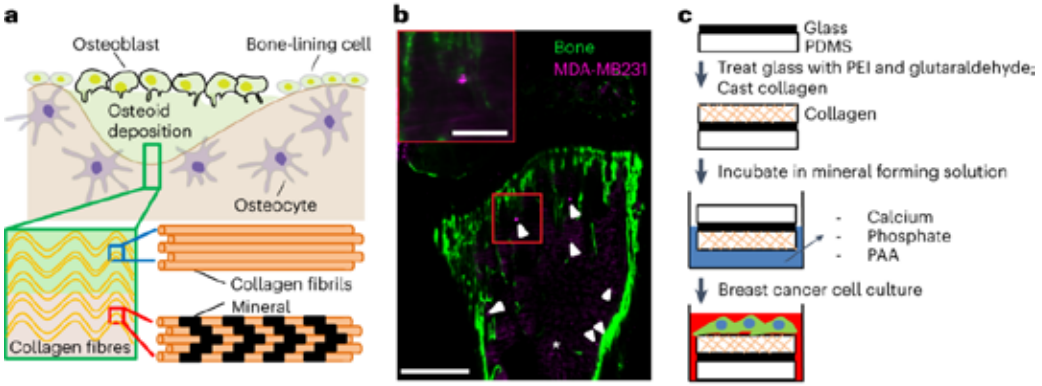

***a**, Schematic of bone ECM formation in osteogenic niches. Osteoblasts first deposit osteoid, which consists primarily of collagen type I fibres (blue box) that become mineralized (red box) over time by intrafibrillar mineralization. **b**, Intracardially injected MDA-MB231 labelled with Cy5-containing silica nanoparticles (magenta) disseminate to regions in which new bone matrix becomes mineralized, as visualized by light-sheet imaging of a calcein-labelled cleared mouse tibia (green). White arrowheads and asterisk indicate MDA-MB231 cells and autofluorescence of bone marrow, respectively. Scale bar, 600 μm and 150 μm (inset). **c**, Experimental setup to mineralize fibrillar collagen type I matrices via the PILP method for subsequent analysis of breast cancer-cell phenotype.*

S. Choi, M. A. Whitman, A. A. Shimpi, N. D. Sempertegui, A. E. Chiou, J. E. Druso, A. Verma, S. C. Lux, Z. Cheng, M. Paszek, O. Elemento, L A. Estroff, C. Fischback, Cornell University This work was performed in part at Cornell NanoScale Facility (CNS).

This work was supported by the Human Frontier Science Program (RGP0016/2017); the National Cancer Institute (IU54CA210184); NIH F31 (F31CA228448). *Nature Biomedical Engineering 7, 1455-1472 (2023)*

National Research Priority: NSF–Understanding the Rules of Life

3D Biomimetic Model of Lymphatics Reveals Cell-Cell Junction Tightening and Lymphedema Via a Cytokine-Induced ROCK2/JAM-A Complex

Impaired lymphatic drainage and lymphedema are major morbidities whose mechanisms have remained obscure. To study lymphatic drainage and its impairment, researchers at Harvard University and Boston University created a 3D microfluidic culture model of lymphatic vessels that emulates lymphatic junctional structure and drainage function. The engineered 3D model provides a unique platform to generate interstitial fluid pressure and measure the drainage of interstitial fluid into lymphatics. Using this model, they reveal a previously unappreciated rho-associated protein kinase (ROCK)2/ junctional adhesion molecule-A (JAM-A) protein complex that regulates lymphatic endothelial cell-cell junctions and the drainage of interstitial fluid into the lymphatic circulation.

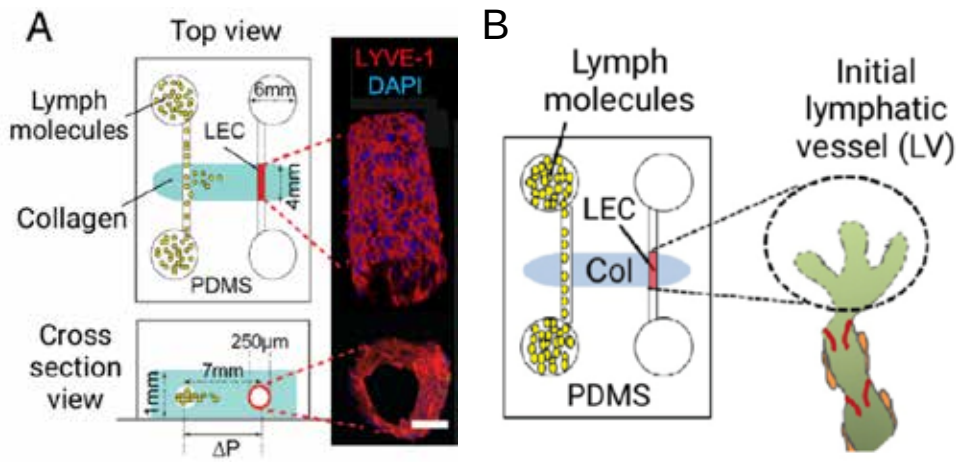

Lymphatic drainage-on-chip recapitulates lymphatic structure, drainage, and dysfunction. (A) *A schematic of the lymphatic drainage-on-chip platform.* ***(B)*** *A schematic of a biomimetic lymphatic drainage-on-chip model system. The engineered lymphatic vessel (LV) in the right-side channel functions as an initial LV to drain interstitial lymph fluid that is introduced through the left-side channel.*

E. Lee, S.L. Chan, Y. Lee, W. J. Polacheck, S. Kwak, A. Wen, D. H. T. Nguyen, M. L. Kutys, S. Alimperti, A. M. Kolarzyk, T. J. Kwan, J. Eyckmans, D. R. Bielenberg, H. Chen, C. S. Chen, Wyss Institute for Biologically Inspired Engineering, Harvard University. This work was performed in part at Cornell NanoScale Facility (CNS).

This work was supported by the NIH (EB025765; EB000262; HL133216; and HL141858), the NSF (CMMI-1548571; EEC-1647837), and the Wellcome Leap HOPE program. *PNAS 120 (41) e2308941120 (2023)*

National Research Priority: NSF–Understanding the Rules of Life

Biphasic Chemokinesis of Mammalian Sperm

The female reproductive tract (FRT) continuously modulates mammalian sperm motion by releasing various clues as sperm migrate toward the fertilization site. An existing gap in our understanding of sperm migration within the FRT is a quantitative picture of how sperm respond to and navigate the biochemical clues within the FRT.

Researchers at Cornell University used CNF to carry out an experimental study and found that in response to biochemical clues (a hyperactivation inducer 4-aminopyridine (4AP)), mammalian sperm display two distinct chemokinetic behaviors which are dependent upon the rheological properties of the media: chiral, characterized by swimming in circles; and hyperactive, characterized by random reorientation events. Their findings suggest that the chiral or hyperactive motion refines the sperm search area within different FRT functional regions.

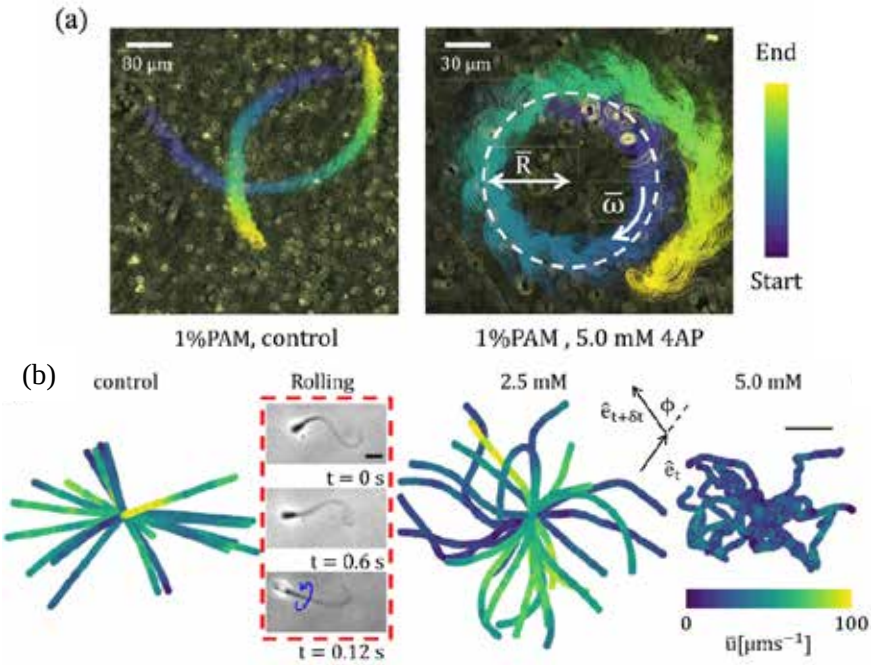

Experimental characterization of sperm motion. (a) Chiral motion. *Overlayed images acquired from the chiral motion in 5 seconds (left) and from the 4AP treated chiral motion in 5 seconds.* ***(b) Hyperactive motion.*** *Sperm trajectories at treatments with 2.5 and 5.0 mM of 4AP.*

Meisam Zaferani and Alireza Abbaspourrad, Dept. of Food Science, Cornell University. This work was performed in part at Cornell NanoScale Facility (CNS).

Phys. Rev. Lett. 130, 248401 (2023).

National Research Priority: NSF–Understanding the Rules of Life

Nanomolding of Metastable Mo_4P_3

Fabricating materials that are not stable at room temperature gives scientists a larger materials toolbox to choose from. Researchers from Cornell University showcase a new approach to make metastable materials at the nanoscale by pressing a bulk feedstock at moderate temperatures through a nanoporous mold.

By nanomolding MoP, the resulting nanowires become Mo_4P_3, a material that is not typically stable at room temperature. This approach can be extended to numerous other compounds that have ideal electronic, optical, and catalytic properties, demonstrating thermomechanical nanomolding is a novel synthesis method to produce high-quality single-crystalline nanowires.

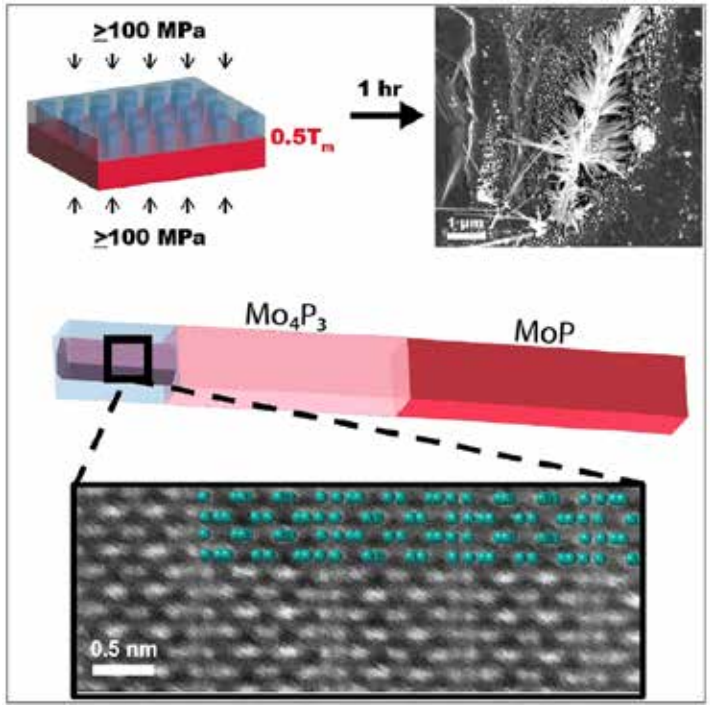

Top: *(left) Schematic of bulk MoP (red) pressed onto a nanoporous mold (blue) to make nanowires (SEM image, right).* ***Bottom:*** *The molded nanowire is metastable Mo_4P_3 and single-crystalline as probed by scanning transmission electron microscopy.*

M. T. Kiani, Q. P. Sam, G. Jin, Betul Pamuk, H. J. Han, J. L. Hart, J. R. Stauff, and J. J. Cha, Dept. of Materials Science and Engineering, Cornell University. This work was performed in part at Cornell NanoScale Facility (CNS).

This work was supported by the NSF DMR 2240956 and the Gordon and Betty Moore Foundation's EPiQS Initiative (GBMF 9062). *Matter 6, 1894-1902 (2023).*

National Research Priority: DoD Critical Technology Area–Microelectronics

15-GHz Epitaxial AlN FBARs on SiC Substrates

High speed communication systems require compact and effective filters in the 6-30 GHz frequency range, which are beyond the capacity of conventional surface-acoustic wave resonators.

Researchers at Cornell University used CNF to demonstrate epitaxial AlN thin-film bulk acoustic resonators (FBARs) on SiC substrates operating at the first-order thickness extensional modes of 15-17 GHz with a qualify factor over 400, the highest resonance frequencies for epitaxial material based FBARs to date. The figure of merit f·Q of the 15 GHz FBARs is ≈ 6.65 THz, comparable to single crystalline FBARs operating in 1-6 GHz. The demonstrated high speed epitaxial AlN FBARs are precursors of monolithic integration of passive acoustic filters and active amplifiers on the SiC substrate.

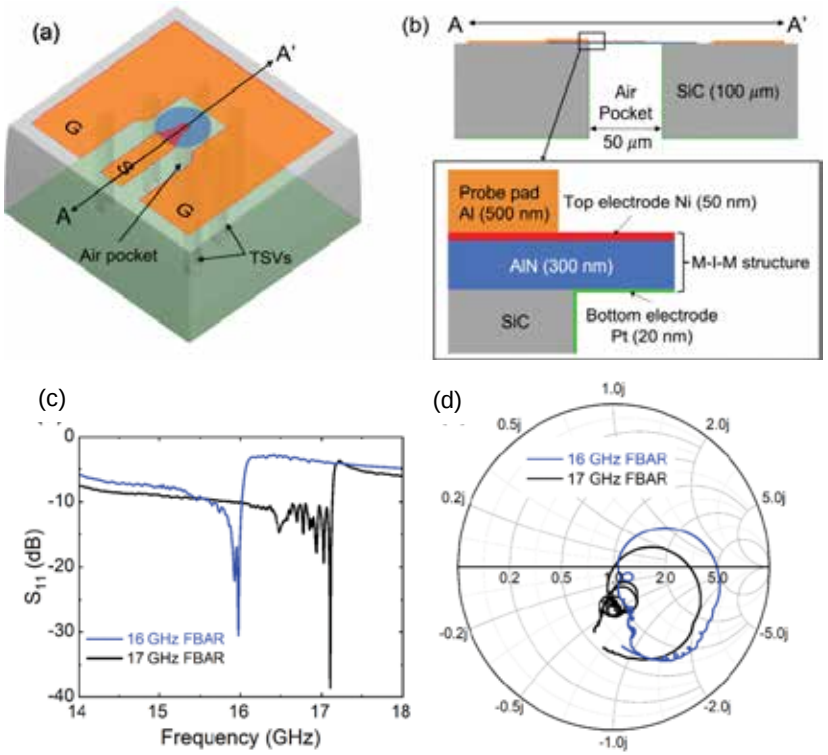

(a) *3D and* ***(b)*** *2D cross-sectional conceptual figures on one-port epitaxial AlN FBAR on the SiC substrate. The vibrating region of the FBAR includes an epitaxial AlN layer (blue), a top electrode (red) and a bottom electrode (green).*
(c) *Magnitude plots of S11 and* ***(d)*** *Smith charts for a 16 GHz and a 17 GHz one-port AlN FBAR driven by a 50 Ω source.*

W. Zhao, M. J. Asadi, L. Li, R. Chaudhuri, K. Nomoto, H. G. Xing, J. C. M. Hwang, D. Jena, Cornell University. This work was performed in part at Cornell NanoScale Facility (CNS).

IEEE Electron Device Letters, 44, p.903-906 (2023)

National Research Priority: DoD Critical Technology Area–Microelectronics

National Nanotechnology Coordinated Infrastructure

CNF Cornell NanoScale Science and Technology Facility

Boron Nitride (BN) Thin Films Grown on Diamond via Pulsed Laser Deposition

Researchers at Rice and Cornell University grew boron nitride (BN) thin films on (100) single-crystal diamonds using pulsed laser deposition and investigated its structural, magnetic, optical, and thermal properties. The BN films exhibited diamagnetic behavior at room temperature; anisotropic refractive index characteristics within the visible-to-near-infrared wavelength range; and cross-plane thermal conductivity of 1.53 $\pm$ 0.77 W/mK at room temperature with the thermal conductance of 20 $\pm$ 2 MW/m^{2}K at the BN/diamond interface.

These findings have significant implications for a range of device applications based on ultrawide bandgap semiconductors (bandgap > 4.0 eV), such as high-power RF electronics, deep-UV optoelectronics, quantum information, and thermal management.

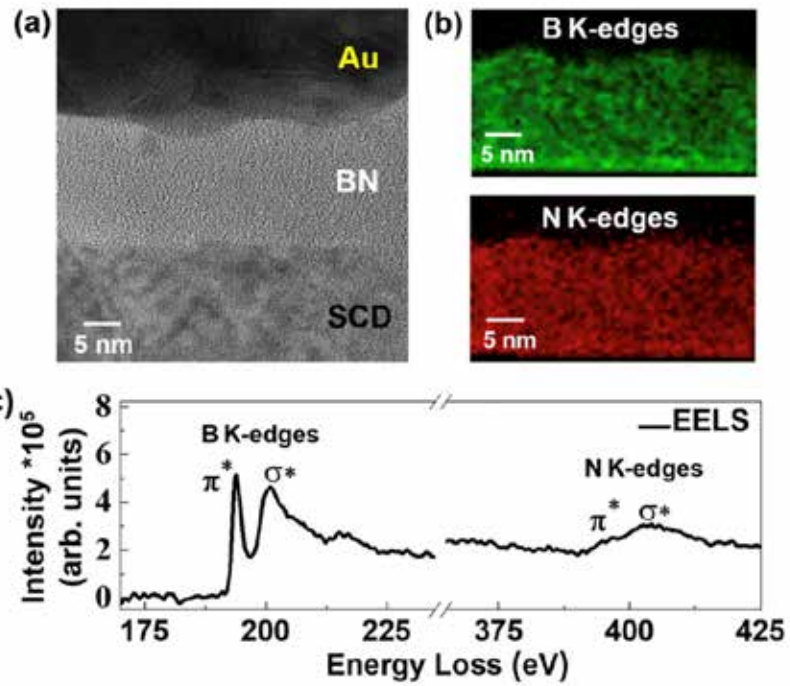

BN thin films on Diamond via Pulsed Laser Deposition. *(a) Cross-sectional high-resolution transmission electron microscopic image of BN film on a SCD. (b) EELS elemental mapping shows the presence of both boron and nitrogen. (c) EELS showing the bands corresponding to boron and nitrogen K-edges.*

A. Biswas, G. A. Alvarez, T. Li, … Z. Tian, P. M. Ajayan, Rice and Cornell University. This work was performed in part at Cornell NanoScale Facility (CNS).

This work was supported by the Army Research Office (W911NF-19-2-0269), DOE EFRC (ULTRA, DE-SC0021230), and SRC JUMP 2.0 (CHIMES). *Phys. Rev. Materials 7, 094602 (2023)*

National Research Priority: DoD Critical Technology Area–Microelectronics

Kentucky Multi-Scale Manufacturing and Nano Integration Node (KY Multiscale)

National Nanotechnology Coordinated Infrastructure

Electrochemical Sculpting of BP and b-As_xP_{1-x} to Produce Nanoribbons

Due to their one-dimensional (1D) structure and high concentration of edge sites, nanoribbons (NRs) display exceptional and tunable electronic and optical properties, rendering them promising nanoscale materials for next-generation energy devices and applications across areas such as energy storage, chemicals and fuels fabrication, catalysis, sensing, and other technologies. However, realizing the full potential of NRs remains a challenge due to the absence of reliable synthetic methods that offer precise control over their structure and properties.

We present a novel two-step method for producing NRs. This method leverages the strong anisotropy of group V layered materials such as black phosphorous (BP) (Fig.1a) and black arsenic phosphorous (b-As_xP_{1-x}) alloys. The method is based on electrochemical sculpting, involving highly anisotropic electrochemical Na^+ intercalation that leads to the formation of uniformly distributed amorphous channels and subsequently, NRs of the host material in between (Fig.1b). Applying this method to BP results in the fabrication of high-density, narrow, and uniform PNRs (Fig.1c-h). The electrochemical sculpting process is also applicable to b-As_xP_{1-x}. However, significant differences exist between b-As_xP_{1-x} and BP due to variations in Na^+ diffusion anisotropy within these materials.

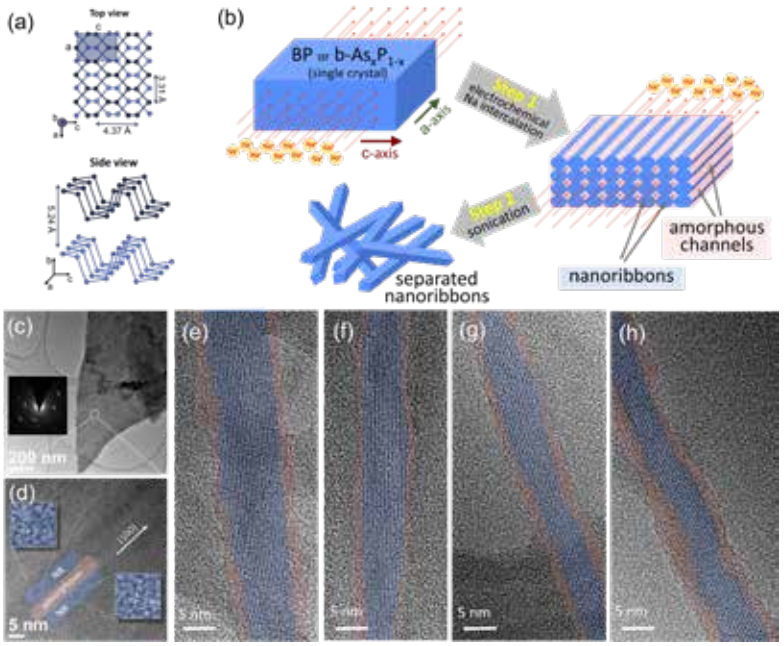

Figure 1. *(a) Crystal structure of BP. (b) Schematic illustrating a two-step NR fabrication process. (c) TEM image of BP particles after electrochemical sculpting. (d) HRTEM of the area shown in (c). (e-h) HRTEM images of seperated BP NRs.*

U.O. Abu, S. Akter, H. Weerahennedige, S. Gupta, G. Sumanasekera, H. Wang, B. Narayanan and J.B. Jasinski. Research is performed at the University of Louisville Conn Center for Renewable Energy Research (KY Multiscale)

This research is supported by the U.S. DOE, Office of Science, Basic Energy Sciences, Award #DE-SC0024131. *Advanced Science*, e2203148 (2022).

National Research Priority: NSF–Growing Convergence Research

Formulation and Characterization of Pressure-Assisted Microsyringe 3D-Printed Scaffolds for Controlled Intravaginal Antibiotic Release

Bacterial vaginosis (BV) is a highly recurrent vaginal condition linked with many health complications. Topical antibiotic treatments for BV are challenged with drug solubility in vaginal fluid, lack of convenience and user adherence to daily treatment protocols, among other factors. 3D-printed scaffolds can provide sustained antibiotic delivery to the female reproductive tract (FRT). Silicone vehicles have been shown to provide structural stability, flexibility, and biocompatibility, with favorable drug release kinetics. This study formulated and characterized novel metronidazole-containing 3D-printed silicone scaffolds for eventual application to the FRT. Scaffolds were evaluated for degradation, swelling, compression, and metronidazole release in simulated vaginal fluid (SVF). For all curing conditions, release of metronidazole after 1 and 7 days showed >4.0-log reduction in *Gardnerella* concentration. Negligible cytotoxicity was observed in treated keratinocytes comparable to untreated cells, This study shows that pressure-assisted microsyringe 3D-printed silicone scaffolds may provide a versatile vehicle for sustained metronidazole delivery to the FRT.

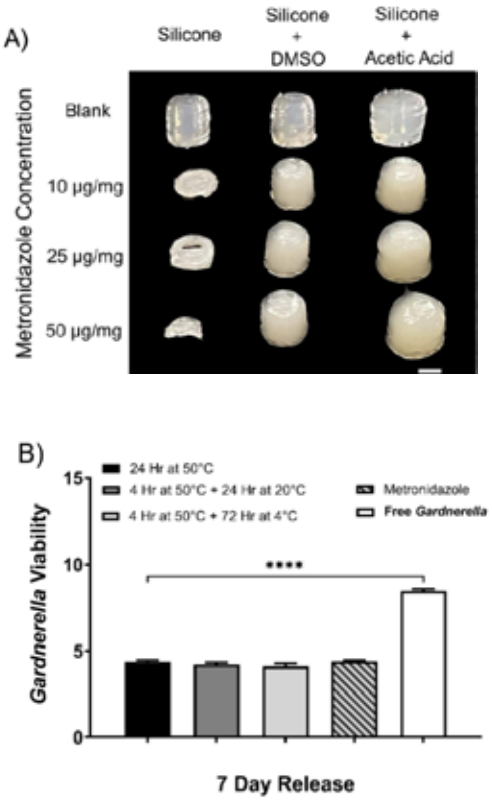

3D-printing silicone ink formulations utilizing were used in dissolution of metronidazole in the ink. Scaffolds were printed with 5 mm height and 4 mm diameter for future murine application. (A) Scaffold resolution was compared between formulations with metronidazole concentrations of 10, 25, 50 µg/mg in ink.

(B) Release of metronidazole from 3D-printed scaffolds at 7 days was conducted in the presence of Gardnerella *for 24 hr. Statistical significance (one-way ANOVA, Tukey HSD post-hoc): *p ≤ 0.05 and ****p ≤ 0.0001.*

AJ Kyser, MY Mahmoud, SE Herold, WG Lewis, AL Lewis, JM Steinbach-Rankins, HB Frieboes. Research performed at the University of Louisville Conn Center for Renewable Energy (KY Multiscale).

Research was supported by NIH R01AI168475. *Int J Pharmaceutics*, 2023.

National Research Priority: NSF–Growing Convergence Research

National Nanotechnology Coordinated Infrastructure

KY MULTISCALE
The NSF NNCI Multi-Scale Manufacturing & Nano Intergration Node

Microfluidic Generation of Alginate Microbeads to Quantify Intra-Tumoral Compression

Cancer progression is highlighted by the emergence of aberrant mechanical features in the tumor micro-environment that present pathological signals to drive tumor progression. Alterations to extrinsic signals such as tumor ECM stiffness and composition have been well described; however, the development of solid stresses *within* the tumor and its effect on tumor evolution is poorly understood. Recent reports have suggested that intra-tumoral stress guides cancer cell escape from tumors, highlighting an emergent mechanobiological driver of cancer progression; however, these aspects are difficult to investigate with standard *in vitro* tools and requires the development of advanced biophysical tools. To address this, we have developed a microfluidic platform (**Figure 1**) that generates deformable alginate microbeads that can be used as force probes to quantify the development of compressive stresses generated within a growing glioblastoma tumorsphere.

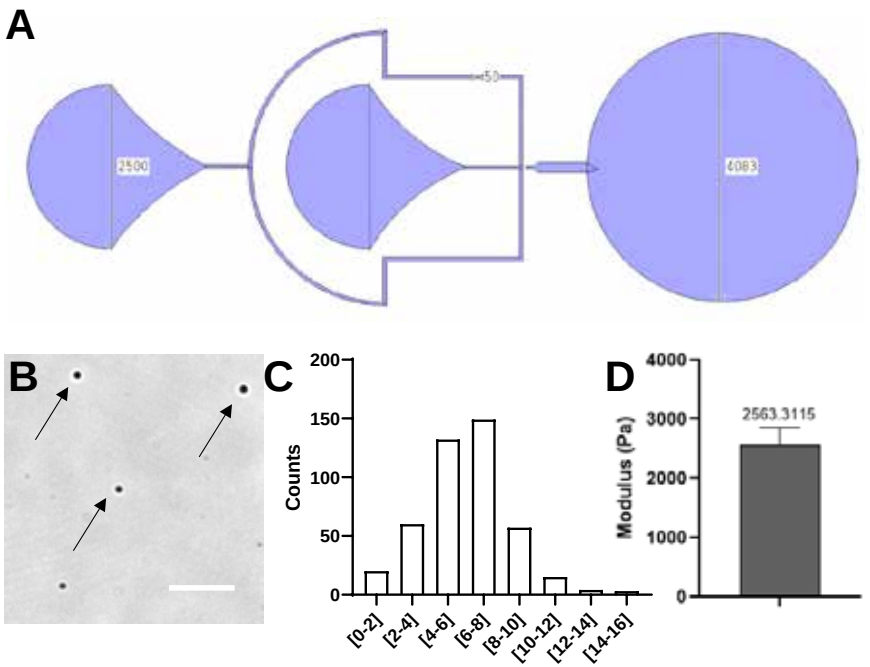

Figure 1. Microfluidic Device Generates Monodisperse Microbeads *(**A**) Schematic of the microfluidic device design. Inlets and outlet diameters shown in microns. (**B**) Collected microbeads show uniform size and size distribution quantification (N = 500) using ImageJ show majority of microbeads are 6-8 μm in diameter. **(C)** Young's modulus for alginate microbeads calculated via AFM (**D**).*

Fowler, ZP and Chen J, Work was performed at at the University of Louisville MicroNano Technology Center (MNTC)

This research was supported by NSF NNCI Award #2025075. Results were presented at the Biomedical Engineering Society Annual Meeting, 2023 and the Brown Cancer Center Retreat, 2023.

National Research Priority: NSF–Understanding the Rules of Life

Scalable Flexible Perovskite Solar Cells by Solution Phase Processing

Solution processing of flexible perovskite solar cells (f-PSCs) provides an avenue for scalable, high-throughput printing of lightweight, scalable, and cost-effective flexible solar cells. However, the deposition of fully solution-processed metal oxide charge transport layers on perovskites has been limited by solvent incompatibilities and high processing temperatures for metal oxide nanoparticles. In this study, we present high-performance, inverted f-PSCs from the direct deposition of yttrium doped SnO_2 nanoparticles functionalized with acetate on top of perovskite as an ink in anhydrous ethanol via blade coating. Yttrium doping improved device performance by improving the charge extraction leading with a decreased series resistance leading to improvements in the open-circuit voltage and fill factor. The champion power conversion efficiency for 0.1 cm2 devices increased from 14.3% for undoped SnO_2 to 18.2% with 2% Y:SnO_2 doping, which is unprecedented for f-PSCs on ITO-PET substrate employing SnO_2 as an ETL.

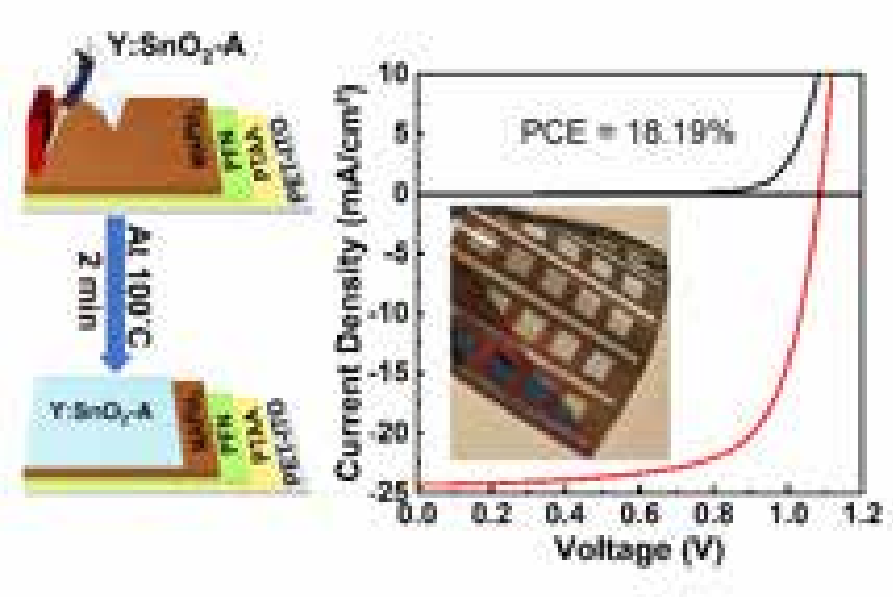

Preparation and deposition of Y:SnO2-A inks, deposition by solution phase blade coating followed by a bried annealing. Performance curve of resulting device and image of flexible perovskite devices.

Chapagain, S., B. Martin, P. Armstrong, C.L. Perkins, M.O. Reese, T. Druffel, C.A. Grapperhaus. Research performed at the University of Louisville Conn Center for Renewable Energy Research (KY Multiscale).

Research supported by DOE SETO Award DE-EE0009752. *ACS Appl. Energy Mater.* 2023, 6, 9, 4496–4502

National Research Priority: NAE Grand Challenge–Make Solar Energy Economical

Performance Evaluation and Model of Spacesuit Cooling by Hydrophobic Hollow Fiber-membrane Based Water Evaporation through Pores

NASA uses a hollow fiber membrane in their Spacesuit Water Membrane Evaporator (SWME) for thermal control of the suit. Understanding the nanoscale pore structure of the membrane proved critical to accurately modeling the thermal performance of the evaporator and to analyzing contamination and failure modes. This new modeling approach will allow engineers to predict thermal performance as a function of key process parameters, contaminants, and foulants, and can likely be extended to ground-based processes such as low-temperature concentration and purification of biomolecules.

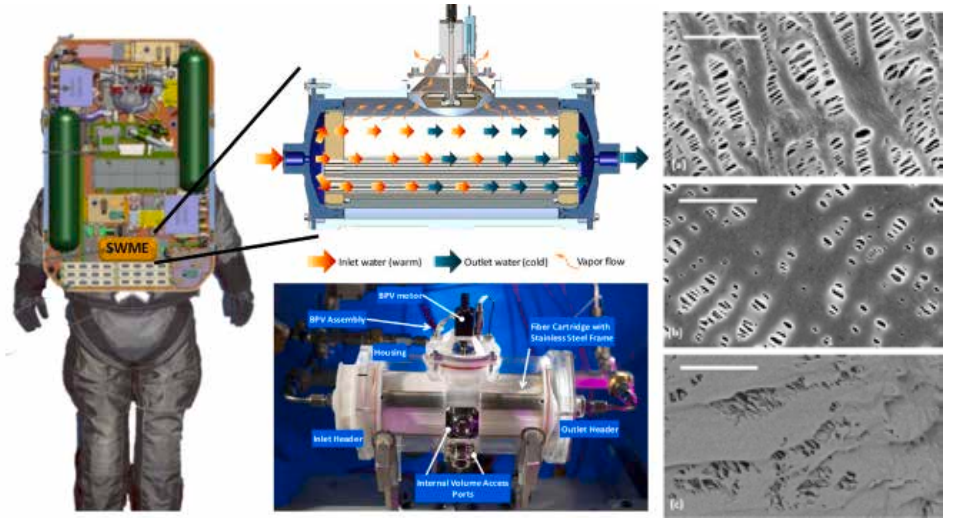

A hollow fiber membrane evaporator is critical to thermal control for NASA's spacesuits (left and center). Visualizing and measuring the nanopore structure of the membrane (right) proved critical for modeling its performance. Scale bar is 1µm.

Prof. Dibakar Bhattacharyya, Chemical Engineering, Univ. of Kentucky. Work performed in part at KY Multiscale.

Research support from NASA Engineering and Safety Center and NIEHS Award P42ES007380. *J. Membrane Science.*, v. 673, 121497 *(2023).*

National Research Priority: NSF–Growing Convergence Research

National Nanotechnology Coordinated Infrastructure

KY MULTISCALE
The NSF NNCI Multi-Scale Manufacturing & Nano Intergration Node

Membrane Functionalization Approaches toward Per- and Polyfluoroalkyl Substances and Selected Metal Ion Separations

Separation technologies are critical for water purification for both drinking water and precision manufacturing. Researchers at the University of Kentucky recently demonstrated that membranes with functionalized nanopores can separate organic and inorganic contaminants from water. Example pollutants included arsenic along with perfluoroalkyl and polyfluoroalkyl substances. The membranes, which employed adsorptive/ion exchange polymers with various complex groups in the pores, demonstrated dramatically improved speed and capacity compared to commercially available solutions. When scaled up, such membranes could provide a new path to widely accessible, safe drinking water.

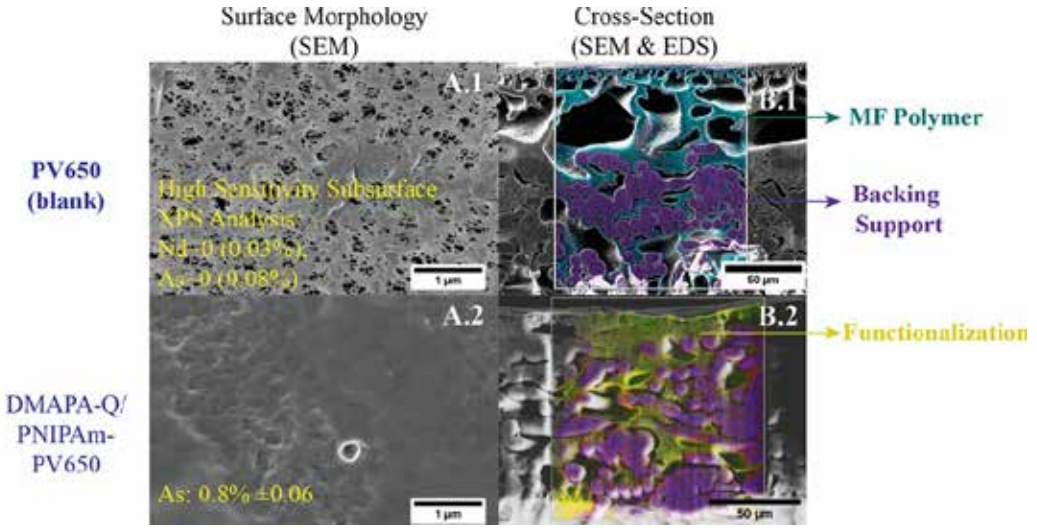

Surface (left) and cross-sectional (right) scanning electron micrographs of membranes for water purification. X-ray photoelectron spectroscopy data (left) and energy dispersive X-ray spectroscopy maps (right) are also shown. A blank (control) membrane is shown at the top and a functionalized (DMAPA-Q/PNIPA) membrane is shown below.

Prof. Julie Zimmerman, Yale Univ. and Dibakar Bhattacharyya, UK Chemical Engineering. Work performed at KY Multiscale.

Research support from NIEHS Awards P42ES007380 and P42ES030990. *ACS Appl. Mater. Interfaces,15, 37, 44224–44237 (2023).*

National Research Priority: NSF–Growing Convergence Research

National Nanotechnology Coordinated Infrastructure

KY MULTISCALE
The NSF NNCI Multi-Scale Manufacturing & Nano Intergration Node

High Hole Mobility Fiber Organic Electrochemical Transistors for next-Generation Adaptive Neuromorphic bio-Hybrid Technologies

Organic electrochemical transistors (OECT) can serve as active electronics in low-cost, wearable systems and for neuromorphic technologies. Researcher at the University of Kentucky recently demonstrated that poly(3,4-ethylene-dioxythiophene):polystyrene sulfonate (PEDOT:PSS) fibers are a promising material system for OECTs. Specifically, their transistors exhibited *record high hole mobilities,* stable contacts, and high mobility-capacitance products (a key figure of merit). Neuromorphic electronics formed from the fibers were responsive to the presence of dopamine and closely matched the geometry of the neuronal axon terminal.

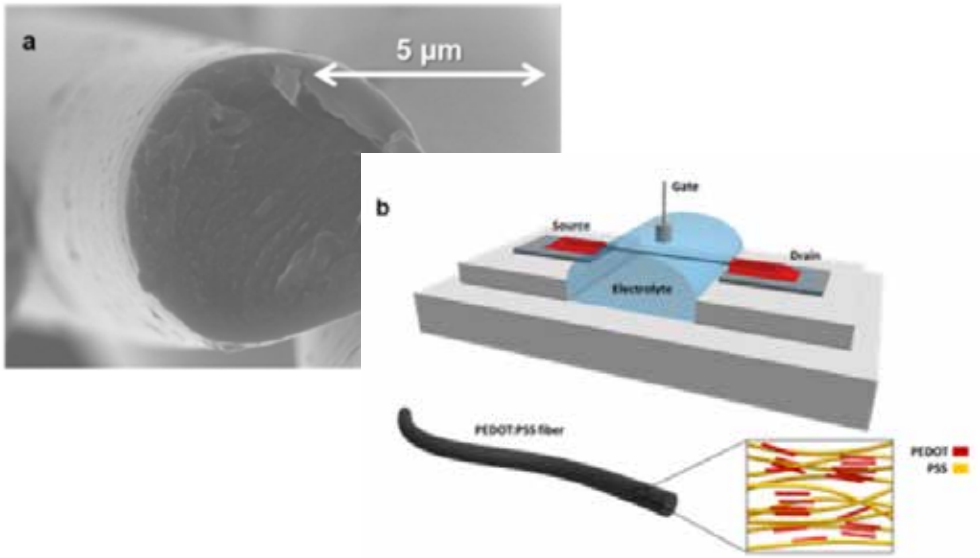

PEDOT:PSS fibers (a, upper left) exhibit extremely high hole mobility and can be used to form organic electrochemical transistors (b, lower right). These transistors subsequently formed the basis for neuromorphic devices that are responsive to the neurotransmitter dopamine.

Prof. Alexandra Paterson (UK Materials Science and Engineering). Work performed at KY Multiscale EMC and CAER.

Research support from NSF OIA 1849213. *Advanced Materials 2305371 (2023).*

National Research Priority: NSF–Growing Convergence Research

National Nanotechnology Coordinated Infrastructure

KY MULTISCALE
The NSF NNCI Multi-Scale Manufacturing & Nano Intergration Node

Effect of Water Vapor Pressure on Positive and Negative Tone Electron-beam Patterning of Poly(Methyl Methacrylate)

Electron-beam lithography is the primary pattern generation technology for almost all bottom-up nanofabrication. Variable-pressure electron-beam lithography (VP-EBL) employs an ambient gas at sub-atmospheric pressures to reduce charging. However, it remains unknown how the gas affects the radiation chemistry of the patterning process. In this work, VP-EBL was conducted on conductive substrates to study the effect of water vapor on poly-methyl methacrylate (PMMA) patterning separately from the effects of charge dissipation. The contrast of PMMA was found to improve significantly with increasing water vapor pressure for both positive and negative-tone patterning. Thus, VP-EBL offers a new means of tuning sensitivity and contrast for electron-beam lithography.

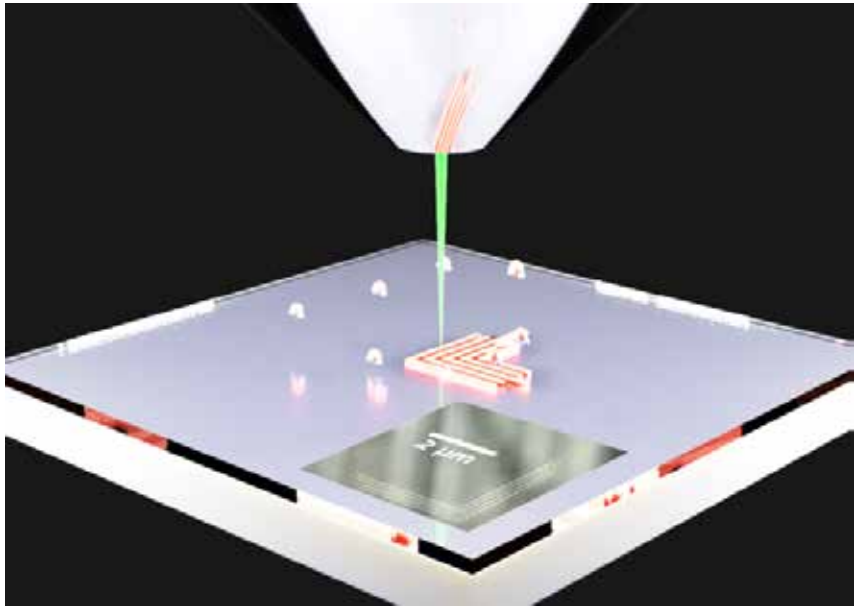

Schematic of electron beam lithography conducted in the presence of a gas. Researchers showed that water vapor improves the contrast of e-beam exposed PMMA opening a path to improving lithographic performance by careful selection of the ambient gas and process parameters. Inset: Experimental micrograph of a “nested-L” pattern exposed using VP-EBL.

Prof. Todd Hastings (University of Kentucky, Electrical Engr.). Work performed at KY Multiscale CeNSE and EMC.

Research support from NSF CMMI-2135666. *J. Vac. Sci. Tech. B, 41, 012604 (2023)*

National Research Priority: NSF–Growing Convergence Research

National Nanotechnology Coordinated Infrastructure

KY MULTISCALE
The NSF NNCI Multi-Scale Manufacturing & Nano Intergration Node

A Jet and Inkjet Printing Technology for Custom MEMS Packaging

In this study we proposed an alternative, low cost, packaging method using both inkjet and aerosol jet printing to fabricate functional interconnects for custom die-level packages assembled on Printed Circuit Boards (PCB).

The interconnects to MEMS microrobots are realized on the NeXus, a unique custom robotic and additive manufacturing system developed at Louisville Automation and Robotics Research Institute (LARRI). Within the NeXus, insulating structures of the package are fabricated using Nordson EFD Pico Pulse® drop-on-demand (dod) Inkjet instrument. Whereas conducting lines connecting die and Printed Circuit Board (PCB) metal pads are fabricated with the help of Optomec Decathlon® Aersol jet printer.

The results show that we successfully fabricated printed interconnects between Cu/Au PCB pads and Si die cleanroom fabricated Au pads, whereas electrical characterization revealed resistances in the 1-10 Ω range.

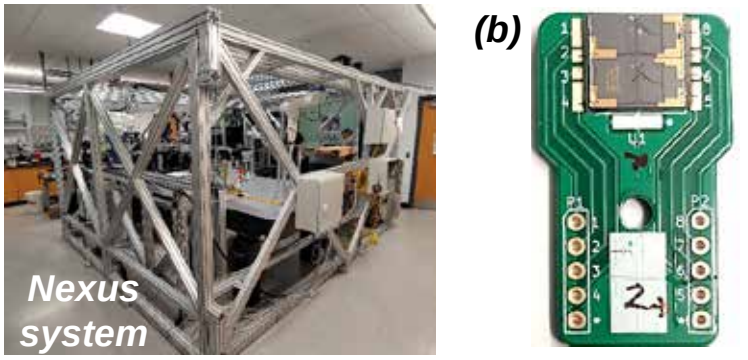

(a) General view of Nexus system. (b) PCB board with packaged MEMS structure-solid Articulated Four Axis Microrobot (sAFAM).

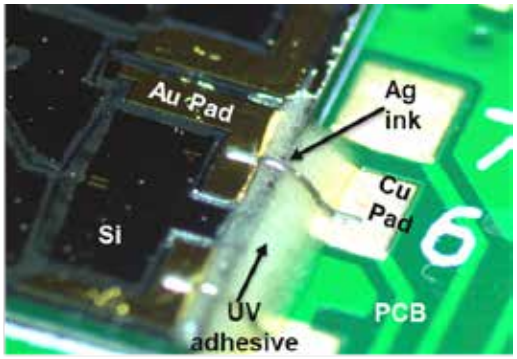

(c) Detailed view of the fabricated electrical interconnects.

Sherehiy, A., Sassa,M., Jackson, D., Sills, D., Ratnayake, D., Zhang, R., Yang, Z., Walsh, K., Naber, J., Popa, D. O.
MEMS structures were fabricated at the University of Louisville MNTC (KY Multiscale).

Research was supported by NSF NNCI REU Summer program 2023 and NSF KY EPSCOR #1849213.

National Research Priority: NSF–Understanding the Rules of LIfe

National Nanotechnology Coordinated Infrastructure

KY MULTISCALE
The NSF NNCI Multi-Scale Manufacturing & Nano Intergration Node

Laser Sintering of RTM385-Boron Nitride Blends

The goal of the research was to explore additive manufacturing using RTM385-Boron Nitride (BN) blends.

The material's high thermal capacity makes it an ideal candidate for high-heat applications. Additive manufacturing with RTM385-BN blends produces green parts that require thermal post-curing to achieve complete cross-linking. Selective laser sintering (SLS) of the material was done to create test chips and tensile testing specimens. The tensile testing specimens were sent to NASA Glenn Research Center for post-curing and testing.

Green parts from SLS machine.

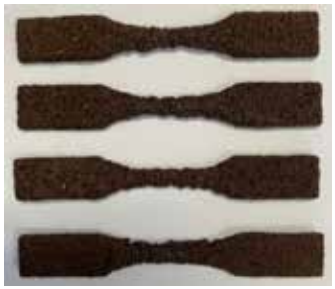

Post cured parts at NASA GRC.

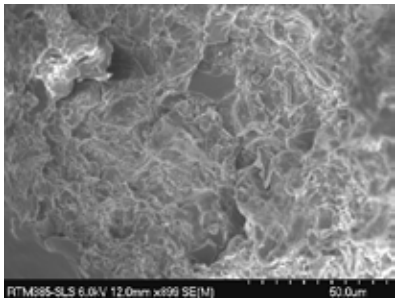

Detailed surface of specimens.

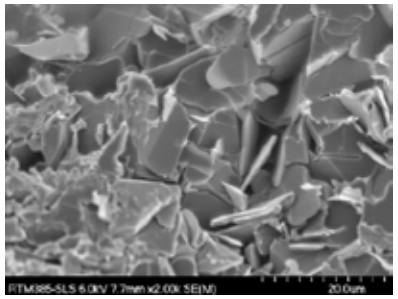

Cross section of dogbone.

Chuang, K., Spade, W., and Gillham, J., Research was performed at the University of Louisville Additive Manufacturing Institute of Science and Technology (AMIST), part of KY Multiscale.

Research supported by NASA Glenn Research Center, Federal Award #80NSSC21M0240.

National Research Priority: NSF–Understanding the Rules of LIfe

National Nanotechnology Coordinated Infrastructure

KY MULTISCALE
The NSF NNCI Multi-Scale Manufacturing & Nano Intergration Node

Mid-Atlantic Nanotechnology Hub (MANTH)

National Nanotechnology Coordinated Infrastructure

Microlaser Chip Adds New Dimensions to Quantum Communication

Researchers at MANTH have created a chip that outstrips the security and robustness of existing quantum communications hardware.

Their technology communicates in “qudits,” doubling the quantum information space of any previous on-chip laser.

In classical communications, a laser can emit a pulse coded as either 1 or 0. These pulses can easily be cloned by an interceptor looking to steal information. In quantum communications with qubits, superposition makes it so a quantum pulse cannot be copied.

The device’s four-level qudits enable significant advances in quantum cryptography, raising the maximum secrete key rate for information exchange from 1 bit per pulse to 2 bits per pulse.

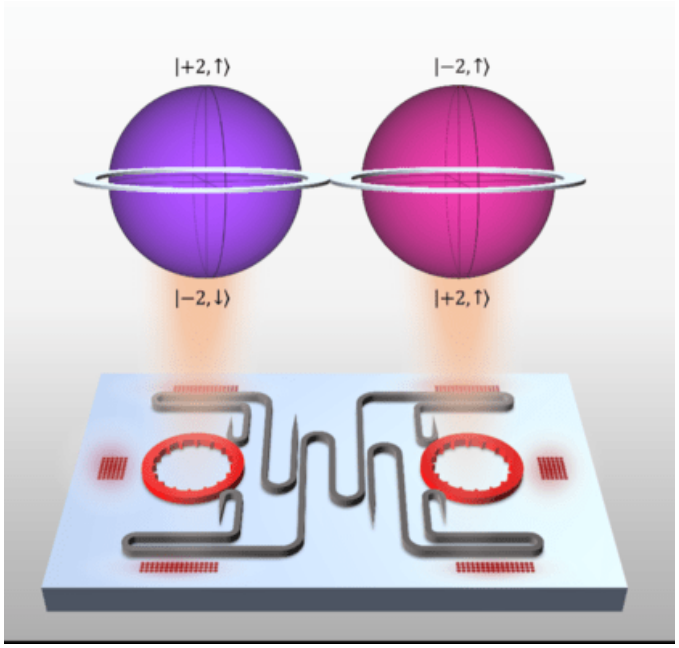

Zhang, Z., Zhao, H., Wu, S. *et al.* This work was performed at MANTH.

Research was supported by the US ARO, NSF, DARPA, ONR, King Abdullah University of Science & Technology, and a Sloan Research Fellowship. *Nature* 612, 246–251 (2022).

National Research Priority: NSF–Quantum Leap

High-Q Factor Multiferroic Resonant MEMS For Low Frequency Magnetic Field Sensors

The heart, brain, skeletal muscles, and nerves all produce magnetic fields at various frequencies and strengths. Magnetomyography (MMG) can detect magnetic fields produced by skeletal muscles, which can provide many medical insights for rehabilitation, health monitoring, diagnosis, and even robotic control of prosthetics.

Researchers at MANTH have created a multiferroic sensor that allows for high resolution, low noise magnetic sensing with low power consumption and a small size for bio-magnetic sensing applications. The MEMS device consists of a layer of a FeCo alloy on piezo-electric AlN. Electrodes are fabricated and the MEMS structure is released to form a free-standing oscillating structure.

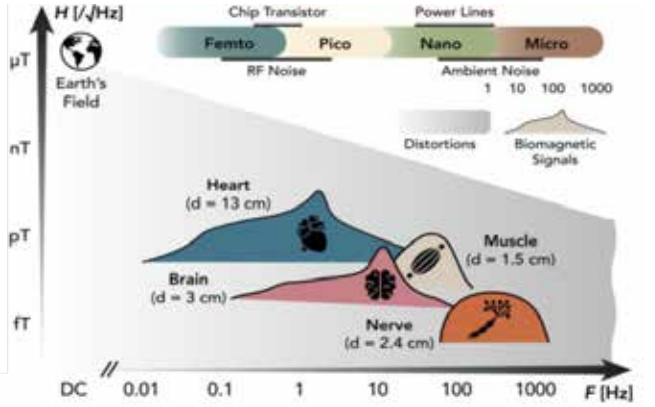

In order to improve sensitivity, the team takes advantage of the high Q factors of the devices at resonance (~8MHz) using a modulation technique. By driving an electrical oscillation through the AlN, the FeCo on top changes its stress state, which alters its ability to strain effectively in the presence of a magnetic field, leading to the modulation effect. Ultimately, the researchers demonstrate a sensitivity of 67 mA/T over a 1kHz bandwidth, with a MEMS resonator Q factor of 1700 and a resolution of 2.2nT/Hz$^{1/2}$. Future work will look to leverage these initial findings into improving the sensitivity and resolution.

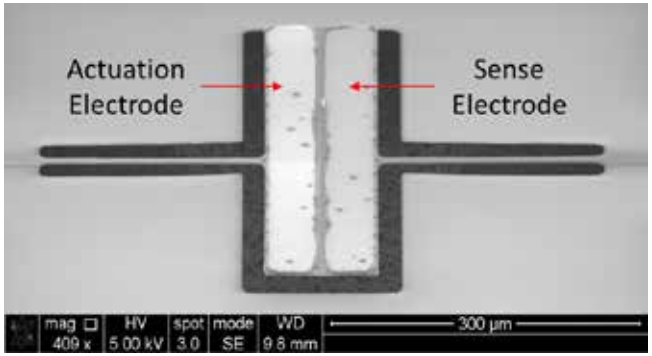

D'Agati, M., Sofronici, S., Huo, Y., Olsson, R.H., Finkel, P., Bussmann, K., Mion, T., Staruch, M., McLaughlin, K. and Wheeler, B.

This work was partially supported by the DARPA QUIVER HR0011-20-C-0098 and based on work supported by a NSF Graduate Research Fellowship. Joint Conference of the European Frequency and Time Forum and IEEE International Frequency Control Symposium (EFTF/IFCS) (pp. 1-3). IEEE.

National Research Priority: NSF–Understanding the Rules of Life

3D Printed Magnetic Microrobots

- MANTH users from the University of Delaware have used the QNF Nanoscribe 3D printer to fabricate magnetically actuated microbots.
- These microbots may play an important role in safely diagnosing diseases, conducting surgery, and transporting drugs in the human body.
- The magnetic actuation offers precise control over the motion of microrobots in terms of their trajectories and on/off mechanisms.
- The phenomenon is demonstrated in the optical micrographs on the right where a Ni coated, 3D printed microrobot is propelled and guided by a magnetic field.

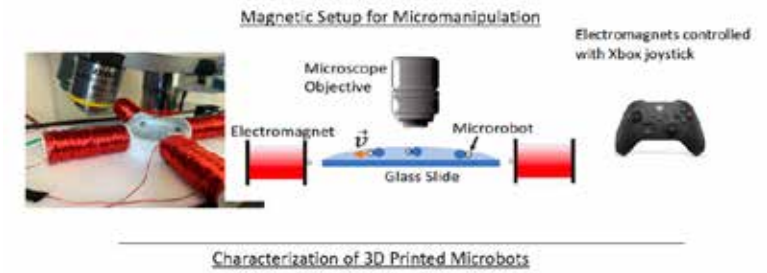

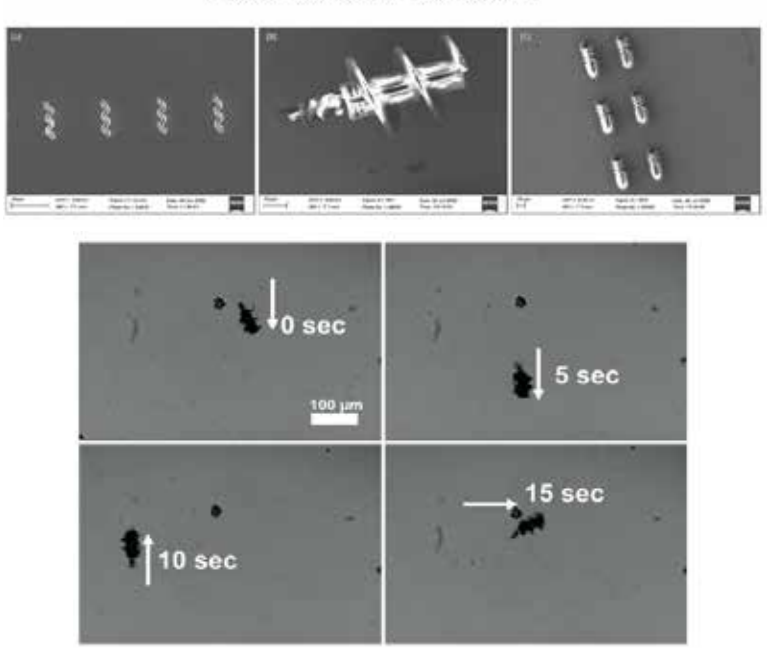

University of Delaware researchers Zameer Hussain Shah, David Rivas, Max Sokolich, and Sambeeta Das, Univ. Delaware. Work conducted at MANTH.

National Research Priority: NSF–Understanding the Rules of Life

Investigating Quantum Dot/Rod Structures

- University of Delaware researchers utilized the JEOL NEOARM TEM at MANTH to obtain spatially-resolved measurements of the alloying composition in colloidal quantum dot nanostructures used for photon up-conversion.
- Nanostructures consisting of two quantum dots separated by a nanorod have been synthesized. One quantum dot serves as the “absorber” – the region where the low energy photons are absorbed – and the second quantum dot serves as the “emitter” – the region where the high energy photons are emitted.
- The nanorod region provides crucial spatial separation between the absorber and the emitter, and its composition has a major impact on the efficiency of the upconversion process.
- They found that the nanorod synthesis resulted in a mix of elongated nanorod particles and shorter tetrapod particles and that the composition varied between differently shaped particles. Elongated nanorods contained primarily Cd and S with very little Se, while the tetrapod particles contained large amounts of Se.

STEM and EDS images of CdSSe nanoparticles from the JEOL NEOARM TEM at the Singh Center. Top row: Tetrapod particle containing Cd, S, and large amounts of Se. Bottom row: Nanorod particle containing only significant amounts of Cd and S.

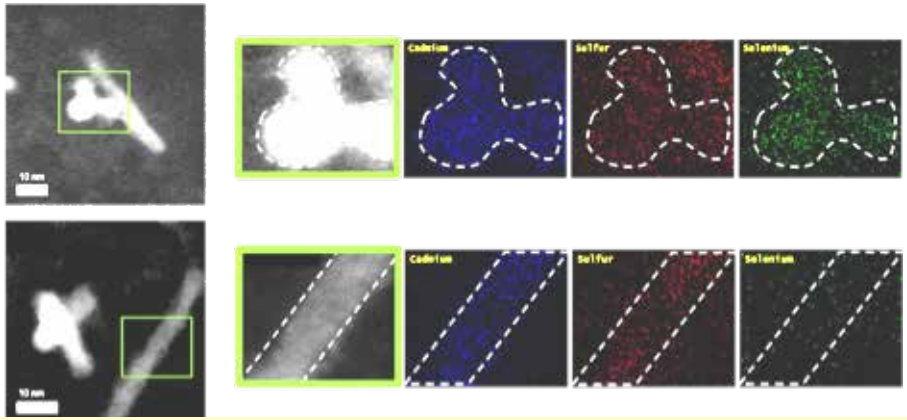

Jill M. Cleveland, Tory A. Welsch, D. Bruce Chase, and Matthew F. Doty, Univ. of Delaware. Work performed at MANTH.

ACS Appl. Opt. Mater. 2023, 1, 4, 810–824.

National Research Priority: DoD Critical Technology Area–Advanced Materials

Magnetic Property Can Manipulate Light in 2D Semiconductor Materials

- MANTH researchers and colleagues have discovered a magnetic property in antiferromagnetic materials that allows for the manipulation of light on the nanoscale, and that links the semiconductor material to magnetism, a gap that scientists have been trying to bridge for decades.
- The 2D material used in this study, $FePS_3$, has unique optical properties that depend on the alignment of its electron spin.
- By applying an external magnetic field to this antiferromagnetic 2D semiconductor, its optical properties can be altered.
- MANTH researcher Deep Jariwala says “Having made the link between magnetism and light manipulation, we are entering into the field of ‘magnetophotonics’.

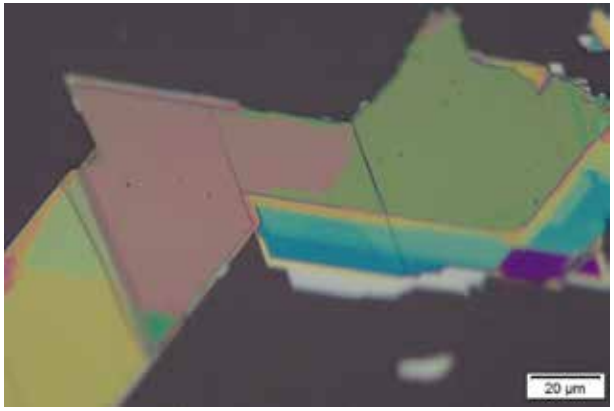

Zhang, H., Ni, Z., Stevens, C.E. et al., U Penn Engineering and Physic, Air Force Research Laboratory, and Kenyon College. Work performed at MANTH.

Nat. Photon. 16, 311–317 (2022).

National Research Priority: NSF–Quantum Leap

Cryo-EM Elucidates Structures of Actin Filaments

- Actin is the most abundant protein in the cytoplasm of most eukaryotic cells. and plays an essential role in multiple cellular functions
- Actin functions in cells as a self-polymerizing filament, both in muscle sarcomeres and in non-muscle cells.
  Capping proteins slow the addition or loss of actin monomers at the ends and are known as Tmod and CapZ.
- The detailed structure of these capping proteins was previously unknown so the MANTH Cryo-EM was employed to further understand these capping mechanisms.

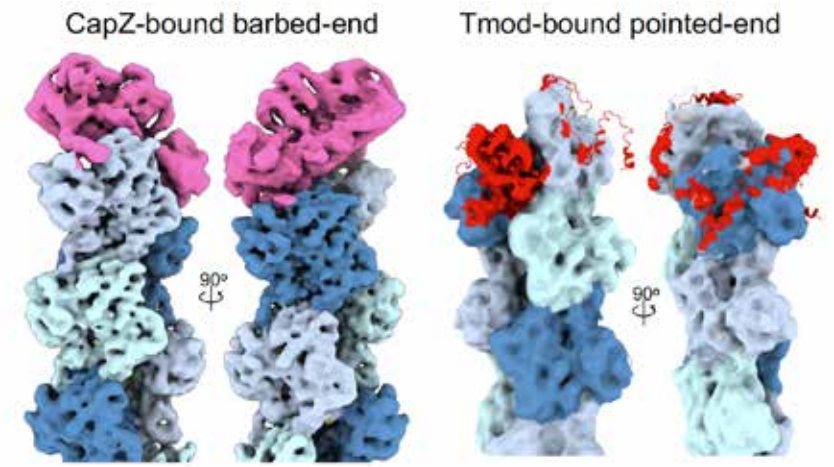

This work was conducted at the UPenn Electron Microscopy Research Labs (EMRL), the Beckman Center for Cryo-EM at the Singh Center, and the Biochemistry Department computing cluster.

This work was supported by NIH R01 GM073791 and a Blavatnik Family Fellowship.

National Research Priority: NSF–Understanding the Rules of Life

Small Company Research in Life Sciences and Medicine

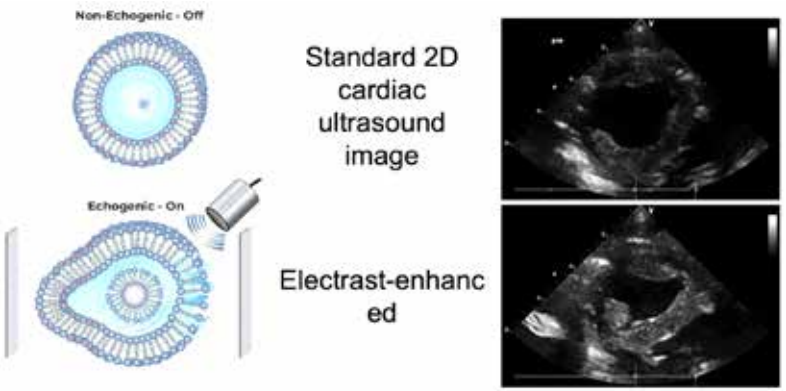

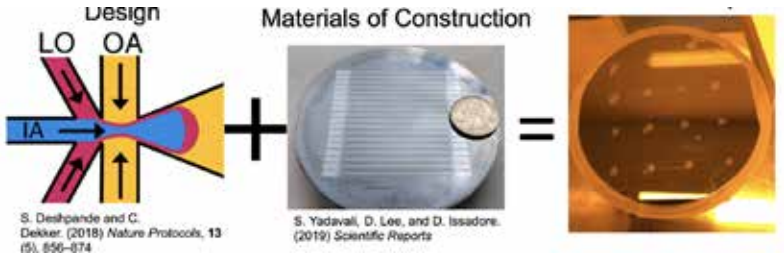

- Transthoracic Echocardiography (TTE) is cost effective, convenient, and safe to diagnose and monitor heart disease. Unfortunately, 20% - 25% of the 35 million TTE exams performed in the U.S. each year are inconclusive.
- Sonnest has developed Electrast, an electrically sensitive ultrasound enhancing agent (UEA), that allows clinicians to evaluate the function, of the heart quickly and cost-effectively at the point of care.
- Sonnest has developed a silicon/glass microfluidic chip for producing double emulsions that transition spontaneously into the desired structure, 1-5 µm liposomes, offering precise control over encapsulation efficiency, particle size, and morphology, leading to increased performance and stability of Electrast.

This work was partially supported by the DARPA QUIVER program under grant number HR0011-20-C-0098. This material is based on work supported by the NSF Graduate Research Fellowship.

National Research Priority: NSF–Understanding the Rules of Life

Midwest Nanotechnology Infrastructure Corridor (MiNIC)

National Nanotechnology Coordinated Infrastructure

Configurational Magnetic States in Mesoscale Square Permalloy Particles

This work was performed by members of Costanzi group at Carlton College, a small Liberal Arts College in southern Minnesota. In this work, the researchers used the EBL, sputter deposition and ion mill systems in the MNC to detect the magnetization configuration in individual magnetic nanoparticles. Magnetization configuration in magnetically soft particles is highly contingent on the shape, size, and symmetry of the particle. They performed experiments which show that edge roughness may cause the “buckle configuration” to persist at smaller sizes than predicted, and that S-state configurations are more stable than in simulation due to the slight symmetry breaking caused by edge roughness.

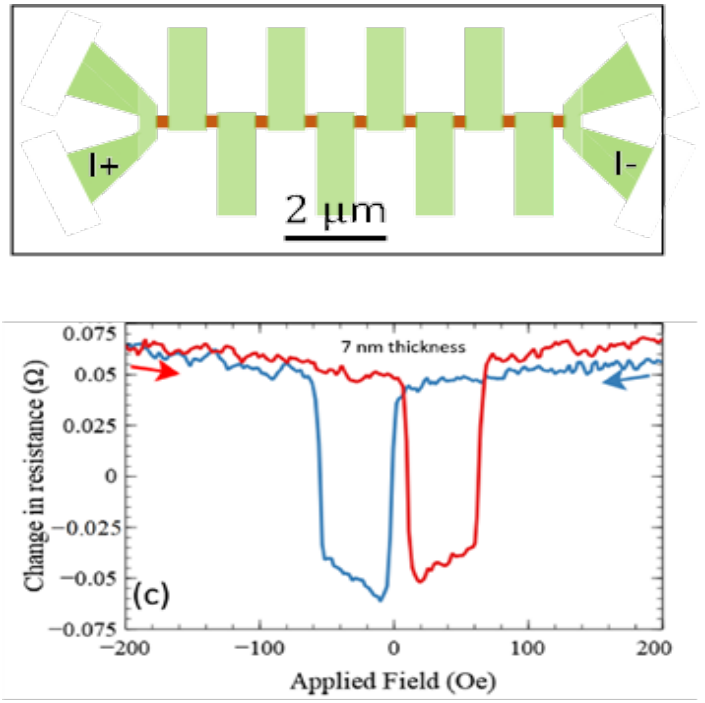

Top: Cartoon of fabricated sample geometry. Bottom: Forward and reverse sweep of magnetoresistance data for particles 175 nm on a side, corresponding to a buckle configuration.

A. Cho, S. Weeden, G. Dairaghi, D. Palenova, and B. N. Costanzi, Carlton College. Work performed at MiNIC.

Appl. Phys. Lett. **121**, 182406 (2022).

National Research Priority: DoD Critical Technology Area–Advanced Materials

National Nanotechnology Coordinated Infrastructure

MiNIC
The Midwest Nano Infrastructure Corridor

Achieving Near-Perfect Light Absorption in 2D Materials

In this project, a unique feature of 2D transition metal dichalcogenide (TMDC) materials called “band nesting” is used to demonstrate near-perfect light absorption using only two or three uniform atomic layers of these materials. The key innovation in this design, verified using theoretical calculations, is to stack monolayer TMDCs in such a way as to minimize their interlayer coupling, thus preserving their strong band nesting properties. Both twisting the layers at a precise angle or using a graphene interlayer was shown to suppress this coupling. The effect was enhanced by the use of a Salsbury screen reflector on the bottom of these layers. Through this strategy, absorption as high as 95% was demonstrated. This work was a collaboration between the Koester and Low groups at the University of Minnesota, and the Hinkle group at the University of Notre Dame.

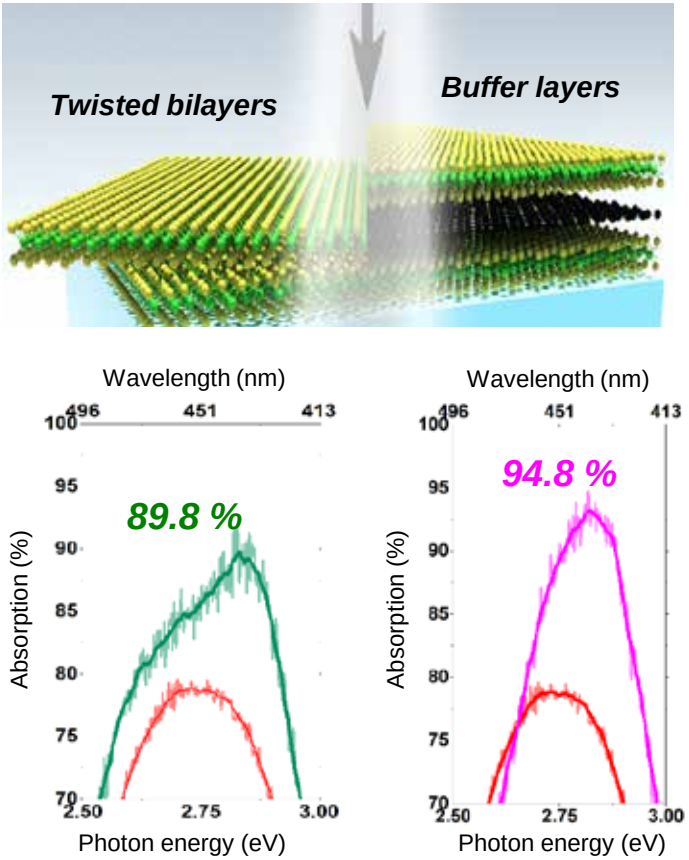

Top: Diagram showing twisted bilayer TMDCs and bilayers with a graphene buffer. Bottom: Demonstration of near-perfect light absorption.

S. Lee, D. Seo, S. H. Park, N. Izquierdo, E. H. Lee, R. Younas, G. Zhou, M. Palei, A. J. Hoffman, M. S. Jang, C. L. Hinkle, S. J. Koester, and T. Low, Univ. Minnesota. Work performed at MiNIC.

This work was supported by NSF Award DMR-1921629. *Nat. Commun*. **14**, 3889 (2023).

National Research Priority: NSF–Quantum Leap

National Nanotechnology Coordinated Infrastructure

MiNIC
The Midwest Nano Infrastructure Corridor

Optical Control of Neuronal Activities with Photo-Switchable Nanovesicles

Precise modulation of neuronal activity by neuroactive molecules is essential for understanding brain circuits and behavior. However, tools for highly controllable molecular release are lacking. In this work, led by the Zhenpeng Qin group at UT Dallas, MiNIC facilities were used to develop and characterize photoswitchable nanovesicles for neuromodulation applications. The nanvescicles were based on reversible photoisomerization of azobenzene-containing phosphatidylcholine (azo-PC). Irradiation with 365-nm light triggers the trans-to-cis isomerization of azo-PC, resulting in a disordered lipid bilayer with decreased thickness and cargo release. Irradiation with 455-nm light induces reverse isomerization and switches the release off. Real-time fluorescence imaging shows controllable and repeatable cargo release within seconds. The researchers demonstrated that SKF-81297, a dopamine D1-receptor agonist, can be repeatedly released to activate cultures of primary striatal neurons. This technology shows promise for precise optical control over the molecular release and can be a valuable tool for molecular neuroscience studies.

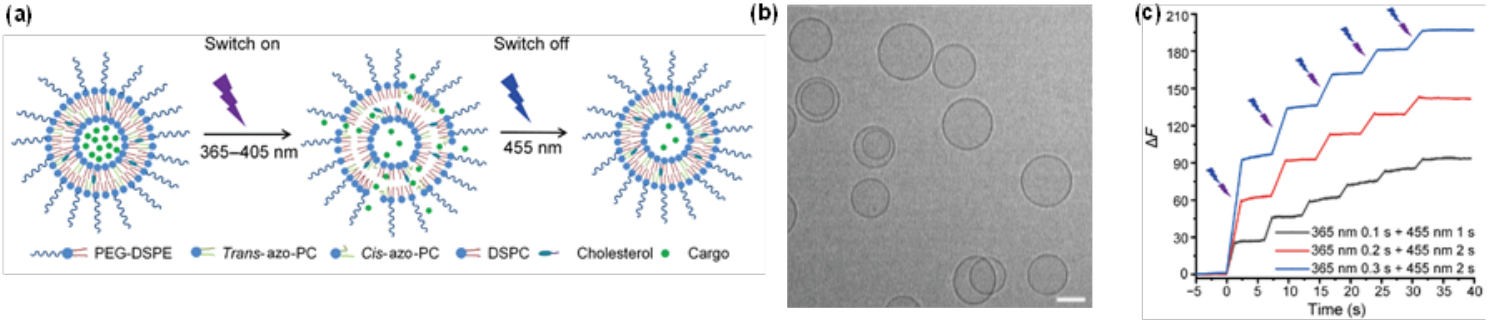

(a) Cartoon of reversible photoswitching isomerization process. (b) Cryo-TEM images of nanovesicles. (c) Real-time fluorescence imaging showing controllable cargo release

H. Xiong, K. A. Alberto, J. Youn, J. Taura, J. Morstein, X. Li, Y. Wang, D. Trauner, P. A. Slesinger, S. O. Nielsen, and Z. Qin. Work performed at MiNIC.

Nano Res. **16**, 1033-1041 (2023).

National Research Priority: NSF–Understanding the Rules of Life

National Nanotechnology Coordinated Infrastructure

MiNIC
The Midwest Nano Infrastructure Corridor

Surprising Size-Independent Swimming Speed of Peritrichous Bacteria

In this international collaboration between researchers at U Minnesota, U Cincinnati, and researchers in S. Korea and the UK, the team showed that the general positive size-speed correlation of swimming objects may not hold at microscopic scales for bacteria, where viscous dissipation overwhelms inertia in their swimming. By combining experiments, simulations, and theory, the team showed that the swimming speed of bacteria with multiple flagella is constant across the natural range of bacterial lengths, settling a long-lasting debate over the size–speed relation of bacterial swimming. This analysis could provide a useful guide for designing artificial micro-swimmers.

Cartoon showing bacteria swimming and the effect of multiflagellarity on their motion

S. Kamdar, D. Ghosh, W. Lee, M. Tătulea-Codrean, Y. Kim, S. Ghosh, Y. Kim, T. Cheepuru, E. Lauga, S. Lim, and X. Cheng. Work performed at MiNIC.

This work was supported in part by NSF Award No. CBET-2028652. *PNAS* **120**, e2310952120 (2023).

National Research Priority: NSF–Understanding the Rules of Life

National Nanotechnology Coordinated Infrastructure

MiNIC
The Midwest Nano Infrastructure Corridor

Flexible Graphene Sensor Arrays for Electrocorticography

In this collaborative effort between Neuroscience and Engineering researchers at the University of Minnesota, graphene electrocorticography (ECoG) electrode arrays conforming to the cortical surface of a mouse were used to record surface field potentials from multiple brain regions. The results were used to provide unique insights into how computations occurred in distributed brain regions to mediate behavior. The arrays were fabricated using a conductive ink produced via liquid exfoliation graphene, and then stencil-printed onto flexible polyimide substrates. The implanted ECoG devices were shown to remain fully functional for up to 180 days.

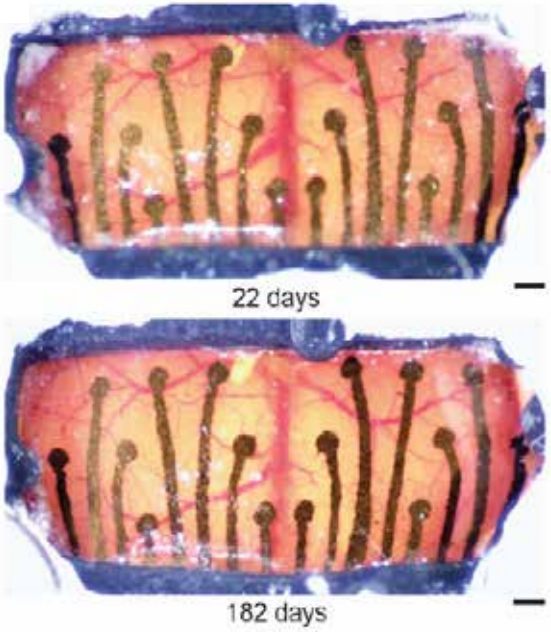

Optical microscope images of a sensor array taken at 2 timepoints after implantation onto a mouse brain.

J. Hu, R. F. Hossain, Z. S. Navabi, A. Tillery, M. Laroque, P. D. Donaldson, S. L. Swisher, and S. B. Kodandaramaiah, Univ. Minnesota. Work performed at MiNIC.

This work was supported by NIH Award No. R01NS111028 and NSF IGERT Award No. ECCS-123456. *J. Neural Eng*. **20** 016019 (2023).

National Research Priority: NSF–Understanding the Rules of Life

National Nanotechnology Coordinated Infrastructure

MiNIC
The Midwest Nano Infrastructure Corridor

Montana Nanotechnology Facility (MONT)

National Nanotechnology Coordinated Infrastructure

How DNA Structure Controls CRISPR

Andrew Santiago-Frangos, a postdoctoral fellow, is the lead author on a new paper, which appeared in the journal **Nature Structural and Molecular Biology** this September. "Structure reveals why genome folding is necessary for site-specific integration of foreign DNA into CRISPR arrays" explains how CRISPR systems record exposures to viral infections. Santiago-Frangos and team used a the new Cryo-EM Facility to take photographs of these changes in real time which helped determine the three-dimensional structure that explains how the DNA is bent and inserted into the CRISPR. This work reveals new DNA-binding surfaces that are critical for DNA folding and site-specific delivery of foreign DNA into a CRISPR array.

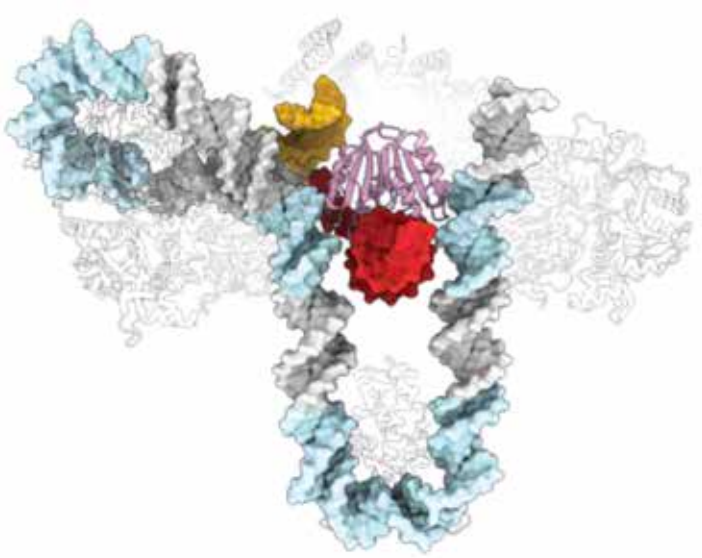

A snapshot of CRISPR enzymes making a DNA-based memory of a viral infection, the first step in a bacterial adaptive immune response. Here, a CRISPR enzyme pastes a fragment of viral DNA (red) into single spot in the bacterial genome called a CRISPR repeat sequence (yellow). CRISPR and additional bacterial proteins recognize extra DNA sequences (light blue) to fold the bacterial genome into a special shape (a U-bend and a loop), that specify this position in the genome.

Andrew Santiago-Frangos, et al, Montana State University. Work performed at Montana State University, Cryo-EM Facility ((NSF 1828765 and the M.J. Murdock Charitable Trust).

Funding provided by NIH 1K99GM147842. *Nature Structural & Molecular Biology 2023 Vol. 30 Issue 11*

National Research Priority: NSF–Understanding the Rules of Life and NAE Grand Challenge–Engineer Better Medicines

Forensic Analysis: 1929 Pumiceous Concrete Nativity Chapel, Flagstaff, Arizona

Nativity of Blessed Virgin Mary Chapel was constructed in 1929 with innovative, portland cement concrete that used local siliceous volcanic pumice as aggregate. The basement concrete remains highly intact. However, the precast pumi-ceous concrete blocks of the belltower and façade, which have pink lime - sand plaster exteriors, are cracked and disaggregated. SEM-EDS and XRD analyses reveal that damage comes from per-vasive fracture derived from freeze-thaw actions. Remarkably, there are few traces of chemical attack and decay. Instead, calcite precipitation partially repairs cracks and sulfur-bearing phases (derived from gypsum in cement) are confined to pores. The analyses inform selection of resilient cast stone materials for the belltower repair as part of a current restoration project. They also provide valuable guideposts for effective use of volcanic pozzolans in environmentally-friendly concretes.

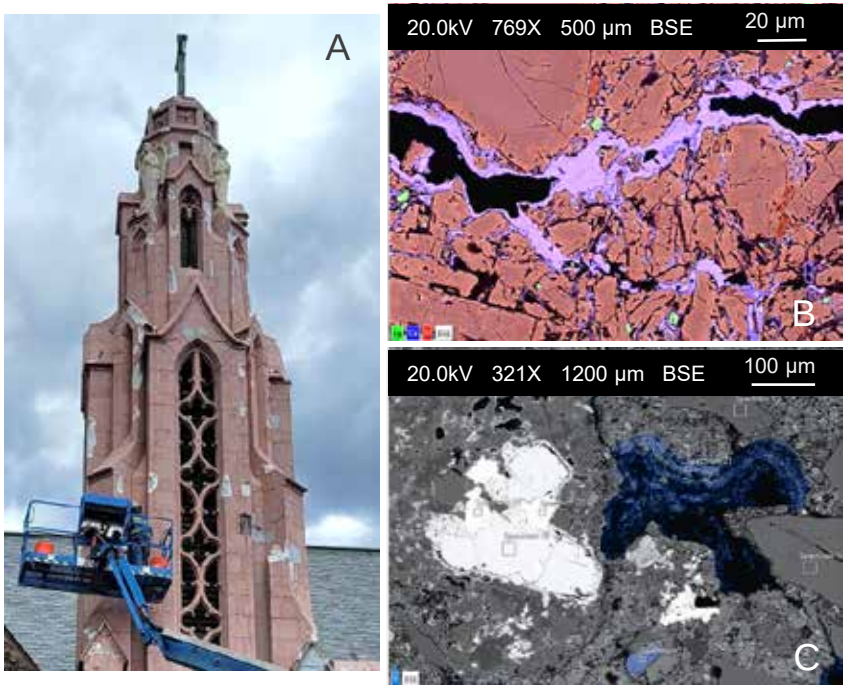

Precast pumiceous concrete. A. Damaged bell-tower, 2022. B. Calcite precipitation (purple) partially seals fracture in feldspar crystal. C. Sulfur mobilization (blue) is segregated in pores, as ettringite. Even so, the pumiceous pozzolan could not mitigate damage from freeze-thaw processes in the porous concrete.

Marie D. Jackson, Dept. of Geology and Geophysics, University of Utah. Work performed at Montana State University, Imaging and Chemical Analysis Laboratory (ICAL).

National Research Priority: NAE Grand Challenge–Restore and Improve Urban Infrastructure

National Nanotechnology Coordinated Infrastructure

MONTANA STATE UNIVERSITY | Montana Nanotechnology Facility

Parasite survey on wolverine hair with FE-SEM

Our research focuses on monitoring rare and elusive carnivores, including wolverine and Canada lynx, in the mountains of Montana. A primary objective of the work is tracking the general health of individual animals.

Hair samples are recovered from animals visiting the monitoring stations in addition to photographs taken by remote cameras. After observing hair loss on multiple wolverines, we brought a collection of hair samples to ICAL from infected wolverines to compare with healthy wolverines. Upon investigation in the FE-SEM, egg cases resembling that of a hair clasping mite were found on infected samples. Analysis of the egg cases is in progress to identify the species and inform researchers of the health effects of different parasites on wolverines.

Wolverine (left pane) showing a bald spot on the lower back (boxed in red) and secondary electron image of a mite egg-case (right pane) on a hair recovered from that wolverine. The SEM image was acquired by the Zeiss Supra 55VP FE-SEM in ICAL .

B.H. Davis and K.C. Baughan, Wild Ideas, LLC. Work performed at Montana State University, Image and Chemical Analysis Laboratory

Funded by MPG Ranch, Florence, MT

Mineral Cements in Ancient Roman Concretes

Roman architectural and marine concretes, fabricated with hydrated lime-volcanic tephra mortar (*materia*) and coarse rock aggregates (*caementa*), provide invaluable guideposts for new concepts of self-sustaining, self-reinforcing and environmentally-friendly concrete infrastructure.

The long-term reactivity of volcanic aggregates with fluids in the concrete produces calcium-aluminum-silicate-hydrate crystals (strätlingite, Al-tobermorite) that toughen interfacial zones, obstruct the propagation of microcracks and increase the ductility of the concrete.

Our Roman analog concrete research (funded, in part, through DOE ARPA-E and USACE-EWN) employs reactive aggregates to create silicate cementing microstructures and durable mechanical resilience, similar to the ancient concretes.

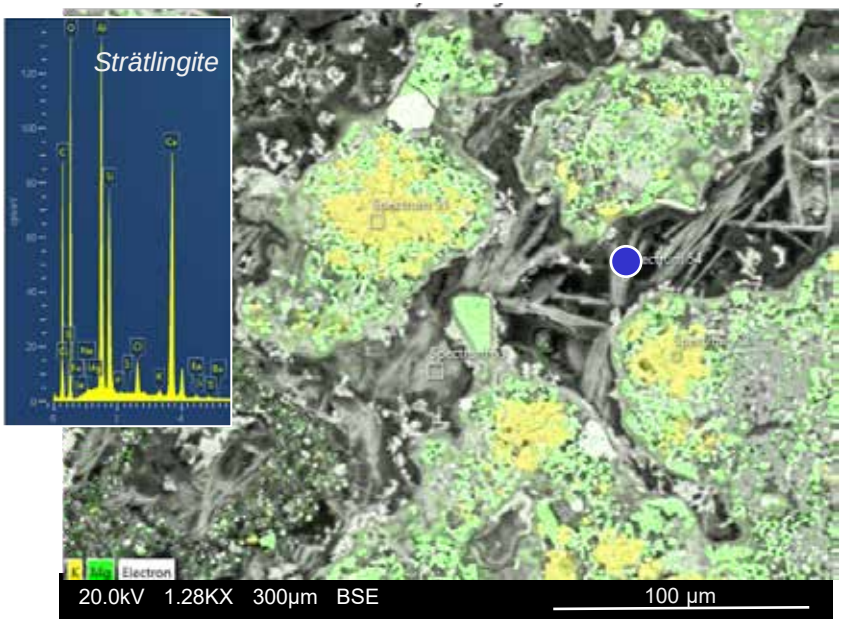

Platey strätlingite ($Ca_2Al_2(SiO_2))(OH)_{10}•2.5(H_2O)$) crystals reinforce the mortar of Markets of Trajan (95 CE) concrete, Rome. Reactive volcanic aggregate contains leucite (yellow) and clinopyroxene (green) crystals and relict volcanic glass.

Marie D. Jackson, Department of Geology and Geophysics, University of Utah. Work performed at Montana State University, Imaging and Chemical Analysis Laboratory (ICAL).

Quantifying the rate copper leaches from a copper drinking vessel into simulated beverages under conditions of consumer use

Carroll College Chemistryundergraduate researchers demonstrated that copper leaches into a Moscow Mule cocktail from the copper mug in which it is held at a rate that exceeds the EPA limit of 1.3 ppm in just over 27 minutes. The article provides insight into the rate, total amount, and the chemical mechanism behind copper leaching from a copper surface into foodstuffs. The copper leaching was found to be dependent on the pH of the solution and the presence of dissolved oxygen.

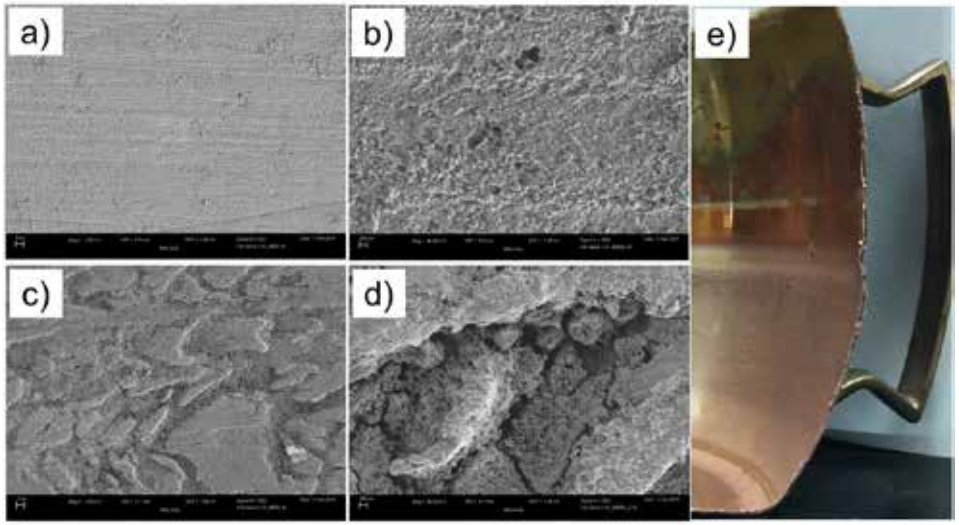

Scanning electron microscope (SEM) images of copper mug surface with (a,b) limited contact with the Moscow Mule cocktail: a) 2 µm and b) 200 nm scale bar; (c,d) after exposure to 26 Moscow Mule cocktails for a cumulative exposure time of 75 h: c) 2 µm and d) 200 nm scale bar. e) Cross-section digital photograph of the copper mug; upper half of the mug was limited contact (a,b) and the lower half of the mug was exposed for 75 h cumulative (c,d).

Pharr, C.R.; Rowley, J.G.; Weber, M.*; Adams, D.*; Gray, I.*; Hanson, E.*; Hilborn, G.*; Kong, V.*; Patello, E.*; Schmidt, S.*; Shulga, D.*, Carroll College, Helena MT. * indicates undergraduate co-author. Work performed at ICAL.

J Environ Health. 2022. 84(6), 8-13.

National Research Priority: Environmental Health and Safety

Mass Spectrometry compatible electronic Immunosensors

Over a decade of mass spectrometry profiling data has determined that integrating abundance levels of multiple biomarkers simultaneously increases the predictive ability of algorithms for early identification of disease. This is important, because early disease identification leads to more successful treatment outcomes and lower medical burden. Despite the value, full realization of the benefits of this knowledge remains underutilized. Here, we present a breakthrough platform for the development of a multi-target metabolic monitoring sensor array, that will enable real-time remote detection of multiple biomarkers, using a low-cost, digitally integrated technology. The technology described, is in development in the Montana Microfabrication Facility and Mass Spectrometry Facility of Montana State University.

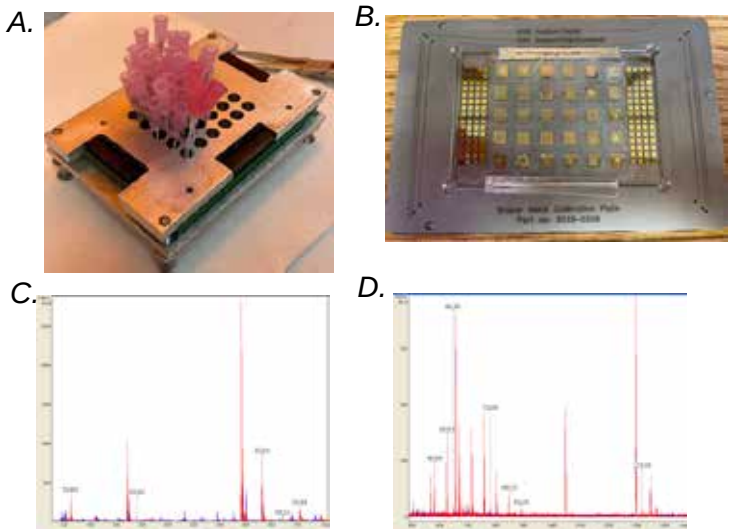

MALDI mass spectra show antibody binding to protein coated electronic surface. A)Microfluidics assembly, B)IDE-MS removed from assembly. C) Mass spectra from Negative controls, and D) Positive controls show peptides associated with antibody surface binding.

Katelyn J. Langguth, Tami R. Peters, Seth Pincus, Joshua Heinemann, Montana State University. Work performed at Montana State University, Mass Spectrometry Facility.

Support from National Institute of Health P20GM103474.

National Research Priority: NSF–Understanding the Rules of Life and Harnessing the Data Revolution

National Nanotechnology Coordinated Infrastructure

MONTANA STATE UNIVERSITY | Montana Nanotechnology Facility

CryoFE-SEM of Lab-Grown Gastric Mucus

Infection with *Helicobacter pylori* can cause gastric inflammation, ulcers, and stomach cancer. To prevent and treat *H. pylori*-related disease, it is crucial to understand the role of the stomach's first line of defense against *H. pylori* pathogenesis: the gastric mucus layer. For many research groups, access to human samples is a critical barrier to obtaining native human mucus[7]. Thus, there is a great need for *in vitro* models for the gastric mucus layer that are physiologically relevant and translatable back to native mucus.

We have recently developed a method for the *in vitro* production of gastric mucus using organoid-derived epithelial monolayers. We have harvested this lab-grown mucus for structural characterization–an important first step in understanding its functionality as a protective barrier. CryoFE-SEM of both native and lab-grown mucus revealed similar cross-sections with honeycomb-like structure as well as pore sizes consistent with those in other mucus literature.

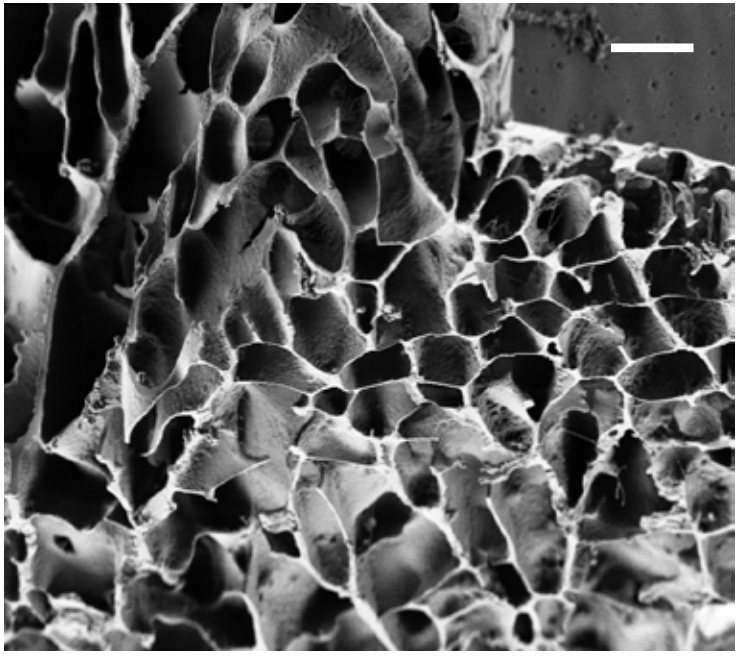

Cross-section of frozen lab-grown mucus (scale bar = 10 µm).

Lyon, K., Davis, B., Zacher, S., Roner, J., Bimczok, D. Work performed at Montana State University, Imaging and Chemical Analysis Laboratory (ICAL).

Support from NSF ECCS-2025391.

National Research Priority: NSF–Understanding the Rules of Life

MEMS Transmissive Beam Scanner

This work concentrates on developing MEMS platform for a transmissive beam scanner. The transmissive beam scanner works by tilting a polarizing wire grid. The tilting platform needs to have an angular deflection of at least +/- 20 ° and a resonant frequency of approximately 1 kHz. Additionally, it needs an operating voltage of less than 400 V and a plate diameter of around 4 mm.

The device is a resonant electrostatic design where electrostatic force is applied between the paddle and handle wafer. A spring design with a stiff outer spring and a flexible inner spring causes the motion of the plate with the grating structure to be amplified. The device is fabricated from a silicon on insulator substrate with the 2 µm thick buried oxide layer providing the insulation and mechanical gap between handle wafer and the mobile device layer.

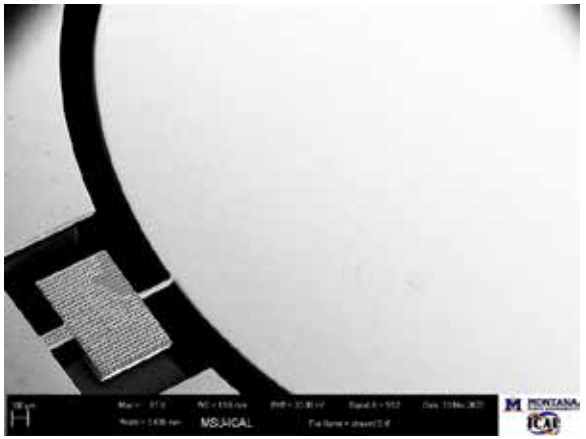

Electron microscope image of transmissive beam scanner

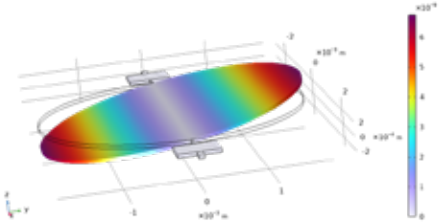

Finite element model of transmissive beam scanner

Samantha “Hunter” Hampshire, Andrew Oliver, and David Dickensheets, Montana State University. Work performed at Montana State University, MMF and ICAL Photomasks were built at the Minnesota Nano Center.

This material (AFRL-2023-4410) is based on research sponsored by Air Force Research Lab under agreement number FA8650-21-1-1176.

National Research Priority: NAE Grand Challenge–Engineer the Tools of Scientific Discovery

Viscoelastic characterization of chondrocyte cells using microfluidics

It is well demonstrated that mechanical properties of cells change when they become infected with diseases such as cancer or osteoarthritis, and these changes can be used as disease biomarkers. Mechanical biomarkers are label-free, so they don't require slow and costly sample labeling and therefore are advantageous to more traditional biochemical biomarkers. However, the existence of a biomarker is not necessarily useful unless it can be exploited in a timely, cost-effective manner. While traditional methods for mechanically characterizing cells are well established, they all suffer a major drawback: low throughput.

The overall goal of this project is to develop a microfluidics-based platform capable of mechanically characterizing viscoelastic properties, namely viscoelastic recovery time, of single chondrocyte cells with the potential of parallel cell measurement for high-throughput instrumentation.

In this work, single primary-chondrocyte cells are compressed between two glass plates. The applied strain is rapidly removed, and the chondrocyte cell is imaged with confocal laser scanning microscopy (CLSM) to image the recovery to its relaxed, spherical shape. Viscoelastic recovery of chondrocyte cells is clearly observed, however fitting these data to a mechanical model is still in progress.

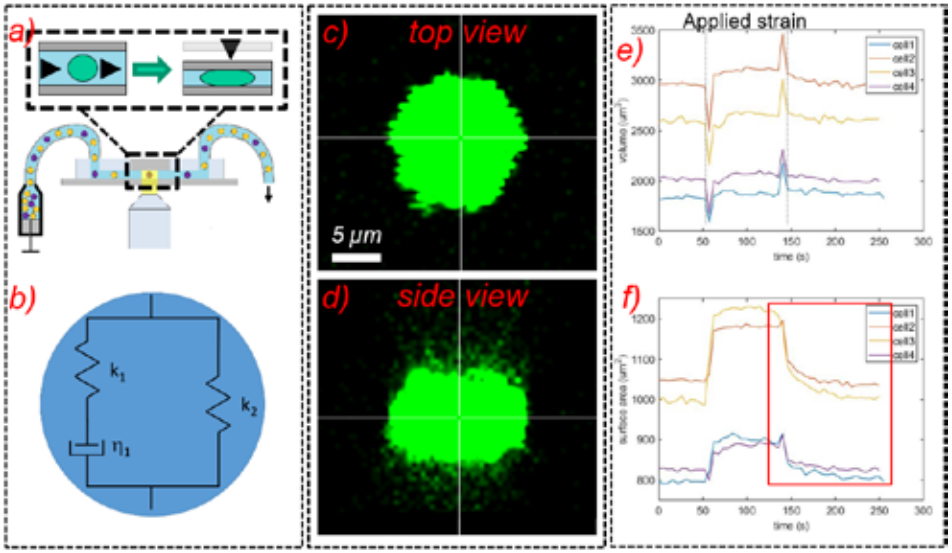

a) Working principle of the microfluidic device. Cells are imaged with CLSM as they are compressed and released by two glass plates. b) Linear-viscoelastic mechanical model for a chondrocyte cell. c) and d) CLSM images of top and side views of a compressed cell, respectively. e) Volume of four cells undergoing compression and relaxation. Importantly, the volume of cells remains nearly constant during compression, excluding the sharp spikes which represent the glass plates moving during the z-stack of the CLSM data. f) Surface area of cells changes dramatically during compressing and shows a roughly 100 second viscoelastic-recovery time (red box). Fitting these data to a mechanical model is in progress.

Michael Neubauer, Ron June, and Stephan Warnat, Montana State University. Work performed at Montana State University, Center for Biofilm Engineering.

Work supported by NIH R01 AR073964 and NSF CMMI-2140127.

National Research Priority: NSF–Understanding the Rules of Life and NAE Grand Challenge–Engineer Better Medicines

National Nanotechnology Coordinated Infrastructure

MONTANA STATE UNIVERSITY | Montana Nanotechnology Facility

Phosphorus-Doped Silicon Nanoparticle Anodes

Silicon is a promising anode material owing to its high theoretical capacity (3579 mAh g^{-1}); however, Si faces severe volume expansion (~300%) and thermal runoff during (de)lithiation. This work aims to achieve electrochemical and thermal stabilization of silicon nanoparticles via chemical doping. Phosphorus is selected as the dopant of choice owing to its large solubility in silicon (~3 at%). However, under high doping concentrations (>1 at%), phosphorus catalyzes the grain coarsening of silicon nanoparticles as evidenced by SEM. To control for the effects of silicon particle size and crystallinity we focused on doping with low phosphorus concentrations (~0.1 at%). This work reveals that phosphorus-doped silicon controlled conditions leads to both thermal and electrochemical stability.

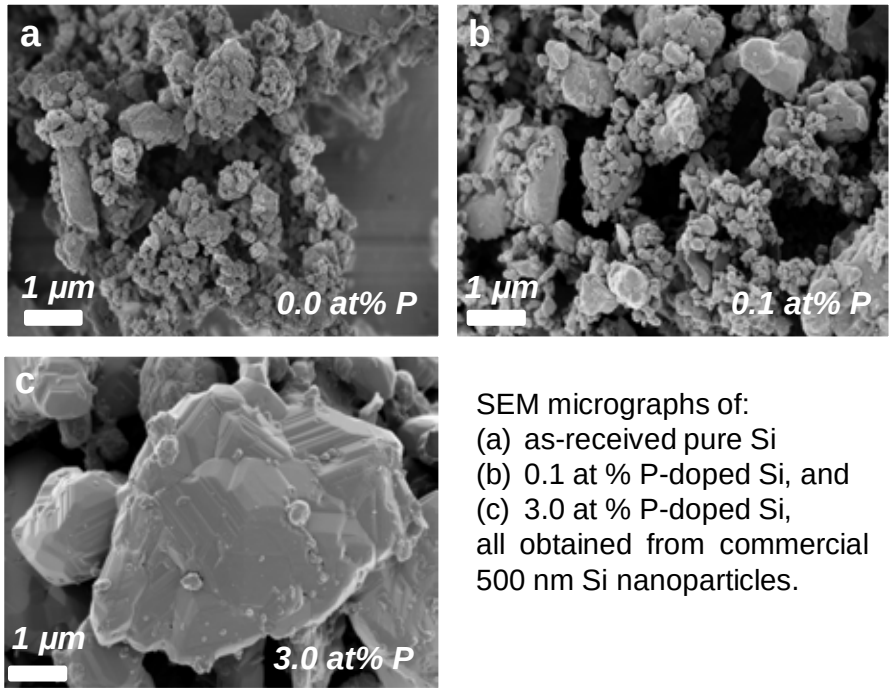

SEM micrographs of:
(a) as-received pure Si
(b) 0.1 at % P-doped Si, and
(c) 3.0 at % P-doped Si,
all obtained from commercial 500 nm Si nanoparticles.

Isabelle P. Gordon, Wei Xu, Sophia Randak, Richard T. Jow, and Nicholas P. Stadie. This research was performed at Montana State University/Stadie Group Laboratories. ICAL & MMF facilities.

This work was supported by a cooperative agreement with the Army Research Laboratory (ARL). *Chem. Mater.* 2023, 35, 2, 549–557.

National Research Priority: NAE Grand Challenge–Make Solar Energy Economical

National Nanotechnology Coordinated Infrastructure

MONTANA STATE UNIVERSITY | Montana Nanotechnology Facility

Nanotechnology Collaborative Infrastructure Southwest (NCI-SW)

National Nanotechnology Coordinated Infrastructure

Porcine Skin Electrosprayed with Silver Nanoparticles Prevents Infections in Deep Burns

Extensive burns represent a significant challenge in biomedicine due to major skin barrier loss. The functionalization of skin grafts with nanostructured antibacterial agents proposes a fast and accessible application to restore barrier function and prevent localized bacterial contamination. The objective of this work was to functionalize skin grafts by electrospray deposition with silver nano-particles and to evaluate its antibiofilm and cytotoxic effects on human fibroblasts. Antibacterial activity combined with excellent bio-compatibility makes this biomaterial a candidate for antibacterial protection by inhibiting bacterial biofilms in deep burns during early stages of development.

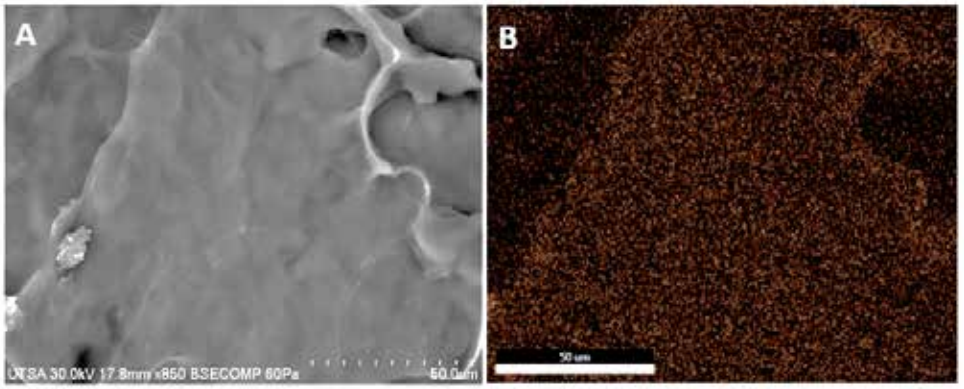

Radiosterilized porcine skin dermis shows a homogeneous distribution of silver nanoparticles. (A) SEM image of the dermis; (B) EDS mapping of the dermis, orange dots represent the distribution of Ag.

Horacio Bach, Department of Medicine, University of British Columbia, Vancouver. Work performed at NCI-SW.

Int. J. Mol. Sci., vol. 23, article 13910.

National Research Priority: NAE Grand Challenge–Engineer Better Medicines

National Nanotechnology Coordinated Infrastructure

NCI Southwest

Erosion of Olivine via Atomic Force Microscopy in Mars Relevant Soils

In this project, olivine is treated as an indicator of past environmental conditions both for in-situ studies on Mars and analysis of returned samples from Mars. Samples are treated to replicate Mars conditions and studied using microscopy and spectroscopy techniques. AFM proved especially important to investigate sample erosion by quantifying variances in the flat-bottomed pit depth of samples. The nature of obersed pitting indicates a potential path for dissolution along grain boundaries encouraged by access of fluid to the olivine surfaces along grain boundaries. AFM proved effective at qualitatively and quantitatively distinguishing between samples in a meaningful manner in which it is possible to assess the importance of climatic dissolution of olivine samples.

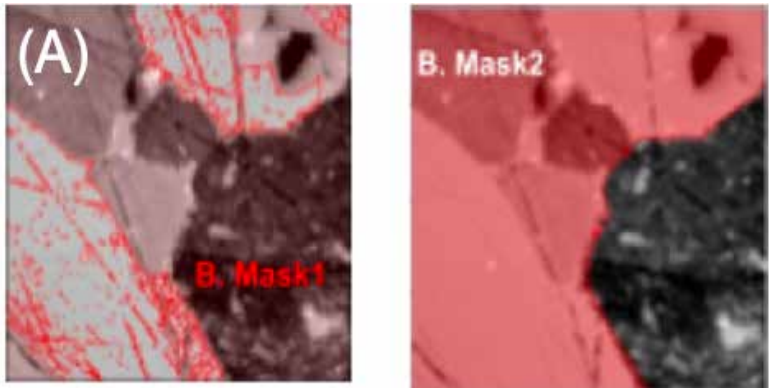

(A) Analysis to quantitatively assess pitting due to erosion of Olivine samples. Red represents Planefit XY, 1 masks to evaluate surface depths and roughness.

Elisabeth Hausrath, Dept. Of Geoscience, University of Nevada, Las Vegas. Work performed at NCI-SW

Geological Society of America CONNECTS, Paper No. 83-7, 9-12 October, 2022, Denver, CO

National Research Priority: NSF–Windows on the Universe

Silver Nanoparticles in Point-of-use Paper Water Filters During Use and After Disposal

It is well known that drinking polluted water can lead to a variety of bacterial diseases, including cholera, dysentery, and typhoid fever. Silver in the dissolved (Ag+) and nanoparticulate (Ag NPs) forms exhibits toxic effects towards myriad single-cell and multicellular organisms. Silver ions disrupt cell homeostasis by interacting with DNA to prevent accurate replication and by denaturing proteins through interaction with thiol groups. Silver NPs have been employed in point-of-use (POU) drinking water treatment devices and shown high bacterial disinfection efficiency. However, beyond showing that such technologies are effective at disinfecting bacteria, it is important to understand A) potential human health effects of the silver itself and B) environmental exposure of silver nanoparticle-containing materials towards end-of-life.

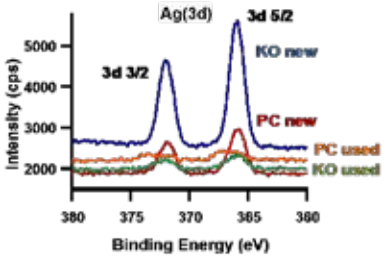

A single Ag peak falls within the BE range of silver oxides/halides for all samples

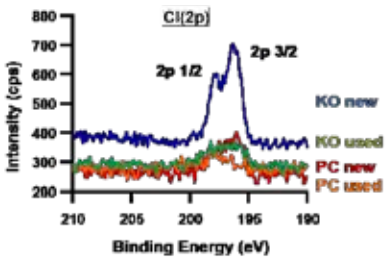

Chlorine is present in all samples and at higher initial concentration

Spectroscopic analysis confirms that the physiochemical characteristics of Ag NPs did not significantly change after use except in that the surface oxide layer (e.g., AgO) partially dissolved into filtered water, causing a reduction in overall Ag mass.

Folia Materials is an NSF SBIR funded company producing POU paper water filters coated with silver nanoparticles. Our results suggest that POU paper water filters containing silver NPs pose limited adverse health or environmental effects and may inform mechanisms of Ag NP toxicity and of how Ag+ ions are released from Ag NPs in water treatment devices.

Teri Dankovich, Folia Water Inc., Boston, MA. Work performed at NCI-SW.

National Research Priority: NAE Grand Challenge–Provide Access to Clean Water

GaN-on-GaN p-i-n diodes with avalanche capability enabled by eliminating surface leakage

Traditional mesa terminations require precise angle design to reduce the electric field at the edge and surface treatment to reduce etch damage. Otherwise, the device usually suffers a premature breakdown. This work proposes the use of easy-to-implement hydrogen plasma treatment to solve the premature breakdown caused by mesa and demonstrates the avalanche capability in GaN-on-GaN p-i-n diodes. The breakdown electric field when the avalanche occurred was □2.3 MV/cm at room temperature for a GaN drift layer with a doping concentration of ~7x1015 cm-3, which is consistent with the theoretical value. The temperature coefficient of the avalanche breakdown voltage of the devices was 4.64–4.85x10-4 K-1. This work shows a simple and effective approach to achieve avalanche capability in vertical GaN power devices, which can serve as an important reference for the future development of efficient and robust GaN power electronics.

Yuji Zhao, Department of ECE, Rice University.
Work performed at NCI-SW.

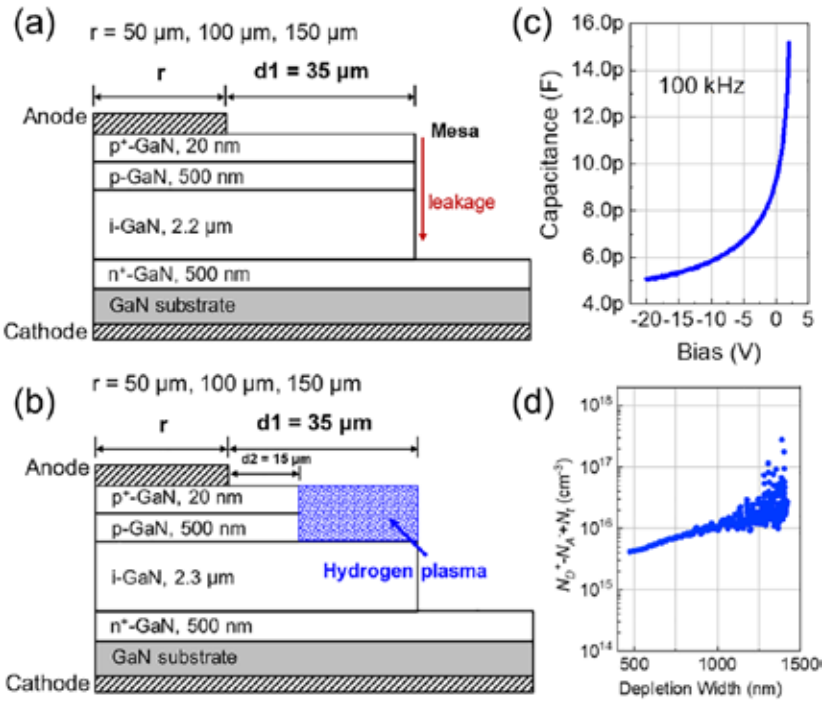

Figure (a) shows the vertical p-i-n diodes with conventional mesa edge termination (Mesa-ET). The hydrogen plasma treatment was applied to the same device on the same sample to form the combined ET (MHP-ET) consisting of the Mesa-ET and hydrogen plasma treatment, as shown in (b). Figure (c) shows the capacitance–voltage (C–V) curve of the sample, and Fig. (d) shows the doping profile in the drift layer extracted from the C–V curve.

National Research Priority: DoD Critical Technology Area–Microelectronics

National Nanotechnology Coordinated Infrastructure

NCI Southwest

Studying Sialic Acid Content in Preeclampsia Using Surface Enhanced Raman Spectroscopy

Silver nanoparticles (NPs) have previously been shown by the Yacaman team as effective enhancers of biological signatures via SERS spectroscopy , dependent upon NP factors such as morphology. Our latest study found that PE patients had higher levels of sialic acid then patients not experiencing PE and proved the efficacy of SERS via Ag NP enhancement for detecting early-stage PE, critical to preventing PE pregnancy complications and even fatal outcomes. The method proposed is effective, rapid, and cost-effective as a diagnostic tool for PE.

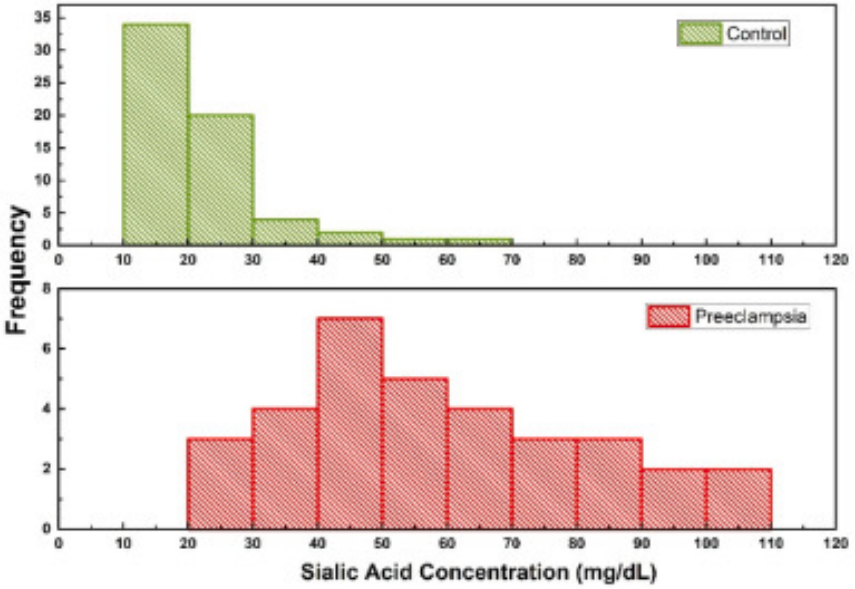

Frequency plot of sialic acid concentration in saliva for healthy (control) and PE patients via SERS.

Miguel Yacaman, Dept. of Applied Physics and Materials Science, Northern Arizona Univ. Work performed at NCI-SW.

Placenta, vol. 13, pp. 12-16, 2022..

National Research Priority: NAE Grand Challenge–Engineer Better Medicines

National Nanotechnology Coordinated Infrastructure

NCI Southwest

High Speed Graphene-Metal Infra-Red Optical Modulators

Graphene is an attractive material for all-optical modulation because of its ultrafast optical response and broad spectral coverage. We present modulator designs based on graphene-metal hybrid plasmonic metasurfaces with highly enhanced light-graphene interaction in the nanoscale hot spots at pump and probe wavelengths. We have demonstrated high-speed all-optical modulators at near and mid-infrared wavelengths (1.56 μm and above 6 μm) with significantly reduced pump fluence (1–2 orders of magnitude) and enhanced optical modulation. The proposed designs hold the promise to address the challenges in the realization of ultrafast all-optical modulators for mid-and far-infrared wavelengths.

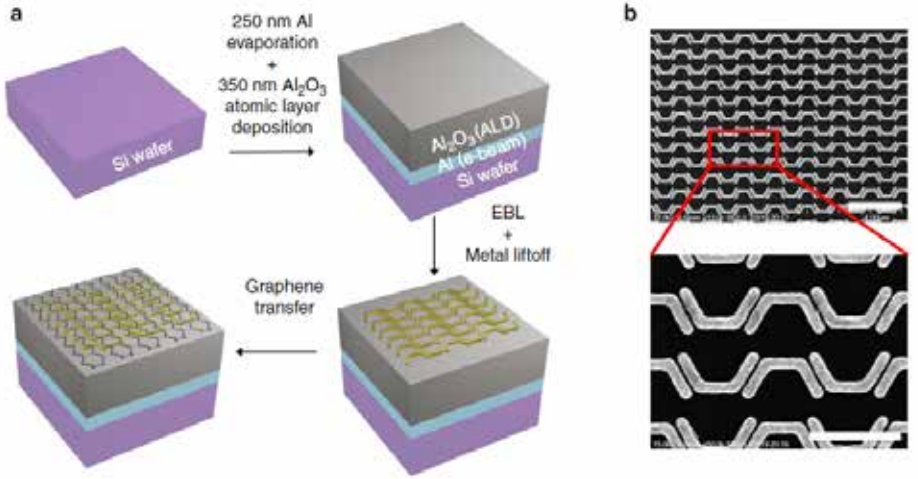

Fabrication of the graphene metasurface absorber all-optical modulator. a) Fabrication steps of the GMMA device. b) SEM images of fabricated Pi-shaped nanoantenna. The scale bars in the top and bottom panels represent 2 μm and 1 mm.

Yu Yao, School of ECEE, ASU. Work performed at NCI-SW

Light: Science & Applications, 11(1), 102.

National Research Priority: Advanced Photonics

National Nanotechnology Coordinated Infrastructure

NCI Southwest

Evaluating Ballistic Transport in n-channel FinFETs

The ballistic transport in state-of-the-art FinFETs has been investigated using a novel 3D-TCAD MonteCarlo device simulator in order to properly understand the underlying scattering mechanisms' relevance. By examining the ballisticity ratio and the percentage of carriers that cross the channel ballistically, it becomes clear that modern FinFETs have not yet reached the ballistic limit. Therefore, there is still room for progress with different devices that may go in the direction of the ballistic limit. The fraction of ballistic carriers in the devices studied is significant, reaching almost 50% for the simulated 14 nm n-FinFETs.

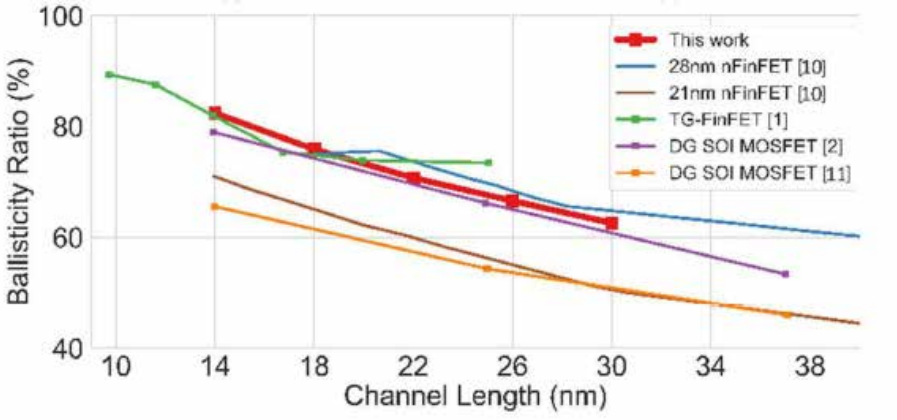

The ballisticity ratio of highly scaled FinFETs compared to other similar work from different CMOS technologies.

Dragica Vasileska, School of Electrical, Computer, and Energy Engineering, ASU. Work performed at NCI-SW.

IEEE Transactions on Nanotechnology, vol. 21, pp. 311-319 (2022).

National Research Priority: DoD Critical Technology Area–Microelectronics

Diamond p-i-n Diodes with Ultra-High Forward Current Density

A diamond Schottky PIN diode (SPIND) supporting a total current of ~1.32 A through a 50 µm wide pseudo-vertical structure demonstrates the highest reported current density to date of ~116 kA/cm^2. The diamond SPIND also provides a maximum power handling capacity of 1.85 MW/cm^2 and a low specific on-resistance R_{ON} of 0.05 mΩ.cm^2 at a forward bias of ~16 V. The SPIND diode shows excellent rectification characteristics with a current on-off ratio of ~ 6×10^{12}. We conclude that the ultimate performance limit in an ultra-wide bandgap material like diamond is the trap-free Mott-Gurney current limit and that the value of R_{ON} keeps on decreasing with increasing forward bias.

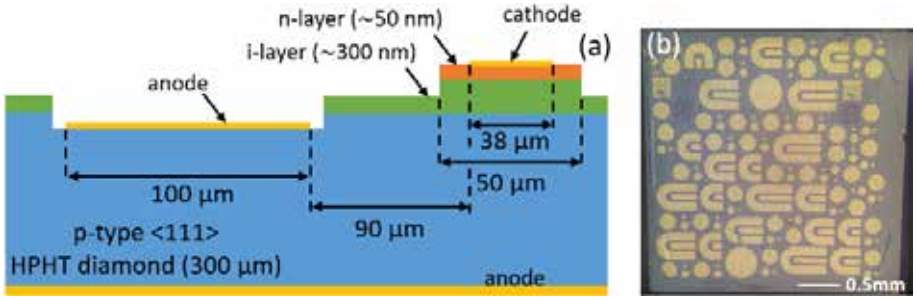

(a) Cross-section of diamond SPIN diode (b) Microscope top-view of the fabricated diamond SPIN diode sample.

Robert Nemanich, Trevor Thornton, and Stephen Goodnick, Dept. of Physics and School of ECEE, ASU. Work performed at NCI-SW.

IEEE Transactions on Electron Devices, vol. 69, no. 1, pp. 254-261, Jan. 2022,

National Research Priority: DoD Critical Technology Area–Microelectronics

National Nanotechnology Coordinated Infrastructure

NCI Southwest

Nebraska Nanoscale Facility (NNF)

National Nanotechnology Coordinated Infrastructure

Interface-Tuning of Ferroelectricity and Quadruple-Well State in $CuInP_2S_6$ via Ferroelectric Oxide

Ferroelectric van der Waals $CuInP_2S_6$ possesses intriguing quadruple-well states and negative piezoelectricity. Its technological implementation has been impeded by the relatively low Curie temperature (bulk $T_C \sim 42$ °C) and the lack of precise domain control. Here we show that $CuInP_2S_6$ can be immune to the finite size effect and exhibits enhanced ferroelectricity, piezoelectricity, and polar alignment in the ultrathin limit when it is interfaced with ferroelectric oxide $PbZr_{0.2}Ti_{0.8}O_3$ films. Piezoresponse force microscopy studies reveal that the polar domains in thin $CuInP_2S_6$ fully conform to those of the underlying $PbZr_{0.2}Ti_{0.8}O_3$, where the piezoelectric coefficient changes sign and increases sharply with reducing thickness. High temperature *in situ* domain imaging points to a significantly enhanced T_C of >200 °C for 13 nm $CuInP_2S_6$ on $PbZr_{0.2}Ti_{0.8}O_3$. Density functional theory modeling and Monte Carlo simulations show that the enhanced polar alignment and T_C can be attributed to interface-mediated structure distortion in $CuInP_2S_6$. Our study provides an effective material strategy to engineer the polar properties of $CuInP_2S_6$ for flexible nanoelectronic, optoelectronic, and mechanical applications.

Kun Wang, Du Li, Jia Wang, Yifei Hao, Hailey Anderson, Li Yang, and Xia Hong, Nebraska Center for Materials and Nanoscience (NCMN) and Dept. of Physics and Astronomy, University of Nebraska–Lincoln and Dept. of Physics, Washington Univ. in St. Louis. Work performed at Nebraska Nanoscale Facility (NNF).

This work was supported by NSF DMR-2118828, OIA-2044049, DMR-2124934. *ACS Nano* 2023, 17, 16, 15787–15795

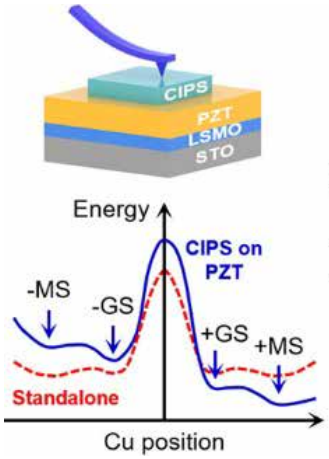

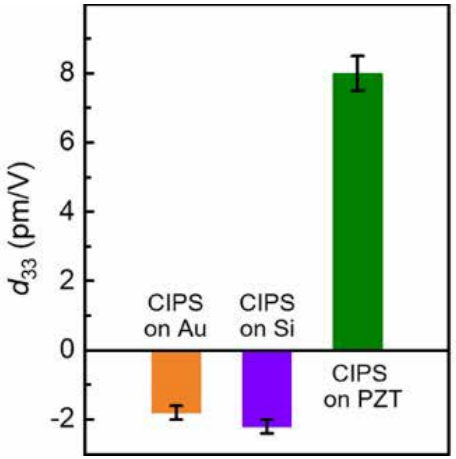

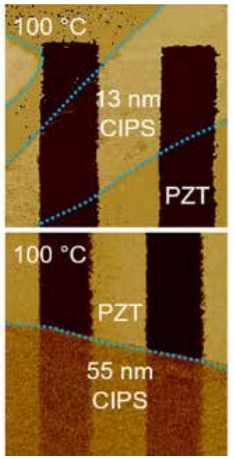

National Research Priority: NSF–Growing Convergence Research

National Nanotechnology Coordinated Infrastructure

Nebraska Nanoscale Facility

Post Deposition Interfacial Néel Temperature Tuning in Magnetoelectric B:Cr_2O_3

Boron (B) alloying transforms the magnetoelectric antiferromagnet Cr_2O_3 into a multifunctional single-phase material which enables electric field driven π/2 rotation of the Néel vector. Nonvolatile, voltage-controlled Néel vector rotation is a much-desired material property in the context of antiferromagnetic spintronics enabling ultralow power, ultrafast, nonvolatile memory, and logic device applications. To facilitate operation of B:Cr_2O_3-based devices in CMOS environments, the Néel temperature, T_N, of the functional film must be tunable to values significantly above room temperature. In this work, Binek and coworkers at NNF:NCMN show that the operation temperature for reliable, voltage-controlled Néel vector toggling, can be thermally tuned within a temperature range as wide as $\Delta T \approx 200$ K via a post-deposition annealing protocol. Magnetotransport data confirm B-accumulation and T_N increase. Neutron and XPS depth profiling map the depth dependent B-concentration.

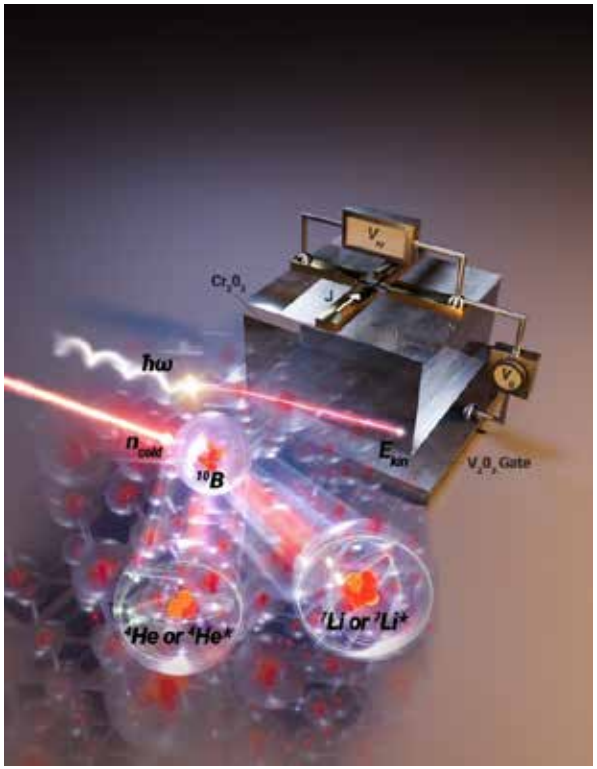

Image shows a device which utilizes an antiferromagnetic, B-doped thin film of magnetoelectric Cr2O3. Voltage applied across the film controls its Néel vector and state variable.

Ather Mahmood, Jamie L. Weaver, Syed Qamar Abbas Shah, Will Echtenkamp, Jeffrey W. Lynn, Peter A. Dowben, Christian Binek. Dept. of Physics and Astronomy, & Nebraska Center for Materials and Nanoscience (NCMN), University of Nebraska–Lincoln, MML and NIST Center for Neutron Research. Part of the work performed at Nebraska Nanoscale Facility (NNF).

Work was supported by NSF EPSCoR RII Track-1: Emergent Quantum Materials and Technologies (EQUATE), Award OIA-2044049. *Advanced Physics Research*, 2023, 2300061.

National Research Priority: NSF–Harnessing the Data Revolution

National Nanotechnology Coordinated Infrastructure

Nebraska Nanoscale Facility

Intrinsic ferroelectricity in Y-doped HfO_2 thin films

Xiaoshan Xu and coworkers at UNL used NNF facilities to demonstrate that stable and enhanced polarization can be achieved in epitaxial HfO_2 films with a high degree of structural order (crystallinity). An out-of-plane polarization value of 50 μC cm^{-2} has been observed at room temperature in Y-doped HfO_2(111) epitaxial thin films, with an estimated full value of intrinsic polarization of 64 μC cm^{-2}, which is in close agreement with density functional theory calculations. The crystal structure of films reveals the *Pca*2$_1$ orthorhombic phase with small rhombohedral distortion, underlining the role of the structural constraint in stabilizing the ferroelectric phase. Our results suggest that it could be possible to exploit the intrinsic ferroelectricity of HfO_2-based materials, optimizing their performance in device applications.

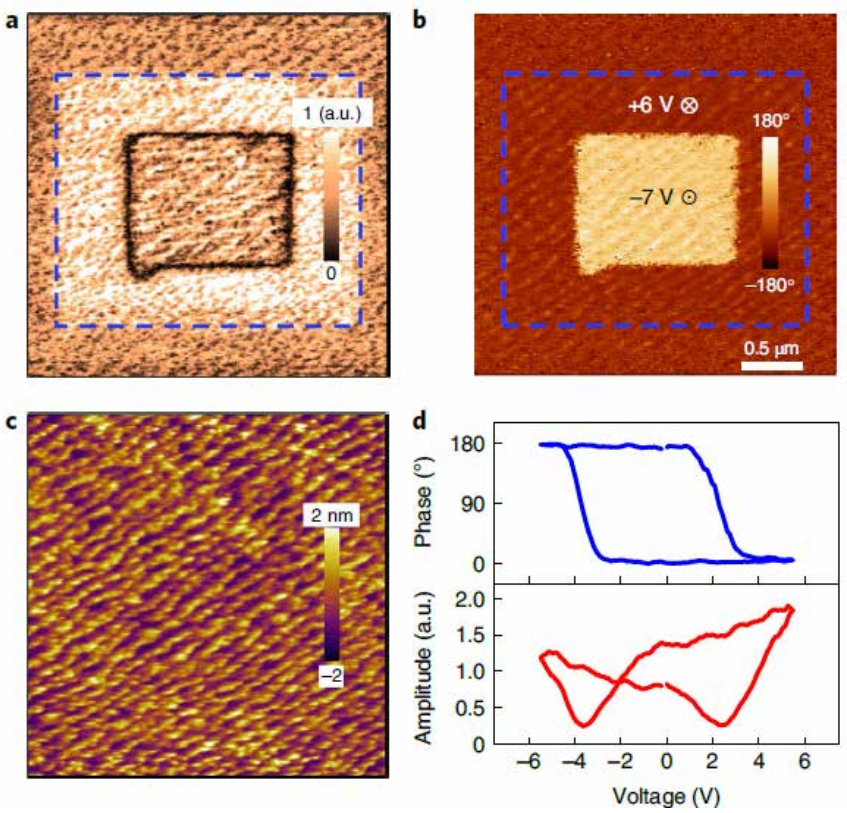

a,**b**, Amplitude (**a**) and phase (**b**) of the PFM image after poling with +6 and –7 V, demonstrating stable, bipolar, remanent polarization states. **c**, Atomic force microscopy image of the surface of the YHO(111)/LSMO(001) film, displaying the atomic step-and-terrace morphology. **d**, Phase- and amplitude-switching spectroscopy loops, demonstrating ferroelectric-like hysteresis on bare surface.

Yu Yun, Pratyush Buragohain, Ming Li, Zahra Ahmadi, Yizhi Zhang, Xin Li, Haohan Wang, Jing Li, Ping Lu, Lingling Tao, Haiyan Wang, Jeffrey E. Shield, Evgeny Y. Tsymbal, Alexei Gruverman & Xiaoshan Xu, Dept. of Phy. & Astron, UNL, Nebraska Center for Materials and Nanoscience (NCMN), MME UNL, SME Purdue Univ., Sandia National Lab, NM. Work performed at Nebraska Nanoscale Facility (NNF).

Nature Materials, 2022, 21, 903.

National Research Priority: NSF–Harnessing the Data Revolution

National Nanotechnology Coordinated Infrastructure

Nebraska Nanoscale Facility

Plasmon Enhanced Quantum Properties of Single Photon Emitters with Hybrid Hexagonal Boron Nitride Silver Nanocube Systems

Hexagonal boron nitride (hBN) has emerged as a highly desirable element for integrated quantum photonic networks. One major challenge of using these SPEs in such applications is their low quantum efficiency. Here, Abdelghani and coworkers at NNF:NCMN studied the quantum single-photon properties of hybrid nanophotonic structures composed of SPEs created in ultrathin hBN flakes coupled with plasmonic silver nanocubes (SNCs). The authors demonstrate 200% plasmonic enhancement of the SPE properties, manifested by a strong increase in the SPE fluorescence. Such enhancement is explained by rigorous numerical simulations where the hBN flake is in direct contact with the SNCs that cause the plasmonic effects. The presented strong and fast single photon emission obtained at room temperature with a compact hybrid nanophotonic platform can be very useful to various emerging applications in quantum optical communications and computing.

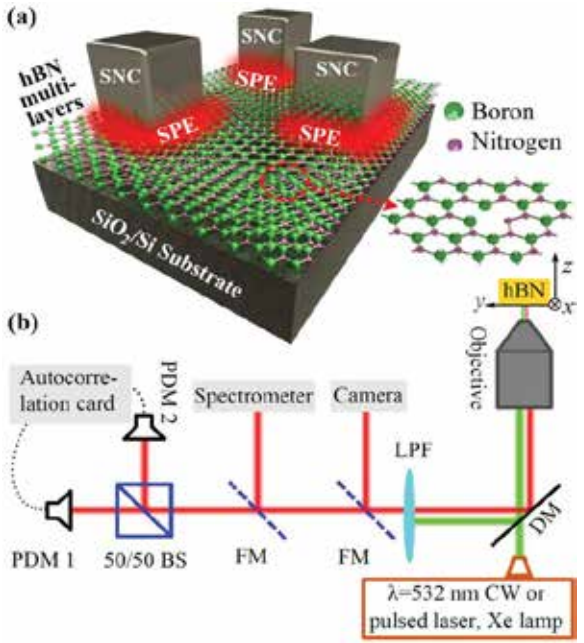

a) Enhanced quantum properties based on hybrid nanophotonic structures composed of SPEs in hBN combined with localized plasmon excitations from SNCs. Insert of a): a sketch of the distribution of hBN flake atoms, composed of boron (green) and nitrogen (purple) atoms in a 2D lattice. b) A schematic of our confocal fluorescence microscope setup consisting of a CCD camera to isolate the hBN flakes, a spectrometer, auto-bunching $g^{(2)}$ setup, lifetime measurements, and fluorescence imaging. DM: dichroic mirror, CW: continuous wave, LPF: long-pass filter, FM: flipped mount mirror, BS: beam splitter.

Mohammadjavad Dowran, Andrew Butler, Suvechhya Lamichhane, Adam Erickson, Ufuk Kilic, Sy-Hwang Liou, Christos Argyropoulos, Abdelghani Laraoui. MME, ECE, and Nebraska Center for Materials and Nanoscience (NCMN), UNL. Part of the work performed at Nebraska Nanoscale Facility (NNF).

Work was supported by NSF EPSCoR RII Track-1: Emergent Quantum Materials and Technologies (EQUATE), Award OIA-2044049 & Office of Naval Research Young Investigator Program (ONR-YIP) (Grant No. N00014-19-1-2384). *Advanced Optical Materials*, 2023, 11, 16, 2300392.

National Research Priority: NSF–Quantum Leap

National Nanotechnology Coordinated Infrastructure

Nebraska Nanoscale Facility

Enhanced Photoresponse in Few-Layer SnS_2 Field-Effect Transistors Modified with Methylammonium Lead Iodide Perovskite

Sinitskii and coworkers at NNF:NCMN demonstrate that decoration with methylammonium lead iodide perovskite ($MAPbI_3$) nanoparticles is an efficient approach to engineer strong visible light photoresponse in electronic devices based on two-dimensional (2D) materials with limited optical absorptivity. This was demonstrated using 2D SnS_2, a promising electronic material with a band gap of about 2.3 eV and poor absorption in the visible range of spectrum. Field-effect transistors based on pristine 2D SnS_2 show an n-type transport with high on–off ratios. Decoration with isolated $MAPbI_3$ nanoparticles qualitatively retains the transfer characteristics of the devices but dramatically increases their photoresponse in the entire visible range of the spectrum. The $MAPbI_3$-decorated SnS_2 devices exhibit stable, reproducible photoswitching over numerous cycles with response times of no longer than 12 ms. The described perovskite decoration approach should be applicable to engineering photoresponse in a variety of other devices based on 2D electronic materials with low optical absorptivity.

Michael J. Loes, Alexey Lipatov, Nataliia S. Vorobeva, Haidong Lu, Jehad Abourahma, Dmitry S. Muratov, Alexei Gruverman, and Alexander Sinitskii. *Dept. of Chemistry and NCMN,* University of Nebraska – Lincoln and Dept. of Chem. and Bio. Eng. South Dakota Sch. of Mines, SD. Part of the work performed at Nebraska Nanoscale Facility (NNF).

Work was supported by NSF EPSCoR RII Track-1: Emergent Quantum Materials and Technologies (EQUATE), Award OIA-2044049. *ACS Appl. Electron. Mater.* 2023, 5, 2, 705–713.

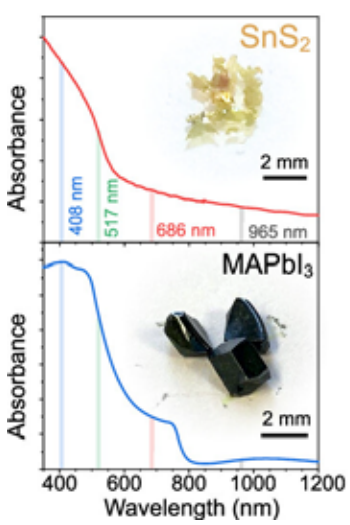

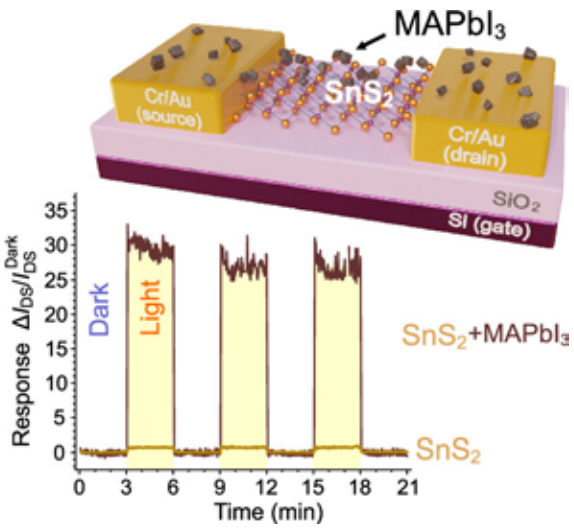

National Research Priority: NSF–Growing Convergence Research

National Nanotechnology Coordinated Infrastructure

Nebraska Nanoscale Facility

WS_2 Nanotube-Embedded SiOC Fibermat Electrodes for Sodium-Ion Batteries

Layered transition metal dichalcogenides (TMDs) such as tungsten disulfide (WS_2) are promising materials for a wide range of applications, including charge storage in batteries and supercapacitors. Nevertheless, TMD-based electrodes suffer from bottlenecks such as capacity fading at high current densities, voltage hysteresis during the conversion reaction, and polysulfide dissolution. To tame such adverse phenomena, we fabricate composites with WS_2 nanotubes. Herein, Gurpreet Singh and coworkers at Kansas State University utilized the NNF Facility and reported on the superior electrochemical performance of ceramic composite fibers comprising WS_2 nanotubes (WS_2NTs) embedded in a chemically robust molecular polymer-derived ceramic matrix of silicon-oxycarbide (SiOC). Such a heterogeneous fiber structure was obtained via electrospinning of WS_2NT/preceramic polymer solution followed by pyrolysis at elevated temperatures. The electrode capacity fading in WS_2NTs was curbed by the synergistic effect between WS_2NT and SiOC. As a result, the composite electrode exhibits high initial capacity of 454 mAh g^{-1} and the capacity retention approximately 2-3 times higher than that of the neat WS_2NT electrode.

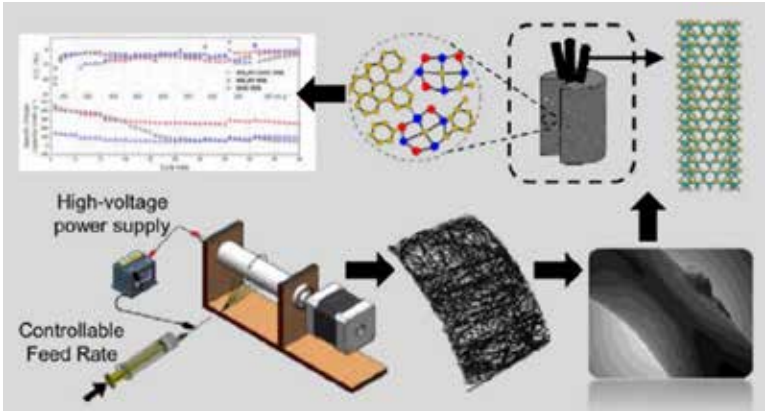

Sonjoy Dey, Krishnappa Manjunath, Alla Zak, Gurpreet Singh, Department of Mechanical and Nuclear Engineering, Kansas State University, Kansas. Part of the work performed at Nebraska Nanoscale Facility (NNF), University of Nebraska - Lincoln.

ACS Omega 2023, 8, 11, 10126–10138.

National Research Priority: NSF–Growing Convergence Research

National Nanotechnology Coordinated Infrastructure

Nebraska Nanoscale Facility

Microplotter-Printed Graphene-Based Electrochemical Sensor for Detecting Phosphates

Enabling an efficient electron transfer from the environment to an atomically thin, two-dimensional material such as graphene and vice versa provides a route to building graphene-based electrochemical sensors. Herein, Suprem Das and coworkers at Kansas State University utilized the NNF Facility and reported the manufacturing of a high-quality graphene nanoink and its use for the first time in fabricating stable and reliable printed phosphate ion electrochemical sensors using a microplotter. These sensors demonstrate a sensitivity of 0.3223 ± 0.025 μA μM^{-1} cm^{-2}, with a limit of detection (LOD) of 2.2 μM and linear sensing range of 1–600 μM. Moreover, they exhibit high selectivity toward phosphates when tested in the presence of NO_3^-, CO_3^-, Cl^-, and SO_4^{2-} interfering ions, affirming their reliability as a sensing platform. Phosphate electrochemical sensing using the proposed printed graphene sensors will pave the way for future development of point-of-care and continuous phosphate monitoring in environmental sensing.

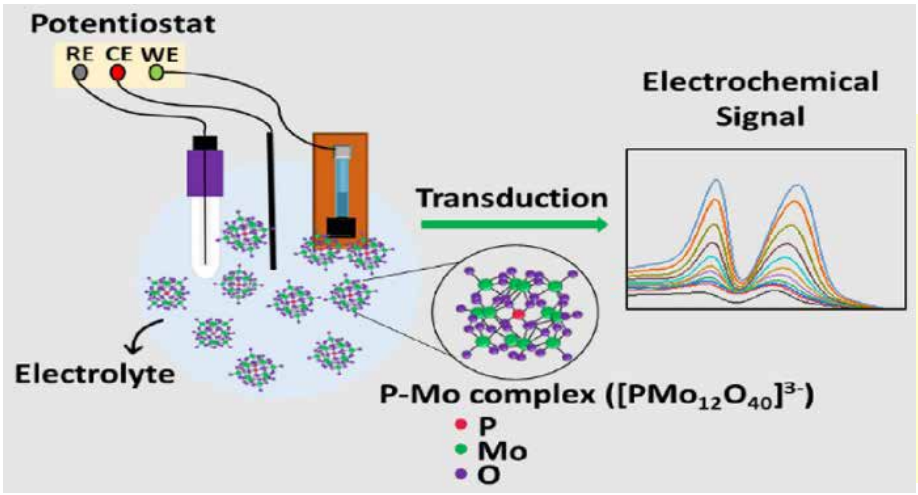

Thiba Nagaraja, Rajavel Krishnamoorthy, Kh M Asif Raihan, Brice Lacroix, and Suprem R. Das. Dept. of Industrial and Manufacturing Systems Eng., Kansas State University, Part of the work performed at Nebraska Nanoscale Facility (NNF), University of Nebraska, Lincoln.

Work supported by NSF Signals in the Soil (SitS) program, # 1935676. *ACS Applied Nano Materials*, 2023, 6, 21, 20288–20297.

National Research Priority: NSF–Growing Convergence Research

National Nanotechnology Coordinated Infrastructure

Nebraska Nanoscale Facility

Ferroelectric Domain Control of Nonlinear Light Polarization in MoS_2 via $PbZr_{0.2}Ti_{0.8}O_3$ Thin Films and Free-Standing Membranes

NNF researchers demonstrated that by interfacing monolayer MoS_2 with epitaxial $PbZr_{0.2}Ti_{0.8}O_3$ (PZT) thin films and free-standing PZT membranes, the amplitude and polarization of the second harmonic generation (SHG) signal are modulated via ferroelectric domain patterning, which demonstrates that PZT membranes can lead to in-operando programming of nonlinear light polarization. The interfacial coupling of the MoS_2 polar axis with either the out-of-plane polar domains of PZT or the in-plane polarization of domain walls tailors the SHG light polarization into different patterns with distinct symmetries, which are modeled via nonlinear electromagnetic theory. This study provides a new material platform that enables reconfigurable design of light polarization at the nanoscale, paving the path for developing novel optical information processing, smart light modulators, and integrated photonic circuits.

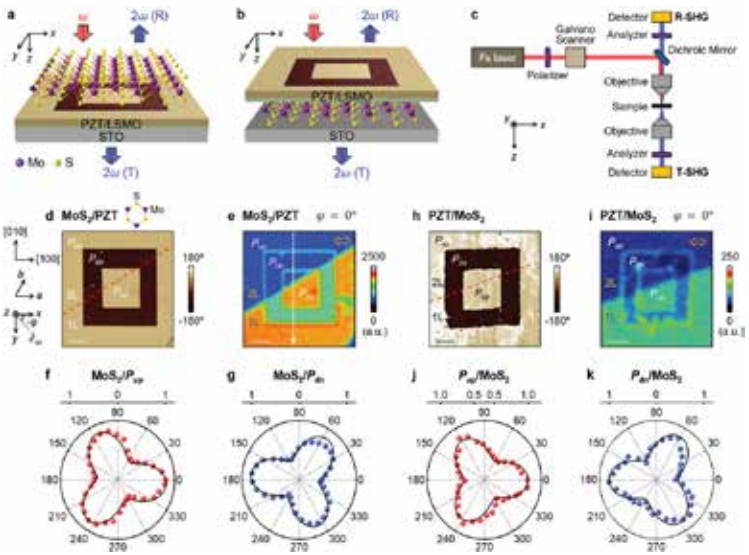

Ferroelectric domain control of SHG singals. a,b) Schematics of a) MoS_2/PZT and b) PZT/MoS_2 samples. c) Schematic of experimental setup. d) PFM phase image and e) T-SHG mapping of MoS_2/PZT. Inset: The laboratory coordinate system and the crystalline orientations of PZT and MoS_2. The dashed and dotted lines in (d) mark the 1L/2L boundary and the edge of MoS_2, respectively. The excitation laser power is 30 mW. Scale bars: 3 µm. f,g) Polar plots of normalized T-SHG intensity versus φ taken on f) P_{up} and g) P_{dn} domains in (e) with fits (solid lines). h) PFM phase image and i) R-SHG mapping of PZT/MoS_2. The dashed line in (h) marks the 1L/2L boundary of MoS_2. The excitation laser power is 7 mW. Scale bars: 2 µm. j,k) Polar plots of normalized R-SHG intensity versus φ taken on j) P_{up} and k) P_{dn} domains in (i) with fits (solid lines). The open arrows in (e) and (i) show the incident light polarization direction.

Dawei Li, Xi Huang, Qiuchen Wu, Le Zhang, Yongfeng Lu, Xia Hong, Nebraska Center for Materials and Nanoscience (NCMN), Dept. of Elect. and Comp. Eng., Dept. of Physics and Astronomy, UNL. Work performed at NNF.

This work was supported by the NSF through DMR-2118828, DMR-1710461, and EPSCoR RII Track-1: Emergent Quantum Materials and Technologies (EQUATE), Award No. OIA-2044049. *Advanced Materials* 2022, 35, 9 2208825.

National Research Priority: NSF–Harnessing the Data Revolution

National Nanotechnology Coordinated Infrastructure

Nebraska Nanoscale Facility

NNCI Site @ Stanford (nano@stanford)

National Nanotechnology Coordinated Infrastructure

A Soft and Flexible Electrochemical Sensor for In-Vivo Detection of Neurotransmitters

Stanford Prof. Bao's group developed a neurotransmitter (NT) sensor that is soft, stretchable, and enables in-vivo, real-time, multiplexed, NT detection in the CNS and GI system. Their work showed the possibility that serotonin can be used as a biomarker for gut inflammation and that their sensor could be adapted to diagnose IBS in humans.

- Fabrication: laser-induced graphene nanofiber networks modified with transition metal nanoparticles and embedded into a block copolymer/elastomer matrix.
- Characterization: HRTEM with EELS, Raman Spectroscopy, Micro X-ray Computed Tomography, mechanical testing.
- In-vivo testing in mammalian brains and colons:
  - o Detected higher serotonin in the colons of mice with acute colitis.
  - o Showed variable serotonin spatial distribution along the colon.

Characterization of the Sensor

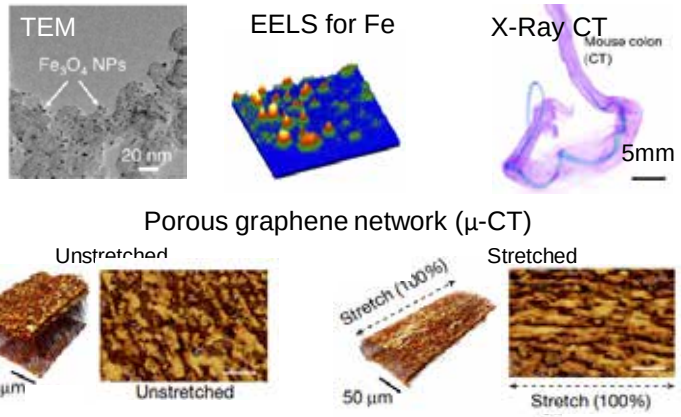

Performance of the Sensor

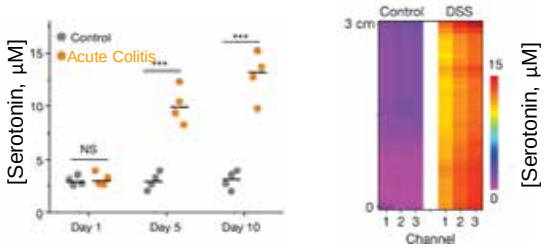

J. Li, et. al., Stanford Univ and Michigan State Univ; Depts. of Chem Eng, Biology, School of Medicine, Mat Sci & Eng, Psychiatry & Behavioral Sciences, Chemistry, Bioengineering, Surgery, Gastroenterology & Hepatology. Work performed in part at nano@stanford.

Supported by NSF (ECCS-2026822), Stanford (IIP & Wu Tsai Neuroscience Institute), NIH (R01DA045664, R01MH116904 & R01HL150566), Firmenich, National Science Scholarship, *Nature* 606, (2022): 94-101.

National Research Priority: NSF–Growing Convergence Research

National Nanotechnology Coordinated Infrastructure

Organic Electrochemical Transistor (OECT): Optimizing Performance with Synthetic Purification

Oxford's Prof. McCulloch developed a new purification method for organic mixed ionic-electronic conductors (OMIECs) to improve the performance of OECTs, which are well-suited for biosensing given their biocompatibility, high sensitivity, and fast switching speeds.

- OMIEC purification by preparative gel permeation chromatography (GPC):
  - Minimized residual catalyst-related impurities (palladium, Pd).
  - Separated polymer batches into molecular weight fractions.
- Characterization Results:
  - ICP-MS at nano@stanford measured 54—97% less Pd after GPC.
  - Electrochemical Impedence Spectroscopy at SHyNE measured 60-80% higher charge carrier mobility (μC) upon Pd reduction.
  - Removing Pd was more crucial than polymer molecular weight for optimizing OECT electrical performance.

GPC Removal of Pd, Measured by ICP-MS

Polymer	Sample ID (MW in kDa)	Palladium Conc. (ppm)
OMIEC = polythiophene ($p(g_4T2\text{-}TT)$)	Unpurified	1769
	Fraction 2 (MW=107.9)	370
	Fraction 1 (MW=180.1)	323
	Fraction 3 (MW = 61.3)	157
	Fraction 4 (MW = 18.4)	73
	Spike	2157
	F1+F2+F3+F4	236

OECT Performance vs Pd Conc. & Polymer Mol. Wt.

(ICP-MS at nano@stanford; electrochemical impedance spectroscopy at SHyNE)

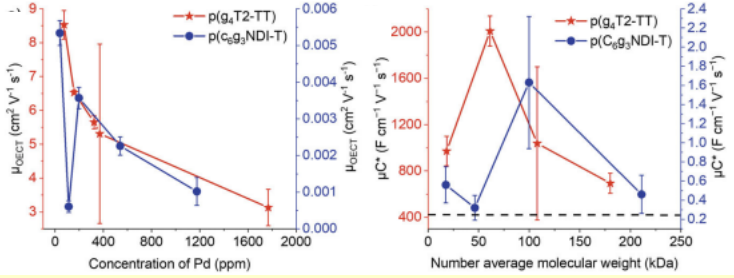

S. Griggs, I. McCulloch, et. al, U of Oxford, Northwestern, KAUST, Stanford, U of Bern; Departments of Chemistry, Materials Science, Biomedical Engineering, Bioengineering, Earth System Science. Work performed in part at nano@Stanford and SHyNE.

This work was supported by NSF (ECCS-2026822, DMR-1751308, ECCS-1542205, & DMR-1720139), EU Horizon 2020 (952911, 862474 &10100708), EPSRC (EP/T026219/1 & EP/W017091/1), Sloan (FG-2019-12046), IIN, Keck Foundation, DOE (DE-AC02-06CH11357), ONR YIP (N00014-20-1-2777), ERC (714586), SNSF (NCCR-MUST), KAUST OSR (OSR-2018-CARF/CCF-3079 & OSR-2019-CRG8-409). *Nature Communications* 13, (2022): 1-11.

5-Atom Wide Graphene Nanoribbons in FETs:
Reducing Transistor Size with Graphene-Based Channeling Materials

Prof. Bokor (UC Berkeley), Dr. Ruffieux (Empa) grew 45-nm long 5-atom wide armchair graphene nanoribbons (5-AGNR, an alternative channeling material) and successfully integrated them into FET devices. Previously, 5-AGNR had only been grown to a few nm long; longer 5-AGNRs may enable the further size reduction of transistors to below 7nm.

- Fabrication:
  - Tungsten/hafnium oxide bottom gate by photolithography and atomic layer deposition.
  - Pd electrodes by electron beam lithography.
  - The source-drain gap was ~18nm
- Characterization Results:
  - Uniaxially aligned 5-AGNR devices had a higher on/off current ratio and significantly higher working device yield, compared to and randomly oriented 5-AGNR devices.

FETs Fabricated with 5-AGNR at nano@stanford

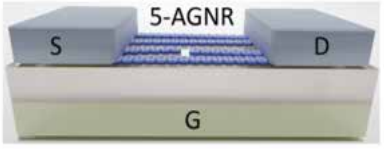

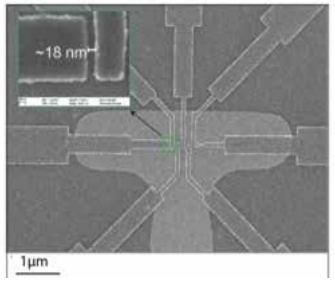

Devices Had p-Type FET Behavior

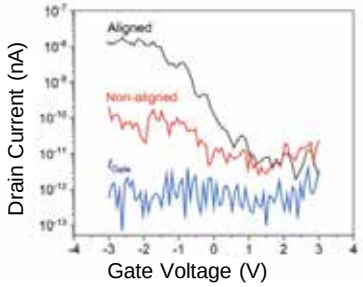

Featured on Journal Cover

G. Barin, Q. J. Bokor, R. Fasel, P. Ruffieux, et. al.; EMPA, Nanki Univ, UC Berkeley, Univ of Regensbergy, RPI, Johannes Gutenberg-Univ Mainz; Departments of Chemistry, Electrical Engineering & Computer Sciences, Theoretical Physics, Physics, and Materials Science. Work performed in part at nano@stanford.

This work was supported by NSF (ECCS-2026822 & DMR-1839098), SNSF (200020_182015 & 159690 & 196795), EU Horizon 2020 (881603), and the Office of Naval Research (N00014-18-1-2708 & N00014-16-1-2921), DOE (DE-AC02-05CH11231). *Small* 18, (2022): 1-10.

National Research Priority: DoD Critical Technology Area–Microelectronics

Multi-Dimensional Data Transmission by Silicon Photonics

Stanford Professor Vuckovic's group developed an integrated multi-dimensional communication scheme for on-chip and chip-to-chip interconnects, combining wavelength- and mode-multiplexing on a Si-based photonic circuit offering a significant enhancement over existing silicon photonic transmitters.

- A photonic inverse design and spectrally flattened microcombs allowed for high-speed (1.12 Tb/S), error-free data transmission through a silicon nanophotonic waveguide.
- Inverse-designed surface-normal couplers enabled multimode optical transmission between two silicon chips via a multimode fiber.
- Fabricated at nano@stanford and used Stanford's SPINS inverse design, open-source software.

Inverse Design Mode-Division Multiplexer

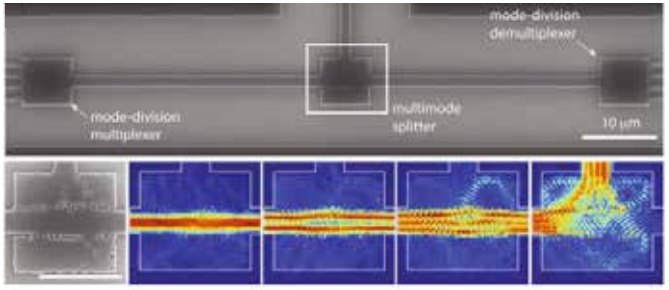

Chip-to-Chip Multimode Link

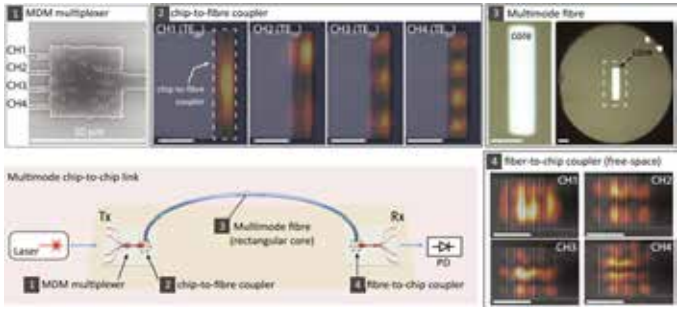

K. Yang, C. Shirpurkar, A. White, J. Vuckovic, et. al. Stanford, U of Central Florida, U of Colorado, UCSB,U of Penn., NIST, USC, Departments of Electrical Engineering, Engineering and Applied Sciences, and Physics, Work performed in part at nano@stanford.

This work was supported by NSF (ECCS-2026822**),** DARPA (PIPES program), AFOSR (FA9550-17-1-0002), AFRL (FA8650-20-C-1105), DOD ONR (N00014-16-1-2813), and Research Foundation—Flanders (12ZB520N). *Nature Communications* 13, (2022): 1-9.

National Research Priority: DoD Critical Technology Area–Microelectronics

Multi-Layered, Self-Healing, Realigning, Electronic Devices

Stanford Prof. Bao's group developed multi-layer, self-healing devices using polymers with similar dynamic bonds but immiscible backbones (e.g., modified PDMS and PPG). The functional, self-healing was demonstrated in a pressure-sensor capacitor, magnetically assembled soft robot, and an underwater LED circuit.

- Characterization: Rheometry, mechanical testing, & nanomechanical imaging by AFM.
- Developed a field-theoretic description for the interfacial self-healing behavior between modified PDMS and PPG layers.
- Reduced interfacial healing allowed for autonomous *realignment* of alternatively stacked films after damage.

Featured on NSF Foundation News!

https://www.youtube.com/watch?v=r7VQugRhFaU

Self-Healing and Realignment of a Capacitor

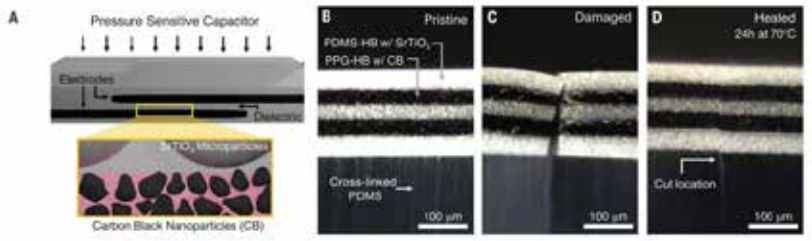

C. Cooper, S. Root, J. Vuckovic, et. al. Stanford University's Departments of Chemical Engineering and Mechanical Engineering, Work performed in part at nano@stanford and SLAC.

This work was supported by NSF (ECCS-2026822, CMMI-2142789, CMMI-2145601, 2138259, 2138286, 2138307, 2137603, 2138296), ARO (W911NF-21-1-0092), DOD (National Defense Science & Engineering Graduate Fellowship), Walter Benjamin Fellowship, DFG (456522816), Stanford's TomKat Center Fellowship, DOE (DE-AC02-76SF00515). *Science* 380, (2023): 935-941.

National Research Priority: DoD Critical Technology Area–Microelectronics

Northwest Nanotechnology Infrastructure (NNI)

National Nanotechnology Coordinated Infrastructure

Directing Polymorph Specific Calcium Carbonate Formation with de novo Protein Templates

Achieving the ability to direct the nucleation and growth of inorganic materials by emulating Nature's use of protein-based templates would enable the design and synthesis of hybrid materials for energy technologies and define a novel approach to carbon capture. Guided by the structure of proteins that control the growth of ice, we developed an approach to designing protein-based templates that direct calcite nucleation and determined the resulting pathways of nucleation and growth. The results show that crystal polymorph, size, and shape can be tuned via protein structure and chemistry, paving the way for the development of hierarchical materials using rationally designed molecular templates.

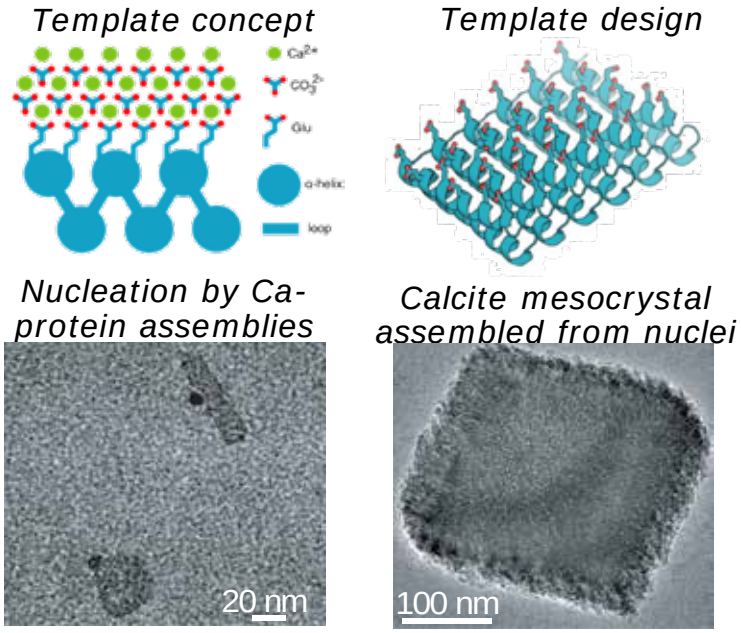

Concept and design of protein template (top) that nucleates nano-calcite, which then assembles to form a calcite mesocrystal (bottom).

Fatima A. Davila (IPD/UW), Biao Jin (MSE/UW), Harley Pyles (IPD/UW), Shuai Zhang (MSE/UW), Chun-Long Chen (ChemE/UW), Jim De Yoreo (MSE/UW), David Baker (IPD/UW), et al. Work (AFM) partially performed at UW Molecular Analysis Facility (MAF)

This work was supported by DOE-BES DE-SC0018940 and DOE-EFRC-CSSAS DESC0019288. *Nature Comm.* 14:8191 (2023).

National Research Priority: NSF–Growing Convergence Research and Understanding the Rules of Life

National Nanotechnology Coordinated Infrastructure

NORTHWEST NANOTECHNOLOGY INFRASTRUCTURE

Novel Biomimetic Membrane for Separation

Generating affordable clean water is essential for communities worldwide, especially in the arid or underdeveloped regions and countries. In this work, we synthesized a novel biomimetic porous membrane by co-assembling CNTPs with peptoid, a sequence-defined synthetic polymer that mimic peptides and proteins. These nanomembranes are highly stable, robust, and self-repairable. By replacing the lipid matrix, we created highly durable artificial membranes with permeability and selectivity. Our results demonstrate a compelling alternative strategy for the design and synthesis of biomimetic membrane. This work provides a new approach for design and synthesis of artificial membranes with potential applications for many global crises, including clean-water shortage.

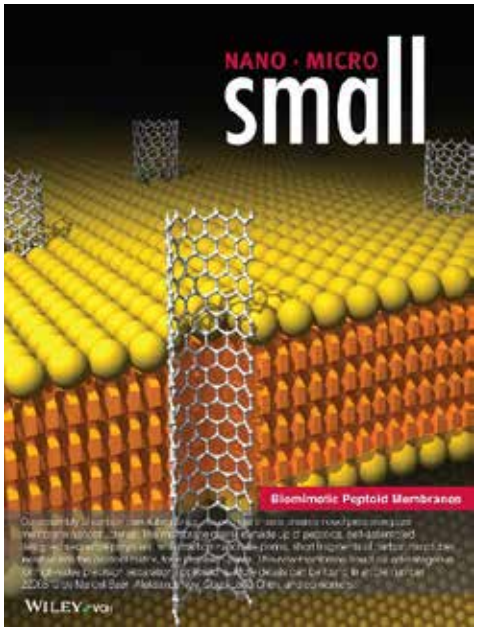

A scheme of peptoid sheet assembling with carbon nanotube porins, based on molecular dynamic (MD) simulation.

Shuai Zhang (MSE/PNNL), Jim De Yoreo (MSE/PNNL), Renyu Zheng (ChemE/PNNL), Chun-Long Chen (ChemE/PNNL).
Work (AFM) partially performed at UW Molecular Analysis Facility (MAF).

This work was supported by the DOE-BES SCW1607 at Pacific Northwest National Laboratory and the Lawrence Livermore National Laboratory. *Small* 2023, 19, 2206810 (Frontispiece)

National Research Priority: NSF–Growing Convergence Research and NAE Grand Challenges–Provide Access to Clean Water

Photonic Advantage of Optical Encoders

Light's ability to perform massive linear operations parallelly has recently inspired numerous demonstrations of optics-assisted artificial neural networks (ANN). However, a clear advantage of optics over purely digital ANN in a system-level has not yet been established. While linear operations can indeed be optically performed very efficiently, the lack of nonlinearity and signal regeneration require high-power, low-latency signal transduction between optics and electronics. Additionally, large power is needed for lasers and photodetectors, which are often neglected in the calculation of the total energy consumption. Here, instead of mapping traditional digital operations to optics, we co-designed a hybrid optical-digital ANN that operates on incoherent light and is thus amenable to operations under ambient light. Keeping the latency and power constant between a purely digital ANN and a hybrid optical-digital ANN, we identified a low-power/latency regime, where an optical encoder provides higher classification accuracy than a purely digital ANN. We estimate our optical encoder enables ~ 10kHz rate operation of a hybrid ANN with a power of only 23mW. However, in that regime, the overall classification accuracy is lower than what is achievable with higher power and latency. Our results indicate that optics can be advantageous over digital ANN in applications, where the overall performance of the ANN can be relaxed to prioritize lower power and latency.

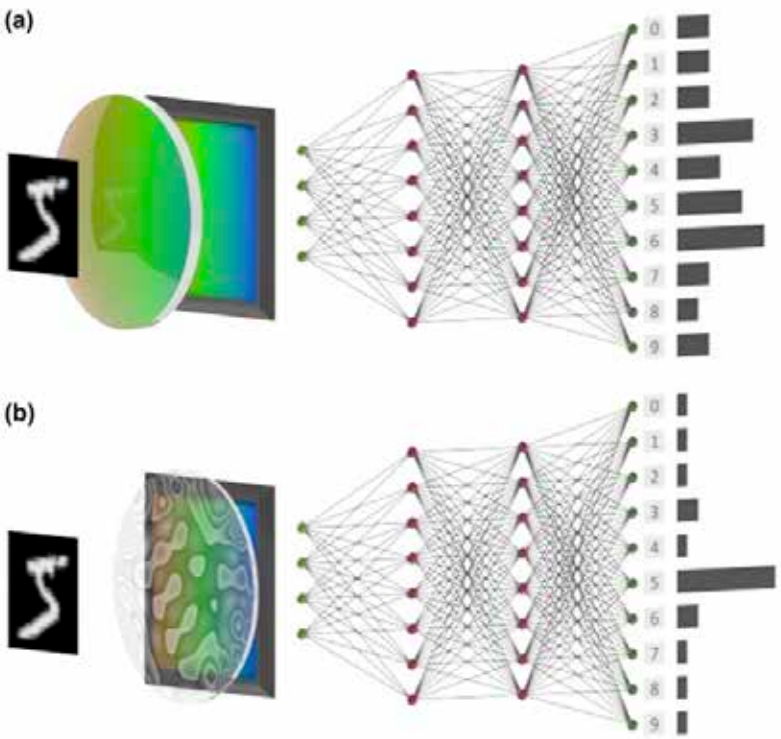

Fabricated meta-optical encoder

Luocheng Huang, Quentin A. A. Tanguy, Johannes E. Fröch, Saswata Mukherjee, Karl F. Böhringer, Arka Majumdar. Work performed in UW Washington Nanofabrication Facility, Molecular Analysis Facility.

Funding Source: NSF-ECCS-2127235, DARPA Contract # W31P4Q-21-C-0043. *Nanophotonics* 2023,

National Research Priority: Advanced Photonics

Miniature Color Camera via Flat Hybrid Meta-Optics

To bridge the gap between the theoretical modeling of wavefront encoding by meta-surfaces and real-life physical implementation, we propose the end-to-end joint design of meta-masks and imaging algorithms in the hardware-in-the-loop (HIL) setup. To model the optics, we use a pixel-wise programmable phase Spatial Light Modulator (SLM) to implement phase encoding physically. Training-based optimization fitting reconstructed and true images obtain the hyperparameter of SLM and image signal processing algorithms. Fundamentally, the HIL-SLM methodology guarantees a proper 'modeling' of the black-box hardware in optimization without discrepancies between mathematical models and physical reality. We demonstrate a miniature colored camera via flat hybrid meta-optics (refractive + meta lenses) implementation of the desired phase modulation found due to HIL methodology. This design produced for EDoF achromatic imaging that achieves high-quality imaging with focal distance 5 mm, aperture 6 mm, F1.0, is an advanced novel development up to date. To illustrate the potential of this hybrid camera, we compare its imaging performance with a compound multi-lens commercial camera showing that the design optics is competitive and even advanced in colored, sharp imaging.

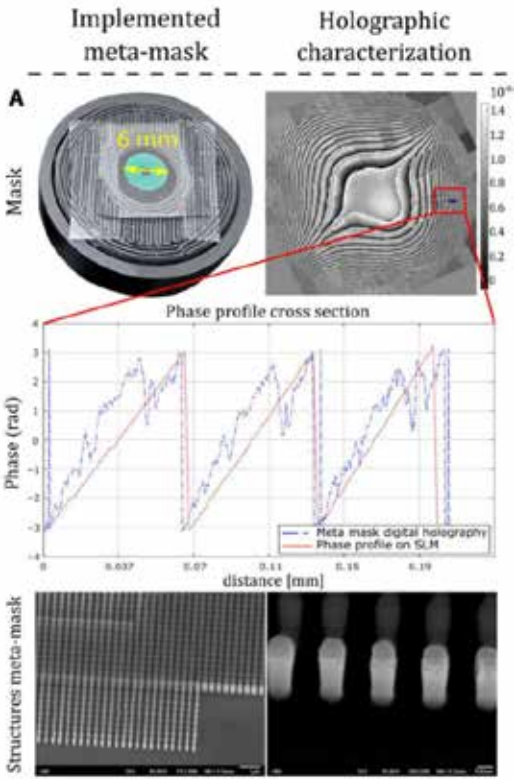

Fabricated meta-optics for miniature color camera

Johannes E. Fröch, University of Washington. Collaborator: Karen Egiazarian, Tampere University, Tampere, Finland. Work performed in UW Washington Nanofabrication Facility (WNF), Molecular Analysis Facility (MAF).

Funding Source: NSF-ECCS-2127235, DARPA Contract # W31P4Q-21-C-0043. *Science Advances* 2023.

National Research Priority: Advanced Photonics

Realizing Arbitrary Tight-binding Hamiltonians Using Site-controllable Cavity Arrays

Analog quantum simulators rely on programmable and scalable quantum devices to emulate Hamiltonians describing various physical phenomenon. Photonic coupled cavity arrays are a promising alternative platform for realizing such simulators, due to their potential for scalability, small size, and high-temperature operability. However, programmability and nonlinearity in photonic cavities remain outstanding challenges. Here, using a silicon photonic coupled cavity array made up of 8 high quality factor (Q up to $\sim 7.1 \times 10^4$) resonators and equipped with specially designed thermo-optic island heaters for independent control of cavities, we demonstrate a programmable photonic cavity array in the telecom regime, implementing tight-binding Hamiltonians with access to the full eigenenergy spectrum. We report a $\sim 50\%$ reduction in the thermal crosstalk between neighboring sites of the cavity array compared to traditional heaters, and then present a control scheme to program the cavity array to a given tight-binding Hamiltonian. The ability to independently program high-Q photonic cavities, along with the compatibility of silicon photonics to high volume manufacturing opens new opportunities for scalable quantum simulation using telecom regime infrared photons.

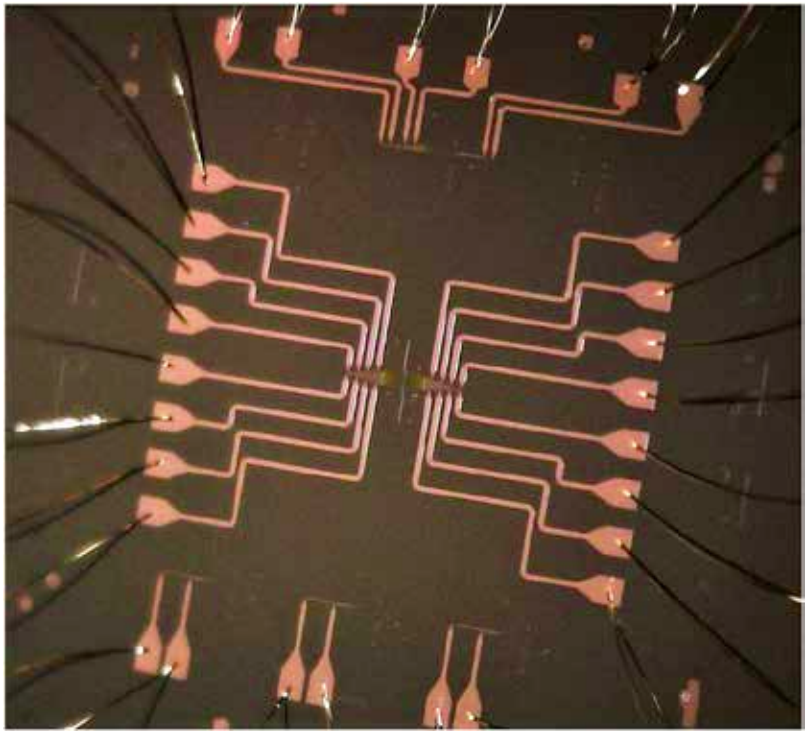

Programmable Coupled Cavity Array

Abhi Saxena, Arnab Manna, Rahul Trivedi, Arka Majumdar, ECE/Physics, University of Washington. Work performed in UW Washington Nanofabrication Facility (WNF), Molecular Analysis Facility (MAF).

Funding Source: NSF-QII-TAQS-1936100, NSF-1845009. *Nature Communications* 14:5260 2023

National Research Priority: NSF–Quantum Leap

National Nanotechnology Coordinated Infrastructure

NORTHWEST NANOTECHNOLOGY INFRASTRUCTURE

Non-volatile Electrically Programmable Integrated Photonics with a 5-bit Operation

Scalable programmable photonic integrated circuits (PICs) can potentially transform the current state of classical and quantum optical information processing. However, traditional means of programming, including thermo-optic, free carrier dispersion, and Pockels effect result in either large device footprints or high static energy consumptions, significantly limiting their scalability. While chalcogenide-based non-volatile phase-change materials (PCMs) could mitigate these problems thanks to their strong index modulation and zero static power consumption, they often suffer from large absorptive loss, low cyclability, and lack of multilevel operation. Here, we report a wide-bandgap PCM antimony sulfide (Sb_2S_3)-clad silicon photonic platform simultaneously achieving low loss (<1.0 dB), high extinction ratio (>10 dB), high cyclability (>1,600 switching events), and 5-bit operation. These Sb_2S_3-based devices are programmed via on-chip silicon PIN diode heaters within sub-ms timescale, with a programming energy density of ~10fJ/nm^3. Remarkably, Sb_2S_3 is programmed into fine intermediate states by applying multiple identical pulses, providing controllable multilevel operations. Through dynamic pulse control, we achieve 5-bit (32 levels) operations, rendering 0.50 ± 0.16 dB per step. Using this multilevel behavior, we further trim random phase error in a balanced Mach-Zehnder interferometer. Our work opens an attractive pathway toward large-scale energy-efficient programmable PICs with low-loss and multi-bit operations.

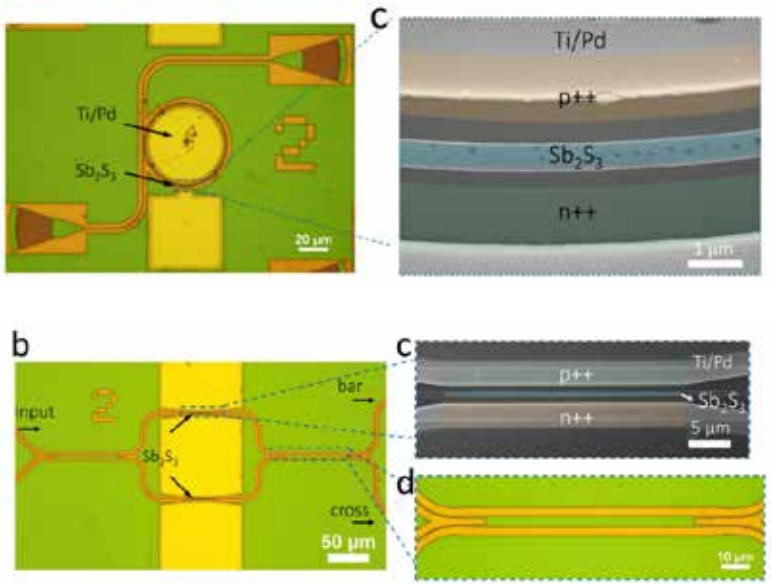

Phase-Change Material Integrated Silicon Photonics

Rui Chen, Zhuoran Fang, University of Washington; collaborator: Kenneth E. Goodson, Stanford; Sarah J. Geiger, Draper Labs. Work performed in Washington Nanofabrication Facility (WNF), Molecular Analysis Facility (MAF).

Funding Source: NSF-1640986, NSF-2003509, ONR-YIP Award, DARPA-YFA Award, NASA-STTR Award 80NSSC22PA980, and Intel. *Nature Communications* 14:3465 (2023).

National Research Priority: Advanced Photonics

Thin On-Sensor Nanophotonic Array Cameras

Today's commodity camera systems rely on compound optics to map light originating from the scene to positions on the sensor where it gets recorded as an image. To record images without optical aberrations, i.e., deviations from Gauss' linear model of optics, typical lens systems introduce increasingly complex stacks of optical elements which are responsible for the height of existing commodity cameras. In this work published in ACM Transactions on Graphics , we investigate flat nanophotonic computational cameras as an alternative that employs an array of skewed lenslets and a learned reconstruction approach. The optical array is embedded on a metasurface that, at 700~nm height, is flat and sits on the sensor cover glass at 2.5~mm focal distance from the sensor. To tackle the highly chromatic response of a metasurface and design the array over the entire sensor, we propose a differentiable optimization method that continuously samples over the visible spectrum and factorizes the optical modulation for different incident fields into individual lenses. We reconstruct a megapixel image from our flat imager with a learned probabilistic reconstruction method that employs a generative diffusion model to sample an implicit prior. To tackle scene-dependent aberrations in broadband, we propose a method for acquiring paired captured training data in varying illumination conditions. We assess the proposed flat camera design in simulation and with an experimental prototype, validating that the method is capable of recovering images from diverse scenes in broadband with a single nanophotonic layer.

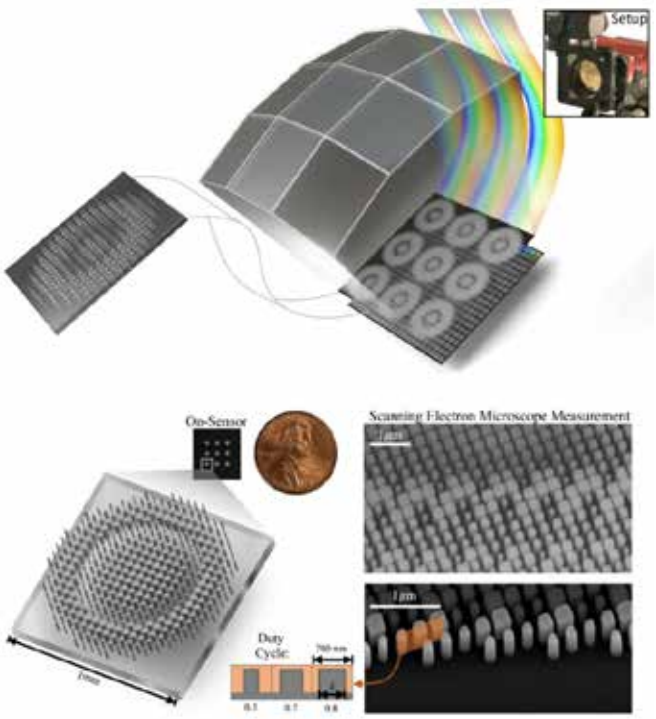

Fabricated meta-optical array for imaging

Johannes E. Fröch, University of Washington. Collaborator: Felix Heide, Princeton. Work performed in UW Washington Nanofabrication Facility (WNF) , Molecular Analysis Facility (MAF).

Funding Source: NSF-ECCS-2127235, DARPA Contract # W31P4Q-21-C-0043. *ACM Transactions of Graphics* 42(6), 2023.

National Research Priority: Advanced Photonics

National Nanotechnology Coordinated Infrastructure

NORTHWEST NANOTECHNOLOGY INFRASTRUCTURE

Toughness Amplification via Controlled Nanostructure in Lightweight Nano-Bouligand Materials

Natural materials like shell, bone and skin have a nanostructured, hierarchical architecture that promotes their simultaneous strength and toughness. While it is accepted that fracture processes across length scales contribute to toughness, toughening mechanisms at the nanoscale are not well understood. Here, we create novel metamaterials made from twisted polymer nanofibers (nano-Bouligand) to demonstrate how toughness changes at the nanoscale. Isolating nanofibers activates size-enhanced ductility and increases the specific fracture energy, while introducing twist between nanofibers creates a nanoscale heterogeneity that impedes crack growth. This work illustrates the potential for creating new, high toughness materials using controlled nanostructures.

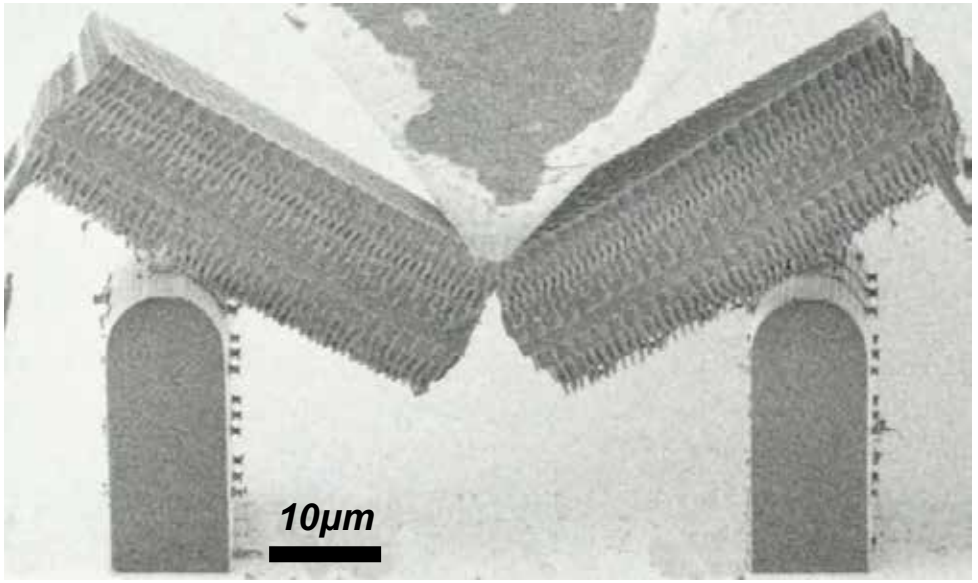

Figure: Microscale fracture experiment on a twisted polymer nanofiber structure demonstrating a great resistance to fracture. The experiment was conducted using an in-situ nanoindenter in a scanning electron microscope.

Lucas R. Meza, UW Seattle, Mechanical Engineering; Zainab Patel, UW Seattle, Materials Science and Engineering.
Work performed at Washington Nanofabrication Facility (WNF) and UW Molecular Analysis Facility (MAF).

This work was supported by NSF Grant #2032539. *Small* 2207779 (2023)

National Research Priority: DoD Critical Technology Area–Advanced Materials

National Nanotechnology Coordinated Infrastructure

NORTHWEST NANOTECHNOLOGY INFRASTRUCTURE

Mechanistic Insights into the Effect of Solvent in Catalytic Reactions

In this investigation, near ambient pressure XPS (NAP-XPS), mass spectrometry and density functional theory calculations were used to identify how the presence of water impacts the breakdown of acetic acid on Pd(111) catalysts. These catalysts serve as a model for understanding the reactions involved in breaking down small oxygenates, mirroring crucial steps in converting fatty acids and biomass. The breakdown of acetic acid involves two primary pathways, resulting in either CO2 or CO formation. Alterations in surface components were tracked under various gas phase conditions. While both pathways compete in pure acetic acid environments, the introduction of water decelerates the CO-forming process, leading to a notable increase in the CO2/CO production ratio. Employing NAP-XPS (within the NNI) enables us to conduct these investigations under higher and more applicable pressures and conditions.

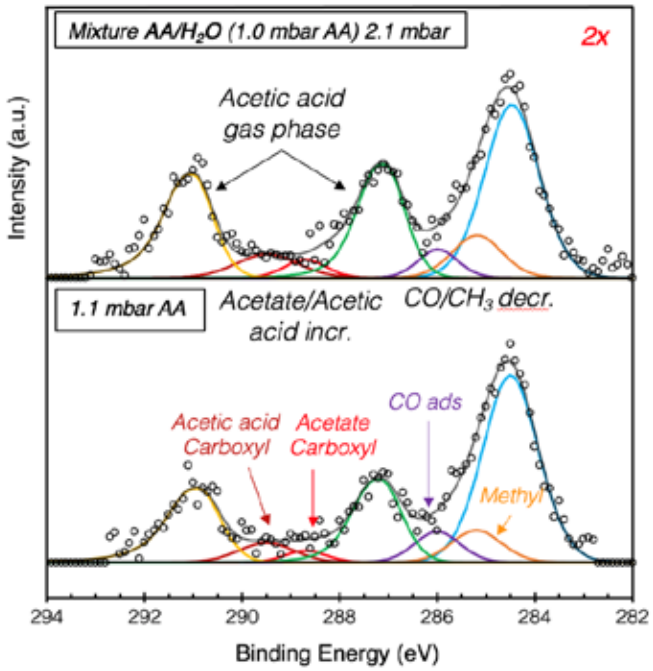

Top: NAP-XPS showing decrease in CO on the surface and an increase in acetate with the addition of water.

Hoan K.K. Nguyen, Kingsley C. Chukwu and Líney Árnadóttir, School of Chemical, Biological, and Environmental Engineering, Oregon State University. Work performed at Northwest Nanotechnology Infrastructure, Oregon State.

This work was supported by NSF Award # CHE 2054933. *J. Phys. Chem.* C 2023, 127, 24, 11472–11480

National Research Priority: NSF–Growing Convergence Research

National Nanotechnology Coordinated Infrastructure

NORTHWEST NANOTECHNOLOGY INFRASTRUCTURE

The Role of Nonmetallic Ion Substitution in Perovskite $LaCoO_3$ for improved OER Activity

This research centers on a Fe and P co-doped $LaCoO_3$ configuration, which here serves as a model system to unravel how the cation and anion sites within perovskite structures influence the performance of the oxygen evolution reaction (OER). This critical relationship between structure and function has been lacking in transition metal perovskites (ABO_3), a burgeoning class of electrocatalysts vital for water splitting to generate green hydrogen. Through a blend of operando/ex-situ X-ray characterization and density functional theory, we're uncovering diverse OER-related phenomena that traditional metal-centered theories have failed to explain.

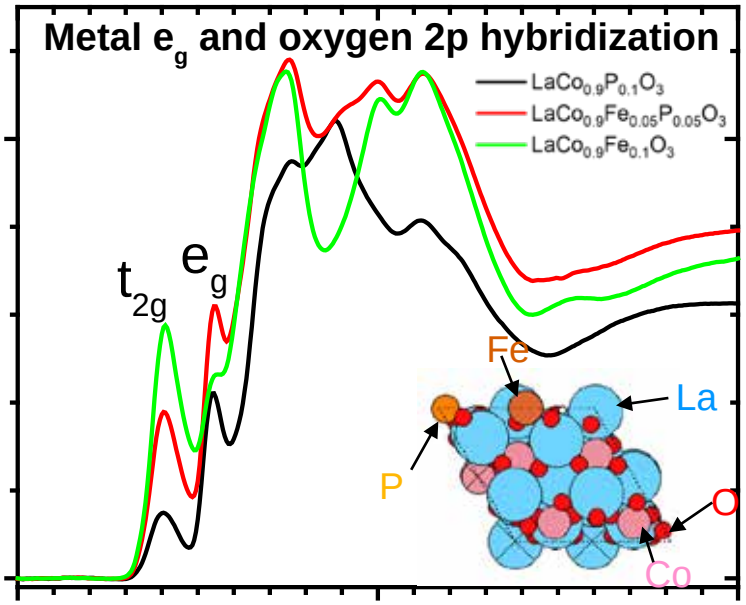

X-ray absorption spectroscopy (XAS) at oxygen K-edge show distinct electronic structure for Fe and P co-doped $LaCoO_3$ oxides. The model from density functional theory is provided to illustrate the surface atomic structure.

Maoyu Wanga, Kingsley Chukwuma Chukwu, Brian A. Muhich, Widitha S. Samarakoon, Líney Árnadóttir, Zhenxing Feng*, School of Chemical, Biological, and Environmental Engineering, Oregon State University. Work performed at Northwest Nanotechnology Infrastructure of Oregon State University.

This work was supported by NSF Award # NNCI-2025489. *Electrochimica Acta* 466, 2023, 145034.

National Research Priority: NSF–Growing Convergence Research

National Nanotechnology Coordinated Infrastructure

NORTHWEST NANOTECHNOLOGY INFRASTRUCTURE

Tuning Surface Chemistry and Topography to Control the Growth of Vascular Tissue

Synthetic small-diameter vascular grafts (<6 mm) are used in the treatment of cardiovascular diseases, including coronary artery disease, but fail much more readily than similar grafts made from autologous vascular tissue. A promising approach to improve the patency rates of synthetic vascular grafts is to promote the adhesion of endothelial cells to the luminal surface of the graft. In this study, we characterized the surface chemical and topographic changes imparted on poly(vinyl alcohol) (PVA), an emerging hydrogel vascular graft material, after exposure to various surface treatments, how these changes dissipate after storage in a sealed environment at standard temperature and pressure, and the effect of these changes on the adhesion of endothelial cells.

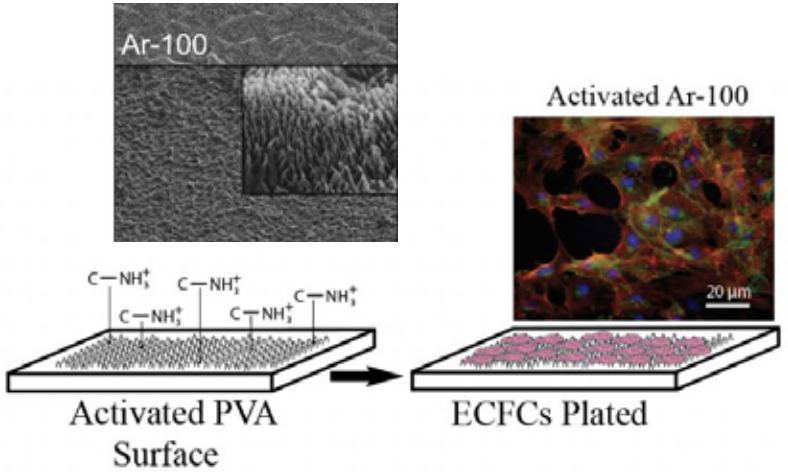

Schematic depicting the experimental procedure for quantifying ECFCs on activated or aged STMP-PVA surfaces. Representative fluorescence images of ECFCs cultured on activated Ar-100 and aged Ar-50 RIP-treated PVA are provided as insets.

Lead PI - Patrick Jurney, Dept. Biomedical Engineering, San Jose State University. Work performed at Northwest Nanotechnology Infrastructure, Oregon State University.

This work was supported by NSF award # CHE 1905091 and NIH awards SC2GM140991, R01 HL144113 and R21 HD096301. *ACS Applied Materials & Interfaces 2023*.

National Research Priority: NSF–Understanding the Rules of Life

National Nanotechnology Coordinated Infrastructure

NORTHWEST NANOTECHNOLOGY INFRASTRUCTURE

Determination of Cu Oxidation State in Supported Metal Catalysts

RenewCat, a burgeoning startup located in Oregon, is focused on significantly enhancing pharmaceutical production yields by revolutionizing the design of new catalysts. Central to their efforts is the management of the oxidation state of copper (Cu) in various heterogeneous catalyst compositions. The company is leveraging the characterization facilities within the NNI to explore diverse preparation techniques for synthesizing heterogeneous copper catalysts. Their goal is to establish correlations between the support material, preparation conditions, and the resulting oxidation state of Cu.

Work performed at NNCI Northwest Nanotechnology Infrastructure, Oregon State University.

This work is supported by RenewCat, Inc.

National Research Priority: NSF–Growing Convergence Research

Research Triangle Nanotechnology Network (RTNN)

National Nanotechnology Coordinated Infrastructure

Sc_2C: a 2D Semiconducting Electride

- The effect of cation electronegativity on the properties of electrides is currently unknown
- Trivalent metal carbides are synthesized experimentally, with varying degrees of electronegativity, exemplified by Sc_2C
- Despite Sc having higher electronegativity than any metal previously found adjacent to an electride site, the material is identified as a two-dimensional (2D) electride
- Computational studies reveal that Sc_2C and Al_2C exhibit higher electronegativity of the cation, leading to increased hybridization between metal and electride orbitals, which opens a band gap in these materials
- Sc_2C is identified as the first 2D electride semiconductor, and a proposed design rule suggests that cation electronegativity drives the change in its band structure

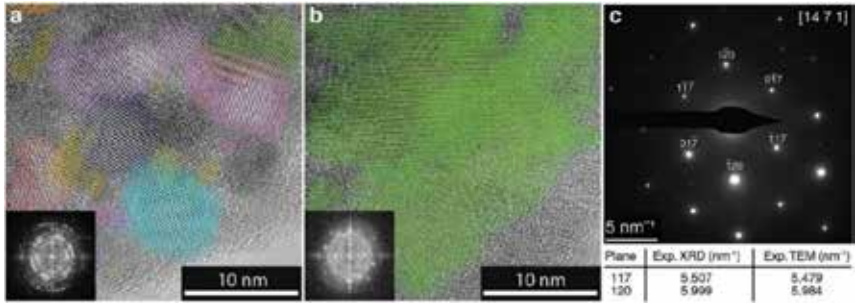

a) High-resolution transmission electron microscopy (TEM) image of Sc_2C before annealing, with colored lattice planes corresponding to different crystallite regions determined through FFTs.

b) High-resolution TEM image of Sc_2C after annealing for 7 days, with the lattice planes of the single crystallite region in green

c) Selected area electron diffraction (SAED) pattern of the [14 7 1] zone axis. The corresponding experimental d-spacings are compared.

Lauren McRae, Rebecca Radomsky, Jacob Pawlik, Daniel Druffel, Jack Sundberg, Matthew Lanetti, Carrie Donley, Kelly White, and Scott Warren, Chemistry Department, University of North Carolina at Chapel Hill; Work performed partially at UNC Chapel Hill Analytical and Nanofabrication Laboratory.

This work also supported by: NSF (DMR-1905294, DGE-1650116, DGE-1650114). *J. Am. Chem. Soc.* 2022, 144, 24, 10862–10869.

National Research Priority: DoD Critical Technology Area–Advanced Materials

Redox Oxide@molten Salt as a Generalized Catalyst Design Strategy for Oxidative Dehydrogenation of Ethane via Selective Hydrogen Combustion

- Ethylene (C_2H_4) is a crucial commodity chemical derived from ethane (C_2H_6), particularly abundant in the US now due to increased shale gas production
- Traditional steam cracking for ethylene production faces challenges like high energy demand, limited conversion, and complex separations
- This study explores oxidative dehydrogenation as an alternative for ethane-to-ethylene conversion, aiming to simplify processes and reduce energy consumption
- A redox catalyst is introduced with a core-shell architecture in a chemical looping process, demonstrating enhanced performance through advanced characterization techniques
- The generalized core-shell redox catalyst design offers exciting opportunities for optimization, aiming to significantly reduce carbon emissions in ethane-to-ethylene conversion

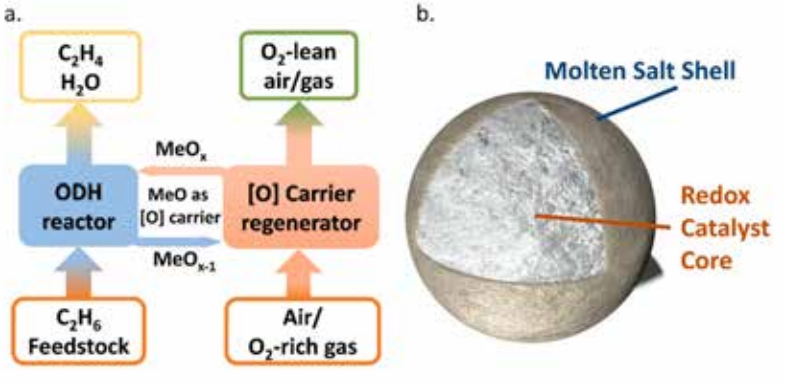

a) Overall scheme of CL-ODH and

b) Schematic illustration of the core shell structured, molten salt promoted redox catalyst (film thickness is ~8–13 nm and the particle diameter is 425–850 μm)

Junchen Liu, Seif Yusuf, Daniel Jackson, William Martin, Dennis Chacko, Kyle Vogt-Lowell, Luke Neal, Fanxing Li, Chemical and Biomolecular Engineering, North Carolina State University; Work performed partially at NC State Analytical Instrumentation Facility and Duke Shared Materials Instrumentation Facility.

This work was supported by NSF (CBET-2116724) and DOE (DE-FE0031918*). Applied Catalysis A: General Volume* 646, 25 September 2022, 118869.

National Research Priority: DOE Energy Earthshots–Clean Fuels & Products Shot

Characterizing Interactions Between Multi-Walled Carbon Nanotubes and Lung Proteins

- Multi-walled carbon nanotubes (MWCNTs) are becoming more widely used in industries like electronics and aerospace, raising concerns about human exposure and potential health effects of inhaling MWCNTs
- This study investigates the interactions between MWCNTs and proteins, focusing on bovine serum albumin (BSA), a predominantly studied lung fluid protein, finding adsorption of BSA onto MWCNTs
- Characterization methods like EDS and XPS used characterize the MWNCTs elementally and SEM imaging reveals BSA adsorbs onto MWCNTs
- Raman spectroscopy reveals that various solutions (water, phosphate-buffered saline (PBS), or Pluronic® F-68 (F-68) are suitable for MWCNT suspension in future work on understanding these interactions

A.

Method	MWCNT composition (%)		
	C	O	Al
EDX	81.8	14.3	3.37
XPS	98.33	1.49	0.18

B.

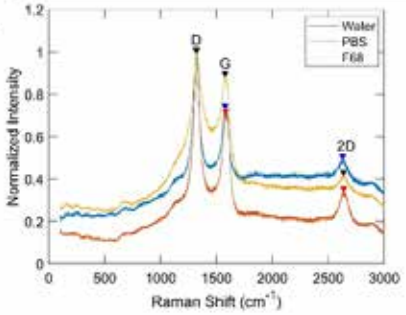

C.

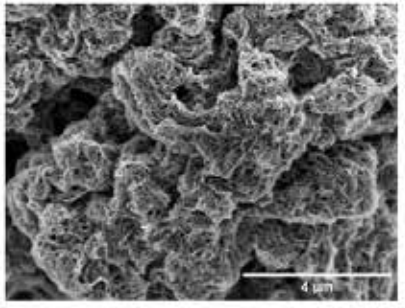

a) *EDS and XPS revealed carbon, oxygen, and aluminum as the primary elements in MWCNTs.*

b) *Raman spectroscopy demonstrated that drying MWCNTs from different suspensions did not alter their physical properties*

c) *SEM depicted the entangled morphology of MWCNTs with absorbed bovine serum albumin, though the proteins were not visibly apparent*

Judith Dominguez, Samantha Holmes, Christine Payne, Department of Mechanical Engineering and Materials Science, Duke University; Work performed partially at Duke Shared Materials Instrumentation Facility.

This work was supported by NSF GFRP. *Publication in progress.*

National Research Priority: White House OSTP R&D Priority–Achieve Better Health Outcomes

Quasi-Continuous Wave Lasing from Directly Patterned and Encapsulated Perovskite Cavity at 260 K

- Metal halide perovskites have emerged as promising gain materials for on-chip lasers in photonic integrated circuits
- To become commercially relevant as economical on-chip light sources, a clear onset of quasi-continuous wave (quasi-CW) and, eventually, continuous wave (CW) lasing at room temperature or Peltier-cooling accessible temperatures from directly patterned perovskite cavities is a critical milestone that must be achieved
- Direct patterning with nanoimprint lithography and encapsulation of the cavity with a thin protective layer of polycarbonate (PC), quasi-CW lasing from $CH_3NH_3PbBr_3$ ($MAPbBr_3$) is demonstrated up to 260 K

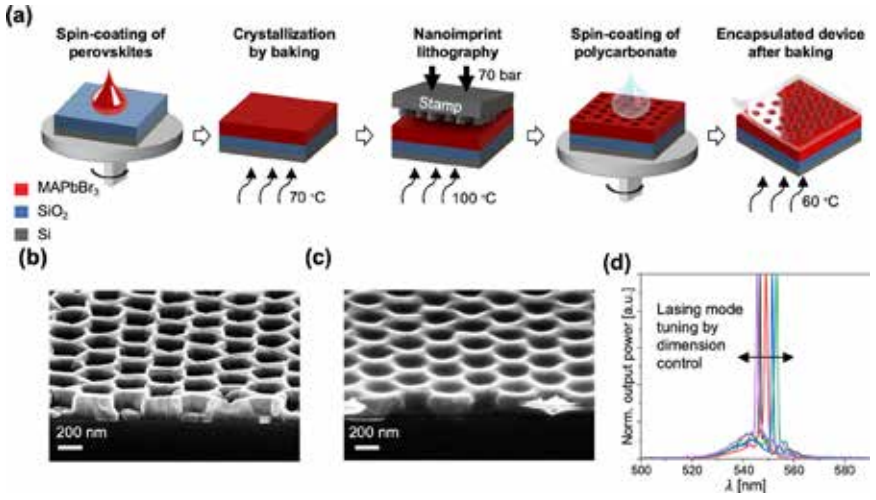

a) Schematic of key fabrication steps

b) SEM images of the nanoimprinted $MAPbBr_3$ 2D PhC laser before PC encapsulation

c) SEM images of the nanoimprinted $MAPbBr_3$ 2D PhC laser after PC encapsulation

d) Lasing mode tuning by PhC dimension control at 200 K

Jiyoung Moon[1], Masoud Alahbakhshi[1], Abouzar Gharajeh[1], Quanwei Li[2], Zhitong Li[1], Ross Haroldson[1], Sunah Kwon[1], Roberta Hawkins[1], Moon J. Kim[1], Walter Hu[1], Xiang Zhang[2], Anvar Zakhidov[1], and Qing Gu[1] , [1]The University of Texas at Dallas [2]University of California, Berkeley; Work performed partially at NC State Nanofabrication Facility.

This work was supported by NSF (ECCS-2209871), ARO (W911NF-19−1−0303), and Welch Foundation (AT-1992−20190330, AT-1617). *ACS Photonics* 2022, 9, 6, 1984-1991.

National Research Priority: DoD Critical Technology Area–Microelectronics

Water Splitting With Silicon p–type-intrinsic–n Superlattices Suspended in Solution

- Particle Suspension Reactors (PSR) are formed by synthesizing high-photovoltage multijunction Si nanowires (SiNWs) that are co-functionalized to catalytically split water
- Spatioselective photo-electrodeposition of oxygen and hydrogen evolution co-catalysts enabled water splitting at infrared wavelengths up to approximately 1,050 nm
- PSR of this type presents a low-cost alternative to traditional rigid (planar) silicon Photoelectrochemical water cell technology

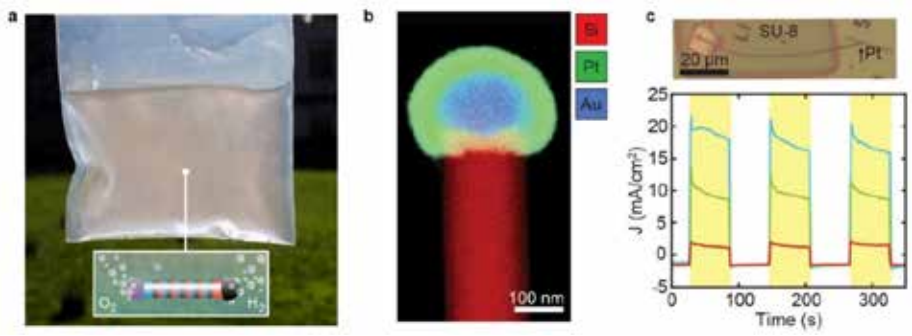

a) *Photo of silicon nanowires suspended in water, demonstrating the PSR architecture; Inset panel shows illustration of a multijunction wire with co-catalysts*

b) *STEM-EDS map of a silicon nanowire with spatioselectively deposited Pt co-catalyst*

c) *Microscope image of a microfabricated single nanowire device for two-electrode photoelectrochemical measurements and the photoelectrochemical current under zero applied bias and chopped illumination at wavelengths of 445 nm (blue), 549 nm (green), and 650 nm (red)*

Taylor S. Teitsworth[1], David J. Hill[1], Samantha R. Litvin[1], Earl T. Ritchie[1], Jin-Sung Park[1], James P. Custer Jr[1], Aaron D. Taggart[1], Samuel R. Bottum[1], Sarah E. Morley[1], Seokhyoung Kim[1], James R. McBride[2], Joanna M. Atkin[1] & James F. Cahoon[1],[1]Department of Chemistry, University of North Carolina at Chapel-Hill, [2]Vanderbilt Institute of Nanoscale Science and Engineering, Vanderbilt University ; Work performed partially at UNC Chapel Hill Analytical and Nanofabrication Laboratory.

This work was supported by NSF (CBET-1914711, CHE-1848278) and DOE (DE-SC0001011). *Nature* 2023, 614, 270-274.

National Research Priority: DOE Energy Earthshots–Clean Fuels & Products Shot

In-Situ Ion Beam-modified Top Contacts to WS_2 Transistors

- 2D semiconductors, having atomically thin bodies, offer improved electrostatic control for transistor scaling
- Unlike 3D bulk semiconductors, the pristine surface of 2D materials lacks dangling bonds, reducing surface traps that hinder device performance
- However, this pristine surface creates a van der Waals gap, acting as a barrier for carrier injection in transistors
- Using an in-situ Ar ion beam, this project modifies a WS_2 2D semiconductor, intentionally breaking chemical bonds and removing sulfur atoms to eliminate the van der Waals gap
- Preliminary results show a significant shift in device polarity, indicating a potential path for tuning polarity through ion beam exposure

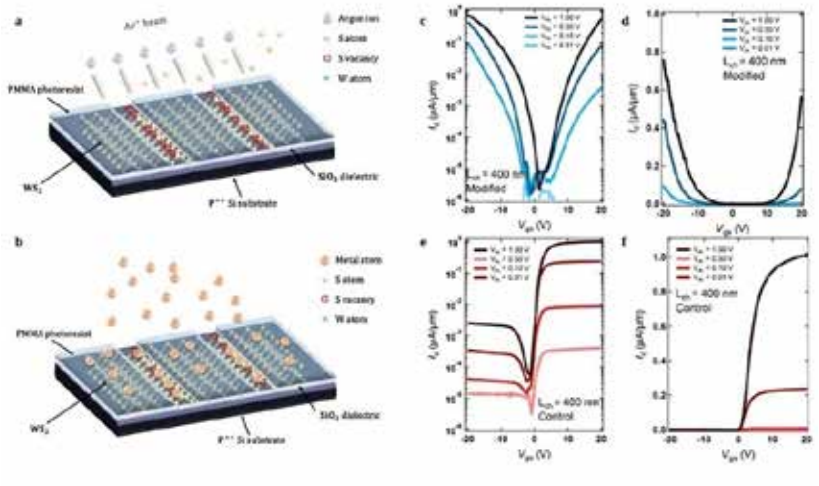

Ion beam-treated 2D semiconductor devices compared to untreated ones. (a) Ar+ beam disrupts WS_2 surface in unprotected areas, creating S vacancies. (b) Metal deposition fills in dangling bonds with W atoms. (c/e) Subthreshold and (d/f) transfer characteristics are compared between ion-beam-modified devices and controls.

Alexander Mangus[1], Baiyu Zhang[1], Hattan Abuzaid[1], Aaron D. Franklin[1,2] , [1]Department of Electrical and Computer Engineering, [2]Department of Chemistry, Duke University; Work performed partially at NC State Analytical Instrumentation Facility and Duke Shared Material Instrumentation Facility.

This work was supported by NSF (ECCS-1508573, ECCS-1508856). *2D Mater.* 6 034005 (2019).

National Research Priority: DoD Critical Technology Area–Microelectronics

National Nanotechnology Coordinated Infrastructure

RTNN

Green MOF-Fabrics: Benign, Scalable Sorption-Vapor Synthesis of Catalytic Composites to Protect against Phosphorus-Based Toxins

- Metal–organic framework (MOF)-fabric composites, crucial for applications like filtration and personal protection, often involve hazardous solvents
- A green synthesis approach is shown using γ-valerolactone (GVL), derived from biomass, as a benign solvent
- GVL proves less toxic, biodegradable, and cost-effective, offering an eco-friendly alternative to solvents like dimethylformamide (DMF)
- The scalable synthesis of MOF-fabrics, evaluated for degrading chemical warfare agents, outperforms DMF-based composites
- This innovative approach broadens MOF-fabric coupling techniques, showcasing a green, scalable sorption-vapor synthesis method applicable to diverse MOFs and fabric chemistries, including Zr MOFs for phosphorus-based chemical decomposition in personal protective equipment

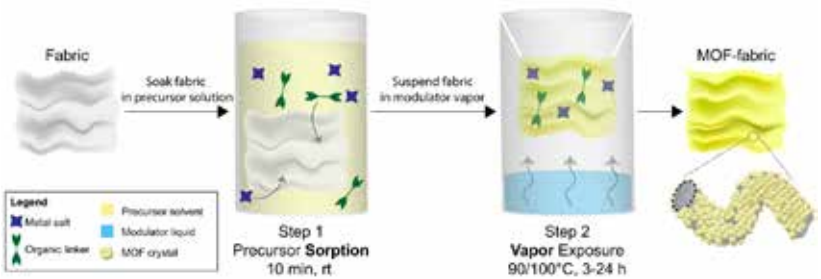

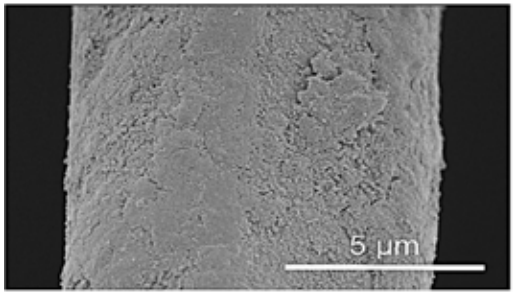

Top: Sorption-Vapor Synthesis of MOF-Fabric Composite: and Schematic of the MOF-Fabric Composite. Bottom: SEM image of spandex@MOF using GVL

Sarah Morgan[1], Morgan Willis[1], Gregory Peterson[2], John Mahle[2], and Gregory Parsons[1], [1]Chemical and Biomolecular Engineering, North Carolina State University, [2]U.S. Army Combat Capabilities Command Chemical Biological Center; Work performed partially at NC State Analytical Instrumentation Facility.

This work was supported by ARO (W911NF-19-2-0154), DOD NDSEG, and DTRA (CB393). *ACS Sustainable Chem. Eng.* 2022, 10, 2699–2707.

National Research Priority: ACS 12 Principles of Green Chemistry–Use of Renewable Feedstocks

Design and Test of a Converging de Laval Nozzle Using Additive Manufacturing

- While compressible flow in nozzles has been extensively studied, the accuracy of experimental results from Additive Manufactured (AM) nozzles remains insufficiently evaluated
- Concerns regarding surface roughness and strength of these nozzles prompted design and testing of converging and “de Laval” nozzles fabricated using ABS filament
- Despite the variable and rough surface profile inherent to AM compared to subtractive manufacturing, the study revealed that at large Reynolds numbers, the surface roughness of 3D-printed nozzles has minimal impact on nozzle flow performance
- Suggests that AM can be effectively employed for nozzle flows at high Reynolds numbers, enabling the rapid demonstration and verification of novel ideas without a significant loss in flow performance

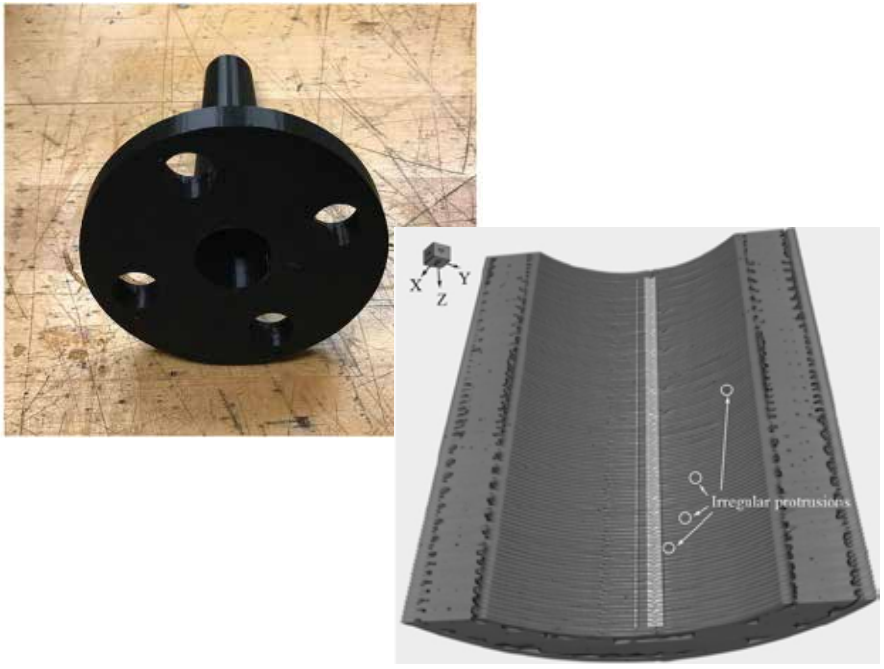

Top/Left: Converging nozzle fabricated by additive manufacturing. Bottom/Right: The converging nozzle topography using a 3D X-ray microscope (nanoCT)

Mingtai Chen[1], Ruksana Baby[2], Seth Dillard[1], Yi Tsung Lee[2], Srinath Ekkad[1], [1]Mechanical and Aerospace Engineering, [2]Materials Science Engineering, North Carolina State University; Work performed partially at NC State Analytical Instrumentation Facility.

*Front. Aerosp. Eng.*1, 2022.

National Research Priority: White House OSTP R&D Priority–Bolster R&D Industrial Innovation (Pre-Commercialization)

National Nanotechnology Coordinated Infrastructure

RTNN

Spark Plasma Sintered, MoNbTi-based Multi-Principal Element Alloys with Cr, V, and Zr

- MoNbTi, MoNbTiZr, CrMoNbTiZr, and MoNbTiVZr multi-principal element alloys (MPEAs) were produced using spark plasma sintering (SPS) for potential use in high-strength applications
- Distinct from traditional arc melting methods, this approach involves cryogenic milling to enhance radiation resistance through defect sinks and increase tensile strength via the Hall-Petch effect
- SPS was selected for consolidation to maintain a fine-grained structure during densification
- Characterization using XRD and SEM revealed the evolution of phases and compositional homogeneity in each alloy
- Thermodynamic analysis highlighted discrepancies between predictions, literature, and characterization, underscoring the need for a thorough investigation into the stability of MPEAs fabricated through solid-state methods for prolonged service life

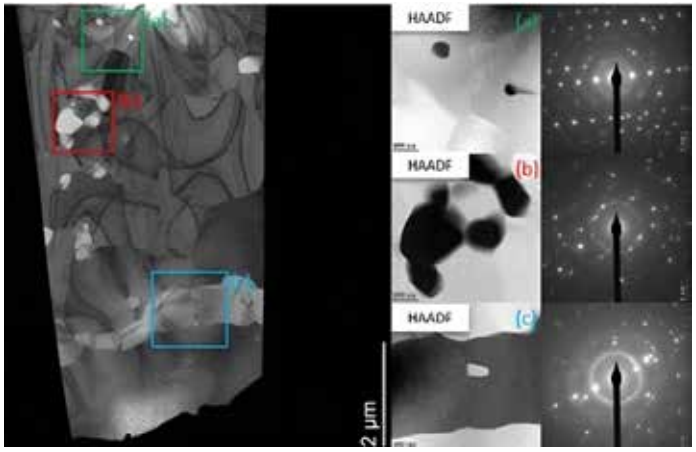

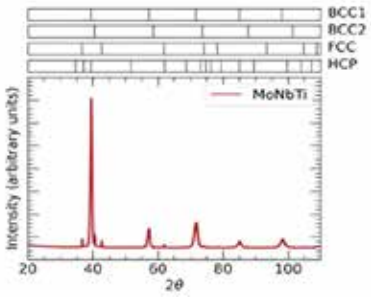

Top: TEM micrograph of the MoNbTi base alloy Higher magnification regions and their associated diffraction patterns are shown in (a), (b), and (c), with XRD spectrum (left)

Geoffrey Beausoleil[1], Djamel Kaoumi[2], [1]Idaho National Laboratory, [2]Department of Nuclear Engineering, North Carolina State University; Work performed partially at NC State Analytical Instrumentation Facility.

This work was supported by DOE (DE-AC07-05ID145142) and NSF (DMR-1726294). *Journal of Alloys and Compounds* 927 (2022)

National Research Priority: DoD Critical Technology Area–Advanced Materials

NeuroLens: Augmented Reality-based Contextual Guidance through Surgical Tool Tracking in Neurosurgery

- External ventricular drain (EVD) insertion, a common neurosurgical procedure, poses challenges in accuracy due to reliance on surgeon expertise and external landmarks
- NeuroLens, an Augmented Reality (AR) system, offers anatomical visualization of a patient's ventricular hologram and contextual guidance for catheter placement
- Utilizing optical tracking and the Microsoft HoloLens 2, NeuroLens achieves real-time, high-accuracy tracking in a patient-specific 3D model
- System was evaluated in a study involving 33 medical students and 9 neurosurgeons, assessing EVD catheter insertion accuracy through MicroCT scans of brain-mimicking molds in a realistic setting

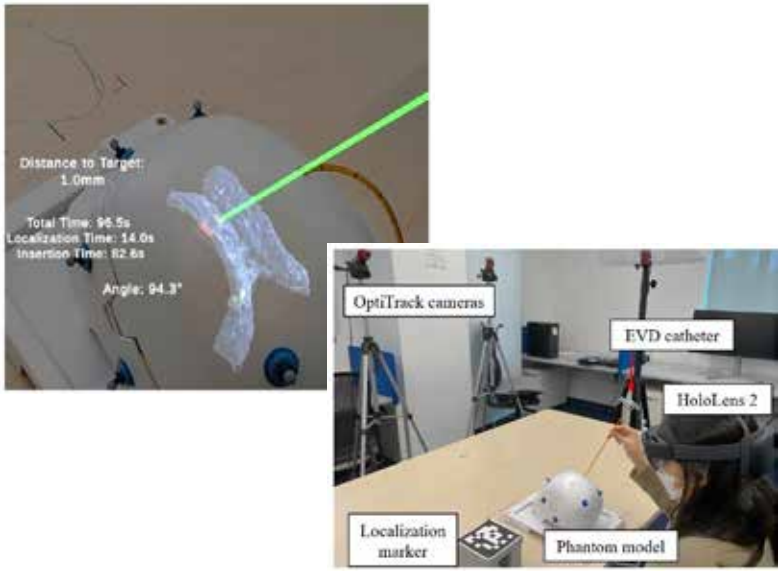

The overall setup of NeuroLens (top-left) and AR-based contextual guidance during the EVD procedure (right)

Sangjun Eom[1], David Sykes[2], Shervin Rahimpour[3], Maria Gorlatova[1,] [1]Department of Electrical and Computer Engineering, Duke University, [2]School of Medicine, Duke University, [3]Department of Neurosurgery, University of Utah; This work performed partially at Duke Shared Materials Instrumentation Facility.

This work was supported by NSF (CNS-2112562, CNS1908051, IIS-2046072). *IEEE International Symposium on Mixed and Augmented Reality (ISMAR)* 2022.

National Research Priority: White House OSTP R&D Priority–Achieve Better Health Outcomes

Enhanced Ferromagnetism in Chemically Reduced 2D $Ti_3C_2T_X$ MXene

- MXenes, a class of 2D transition metal carbides, carbonitrides, and nitrides, are gaining prominence in spintronic nanodevices applications
- This study seeks to overcome the challenges of robust ferromagnetism by enhancing$Ti_3C_2T_x$ MXene through chemical reduction with L-ascorbic acid
- Ferromagnetic loops were observed below 50 K for $Ti_3C_2T_x$ prepared by hydrofluoric acid etching, while L-ascorbic acid treatment significantly increased ferromagnetic ordering, extending it up to 150 K
- The improved ferromagnetism and transition temperature shift could be a result of localized unpaired electrons in Ti-3d orbitals and increased unsaturated Ti atoms
- Chemical reduction via L-ascorbic acid emerges as a promising approach to enhance magnetism in MXenes for developing 2D metallic soft ferromagnets and spintronic devices

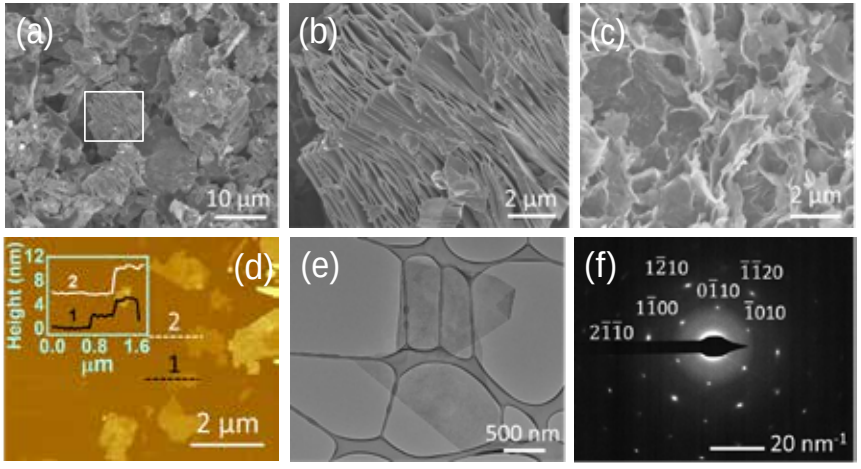

SEM micrograph of (a) multilayered-$Ti_3C_2T_x$ crystals after HF etching of Ti_3AlC_2 MAX phase, (b) multilayered-$Ti_3C_2T_x$ crystal showing the accordion-like structure, and (c) $Ti_3C_2T_x$ powder. (d) Tapping mode AFM image of $Ti_3C_2T_x$ nanosheets on SiO_2/Si, (e) high magnification TEM image of a $Ti_3C_2T_x$ nanosheet suspended over a holey carbon grid, and (f) selected area electron diffraction (SAED) pattern.

Tej Limbu[1], Fei Yan[2], [1]College of Science and Engineering, University of Houston Clear-Lake, [2]Department of Chemistry and Biochemistry, North Carolina Central University; This work performed partially at NC State Analytical Instrumentation Facility.

This work was supported by NSF 1831133, 1523617, 2122044, 1905833, DMR-1420620, DMR-1523617) and DOE (FG02-08ER46531). *Materials Chemistry and Physics* 285 (2022) 12615.

San Diego Nanotechnology Infrastructure (SDNI)

National Nanotechnology Coordinated Infrastructure

Scalable single-mode surface-emitting laser via open-Dirac singularities

Breakthrough in quantum system: Single-aperture cavities are a key component of lasers. However, a suitable physical mechanism that allows single-mode lasing irrespective of the cavity size-a 'scale invariant' cavity or laser-has not been identified yet. The work demonstrates that open-Dirac electromagnetic cavities with linear dispersion exhibit unconventional scaling of losses in reciprocal space, leading to single-mode lasing that is maintained as the cavity is scaled up in size. We demonstrate that their far-field corresponds to a topological singularity of charge two. Open-Dirac cavities unlock avenues for light-matter interaction and cavity quantum electrodynamics.

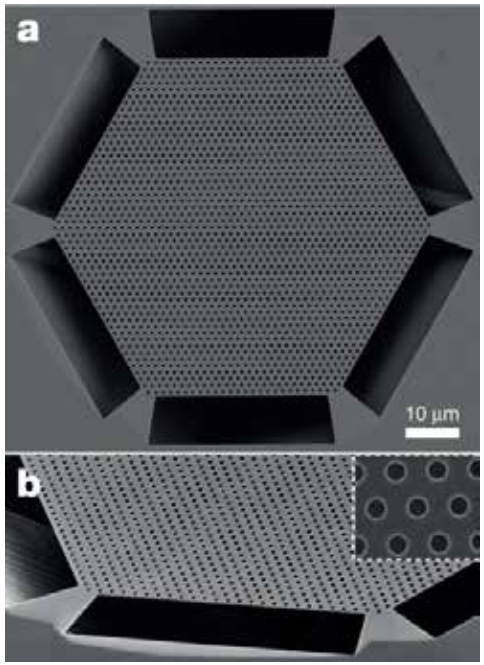

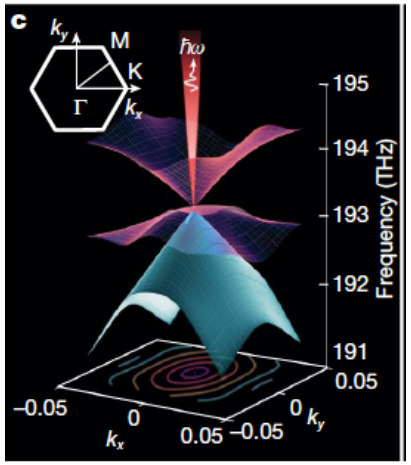

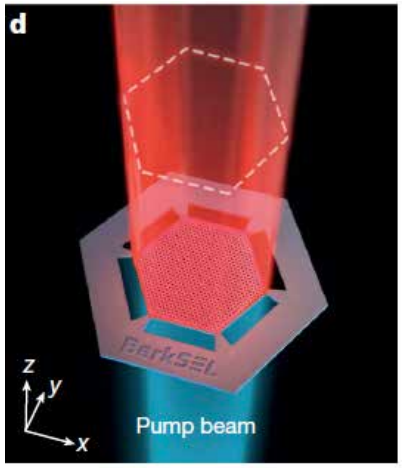

Prof. Boubacar Kante (UC Berkeley). Work performed in part at SDNI.

Nature, 2022 Aug;608(7924):692-698.

National Research Priority: NSF–Quantum Leap

National Nanotechnology Coordinated Infrastructure

sdni San Diego Nanotechnology Infrastructure

A fully integrated autonomous wearable ultrasonic-system-on-patch

Breakthrough in nano medical device: A fully integrated wearable ultrasound system to monitor deep tissues in moving subjects.

The USoP allows continuous tracking of physiological signals from tissues as deep as 164 mm, continuously measuring central blood pressure, heart rate, cardiac output, and other physiological signals for up to 12 hours at a time.

- A fully integrated autonomous wearable ultrasonic-system-on-patch (USoP).
- Machine learning is used to track moving tissue targets and assist the data interpretation.
- Continuous tracking of physiological signals from tissues as deep as 164 mm.
- IoMT: internet-of-medical-things.

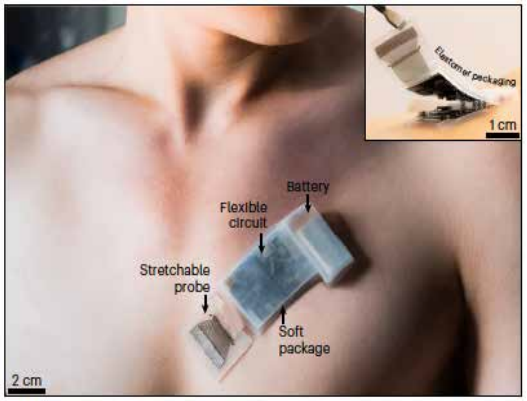

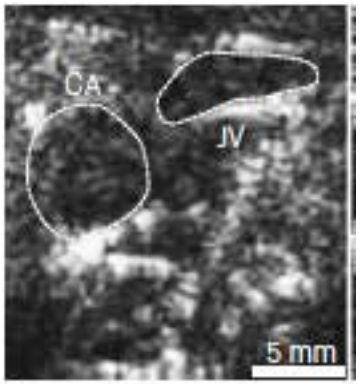

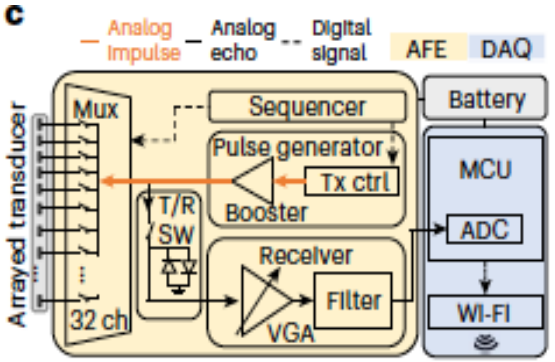

Profs. Sheng Xu, Nuno Vasconcelos, Joe Wang, Erik B. Kistler. Work performed in part at SDNI.

Nature Biotechnology (2023)

National Research Priority: NSF–Growing Convergence Research

National Nanotechnology Coordinated Infrastructure

sdni San Diego Nanotechnology Infrastructure

Scalable Phased-Arrays at 140 GHz using RF and IF Beamforming Techniques

Advances in 5G/6G communications: The paper presents large RF-beamforming arrays (64 elements and higher) capable of 24 Gbps communication systems at 140 GHz and with ±60-degree scanning. The arrays are on grid and can be expanded to 256-elements for 4x8x8 MIMO or other configurations. Also, 2x4 arrays with IF beamforming and with up to 16 Gbps in Tx and Rx modes will be presented. This work shows that standard 45RFSOI and standard packaging used at 28 GHz result in state- of the art performance at D-band, thus ensuring low-cost systems for 6G applications.

The work shows that D-band arrays are a good candidate for high-data rate communications in 5G/6G communications.

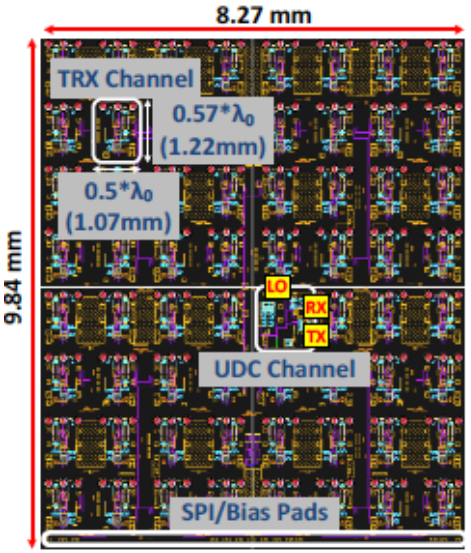

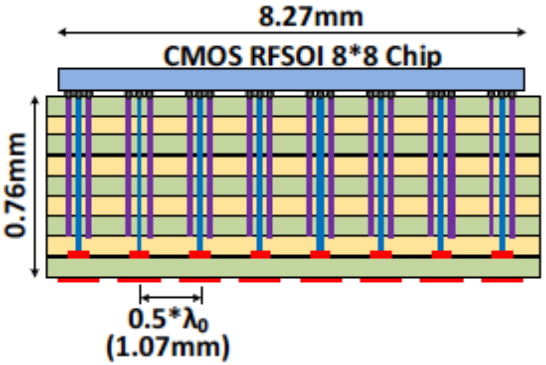

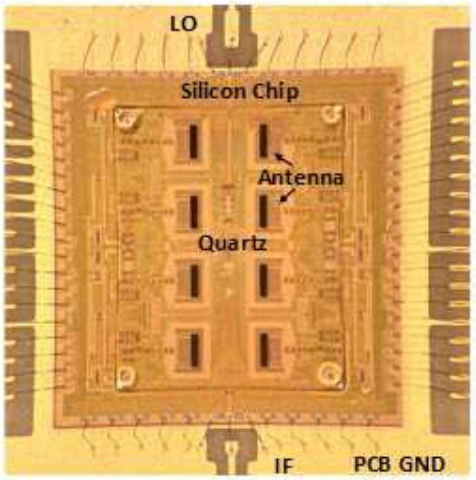

Gabriel Rebeiz (UCSD). Work performed in part at SDNI.

2023 53rd European Microwave Conference (EuMC) (2023*). IEEE Transactions on Microwave Theory and Techniques* (2023)

National Research Priority: CHIPS and Science Act–Semiconductors

A compute-in-memory chip based on resistive random-access memory

Realizing increasingly complex artificial intelligence (AI) functionalities directly on edge devices calls for unprecedented energy efficiency of edge hardware. Compute-in-memory (CIM) based on resistive random-access memory (RRAM) promises to meet such demand by storing AI model weights in dense, analogue and non-volatile RRAM devices, and by performing AI computation directly within RRAM, thus eliminating power-hungry data movement between separate compute and memory. By co-optimizing across all hierarchies of the design from algorithms and architecture to circuits and devices, we present NeuRRAM—a RRAM-based CIM chip that simultaneously delivers versatility in reconfiguring CIM cores for diverse model architectures, energy efficiency, and inference accuracy comparable to software models quantized to four-bit weights across various AI tasks.

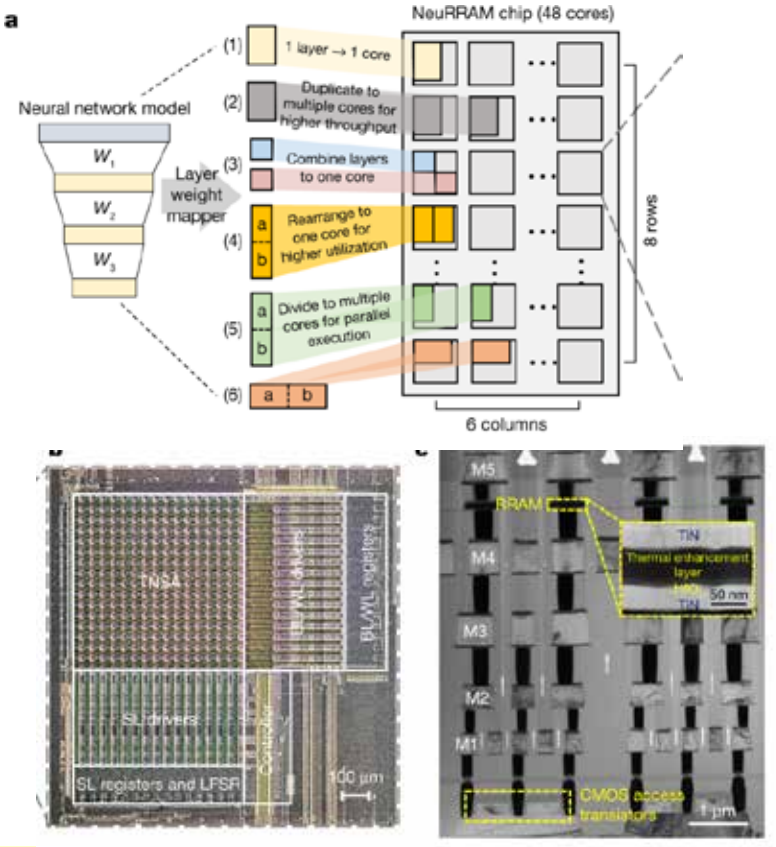

Bin Gao, Siddharth Joshi, Huaqiang Wu (Tsinghua University), H.-S. Philip Wong (Stanford) Gert Cauwenberghs (UCSD). Work performed in part at SDNI.

Nature, 608, 504–512 (2022)

National Research Priority: NSF–Growing Convergence Research

National Nanotechnology Coordinated Infrastructure

sdni San Diego Nanotechnology Infrastructure

Coupling of multiscale imaging analysis and computational modeling for understanding cathode degradation

Advances in energy and sustainability: The lithium-ion battery is a complex system whose electrode thickness ranges from a few tens to several hundred micrometers and consists of components that can be nanosized. This makes it difficult to capture both the structure of the nanosized particles and the volume of the electrode.

Plasma focused ion beam-scanning electron microscopy (PFIB-SEM) enables fast-milling, hence a larger resolved volume compared with FIB-SEM. This method is applied to a thick positive electrode, allowing to resolve the 3D structure of the whole thickness. The electrodes before and after cycling are compared to highlight the structural evolution and degradation mechanisms. The experimental observations are complemented with modeling insights built from the resolved electrode.

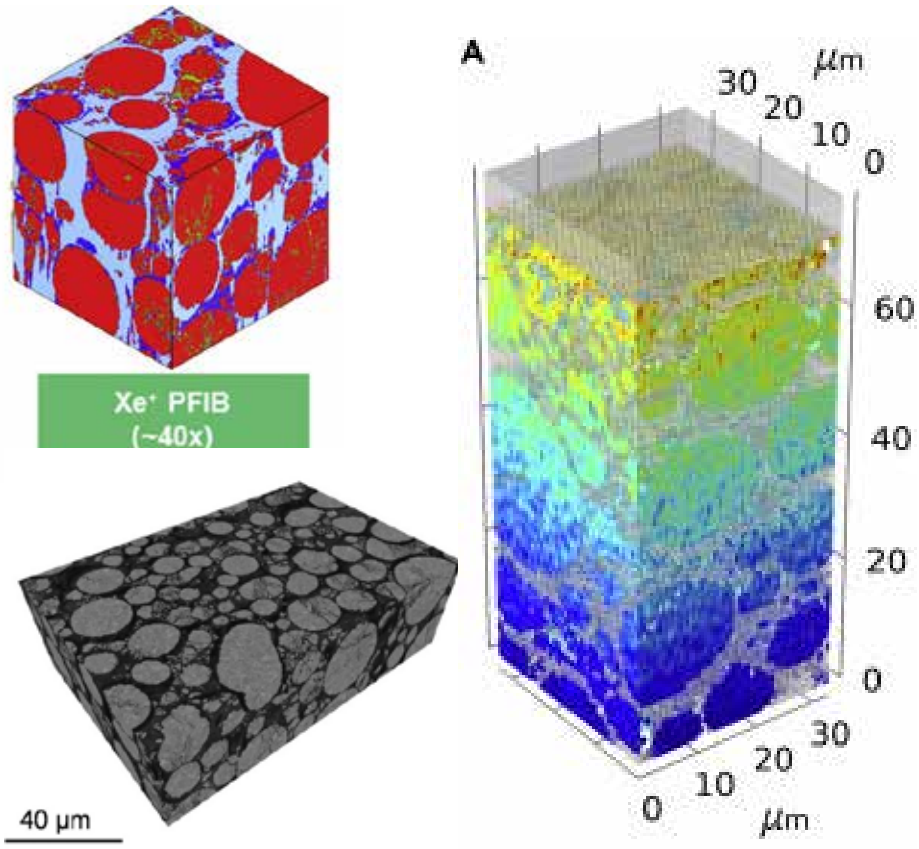

Alejandro A. Franco (LRCS, France), Ying Shirley Meng (U Chicago). Work performed in part at SDNI.

Joule, Volume 7, Issue 1, 18 January 2023, Pages 201-220

National Research Priority: NSF–Growing Convergence Research

National Nanotechnology Coordinated Infrastructure

sdni San Diego Nanotechnology Infrastructure

Soft and Hybrid Nanotechnology Experimental (SHyNE) Resource

National Nanotechnology Coordinated Infrastructure

Artificial extracellular matrix (ECM) scaffolds of mobile molecules enhance maturation of human stem cell-derived neurons

Researchers from **Stupp** and **Kiskinis** labs at Northwestern University focused on the challenge of differentiating induced pluripotent stem cells (iPSCs) into mature neuronal cells in vitro.

They showed that supramolecular peptide amphiphile materials with less cohesive and more fluid-like structure were capable of enhanced bioactivity and increased functional maturation of human iPSCs. These artificial ECM mimetic materials hold promise for aiding functional recovery in central nervous system.

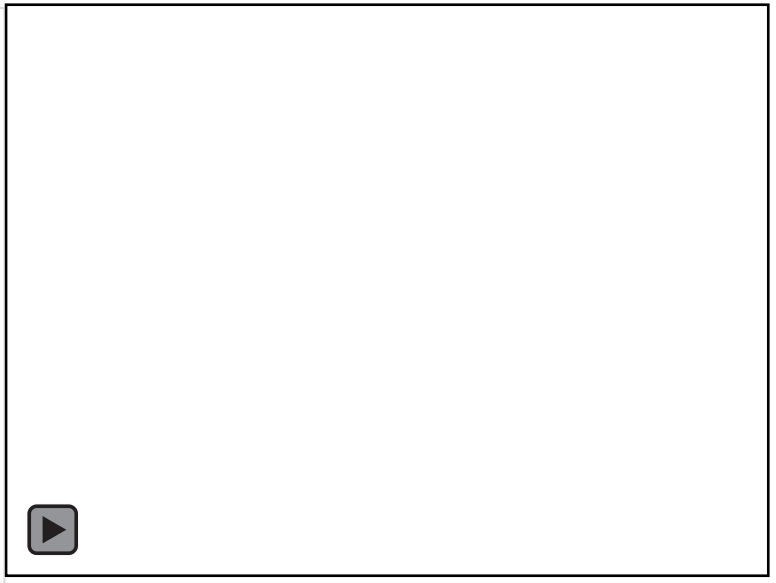

3D illustration of motor neuron (MN) surface receptors interacting with bioactive nanofibers. Illustration by Mark Seniw (ANTEC).

Álvarez, Z.; Ortega, J. A.; Sato, K.; Sasselli, I. R.; Kolberg-Edelbrock, A. N.; Qiu, R.; Marshall, K. A.; Nguyen, T. P.; Smith, C. S.; Quinlan, K. A.; et al., Northwestern University. This work was performed using SHyNE facilities, including Analytical bioNanotechnology Equipment Core (ANTEC) and Peptide Synthesis Core (PS Core) at SQI, as well as at BioCryo and SPID facilities at NUANCE.

Cell Stem Cell **2023**, 30 (2), 219-238.e214.

National Research Priority: NSF–Understanding the Rules of Life

C. elegans Clarinet/CLA-1 recruits RIMB-1/RIM-binding protein and UNC-13 to orchestrate presynaptic neurotransmitter release

Caenorhabditis elegans is a round worm that has been successfully used to study synaptic transmission, the process by which neurons communicate with targets cells in the nervous system through the release of chemical neurotransmitters. Here, we examined how the C. elegans protein, clarinet (CLA-1), an elusive member of the Piccolo, Fife and Rab3-interactingmolecule (Rim) protein family, fits into the organization and function of synaptic release sites in the worm. Using CRISPR/Cas-9 to endogenously tag key synaptic players, we determined the functional hierarchy of these C. elegans synaptic proteins and provide insights into conserved design principles that govern nervous system function.

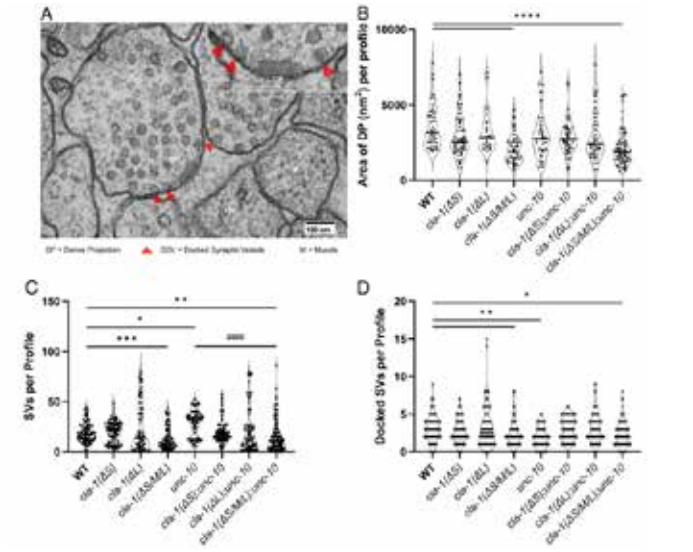

*Fig. 2. Analysis of cla-1 isoform single and double unc-10 mutants using HPF/FS electron microscopy demonstrates that loss of all CLA-1 isoforms is necessary to disrupt synaptic morphology. (A) A single 40-nm cross-section of a synapse from a young adult worm prepared by HPF/FS. Examples of a dense projection and docked SVs (SVs 0 nm distance to the plasma membrane) measured and quantified in this study. (B–D) These data show that loss of CLA-1(L) or (S) alone does not result in the same morphological defects as observed in the cla-1(ΔS/M/L) mutant, indicating that loss of all CLA-1 protein is necessary to disrupt the (B) dense projection and reduce the number of (C) cytosolic and (D) docked SVs. *P < 0.05, **P < 0.01, ***P <0.001, ****P < 0.0001 (C) SV number in cla-1(ΔS/M/L);unc-10 are significantly reduced when compared to unc-10 (####P < 0.0001) and not different from cla-1(ΔS/M/L). One way ANOVA with Tukey's post hoc analysis.*

Krout, Mia, et al. Work performed in part at SHyNE Resource.

Proceedings of the National Academy of Sciences 120.21 (2023): e2220856120.

National Research Priority: NSF–Understanding the Rules of Life

National Nanotechnology Coordinated Infrastructure

SHyNE Soft Hybrid Nanotechnology Experimental Resource

Formation mechanism of high-index faceted Pt-Bi alloy nanoparticles by evaporation-induced growth from metal salts

- This work details the creation of complex, ligand-free high-index faceted Pt nanoparticles using in situ gas-cell transmission electron microscopy (GC-TEM)
- The dynamic behaviors of an alloying and de-alloying process, which involves the coarsening of nanoparticles and a consequent facet regulation stage, has been captured in the real time with nanoscale spatial resolution.
- This work reveal the roles of low melting point metal Bi during the alloying-dealloying process, which provides deep insight in exploring the potential facet regulation of other base metals.

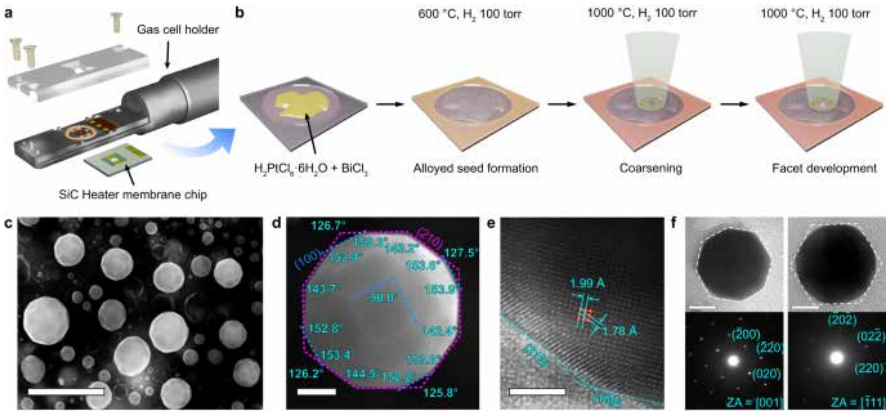

Top: Schematic synthesis process of tetrahexahedral Pt nanoparticles, starting with Bi/Pt salt precursors. Bottom: (S)TEM characterization

Koo, K., Shen, B., Baik, S. I., Mao, Z., Smeets, P. J. M., Cheuk, I. He, K. dos Reis, R., Huang, L., Ye, Z., Hu, X., Mirkin, C. A., Dravid, V. P. Work was performed in part at SHyNE Resource.

This work was supported by NSF ECCS-2025633, DMR-1720139, DMR-0420532, ONR-DURIP N00014-0400798, N00014-0610539, N00014-0910781, N00014-1712870), DMR-1720139, ECCS-1542205. *Nature Communications* 14, 3790 (2023).

National Research Priority: NSF–Growing Convergence Research

National Nanotechnology Coordinated Infrastructure

SHyNE Soft Hybrid Nanotechnology Experimental Resource

Novel in vivo topical treatment of rat tooth enamel to inhibit enamel damage (tooth decay) and biofilm formation

- Dental caries (tooth decay) is the most prevalent human disease caused by oral biofilms, affecting nearly half of the global population despite increased use of fluoride, the mainstay anticaries (tooth-enamel protective) agent
- Ferumoxytol (Fer), a recently FDA-approved iron oxide nanozyme formulation, and stannous fluoride (SnF_2), as anticaries agent, work synergistically to inhibit biofilm accumulation and preventing enamel damage
- STEM-EDS characterization indicates co-delivery of Fer and SnF_2 at tooth surface, and reveals good enamel quality from outward surface inwards

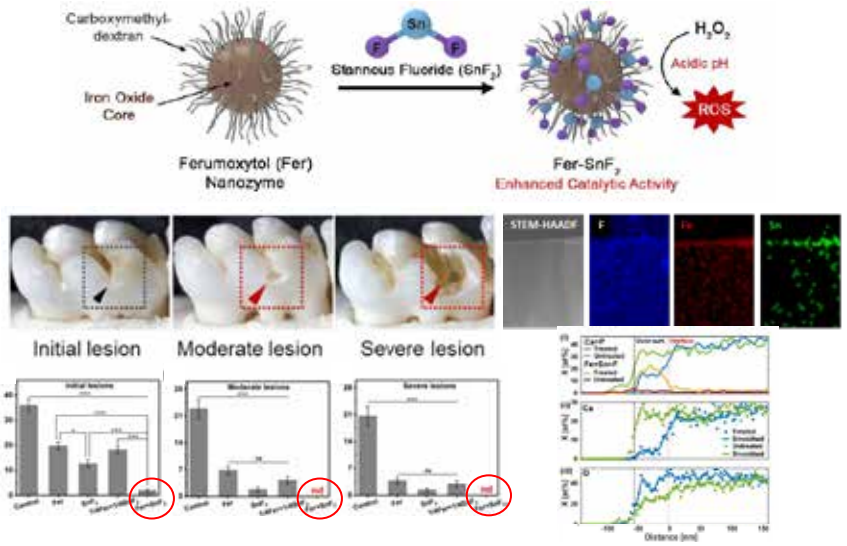

Top: interaction of Ferumoxytol and SnF_2. Bottom left: Fer&SnF_2 synergy in preventing lesions of various severity (red circles). Bottom right: STEM-EDS characterization of treated enamel surface

Huang, Y., Liu, Y., Pandey, N. K., Shah, S. Simon-Soro, A., Hsu, J. C., Ren, Z., Xiang, Z., Kim, D., Ito, T., Oh, M. J., Buckley, C, Alawi, F., Li, Y. Smeets, P. J. M., Boyer, S., Zhao, X., Joester, D., Zero, D. T., Cormode, D. P., Koo. Work was performed in part at SHyNE Resource.

This work was supported by NIH R01-DE025848, S10OD026871, TL1TR001423, R90DE031532 and NSF ECCS-2025633. *Nature Communications* 14, 6087 (2023).

National Research Priority: NSF–Understanding the Rules of Life

Unveiling the influence of selective-area-regrowth interfaces on local electronic properties of GaN p-n junctions for efficient power devices

Correlated nanoscale mapping of doping, conductivity, and dopant complexes was achieved with atom probe tomography (APT), scanning spreading resistance microscopy (SSRM), and cathodoluminescence (CL) spectroscopy to identify how etching and non-planar regrowth processes limit diode performance via the introduction of unintentional dopants and defect states.

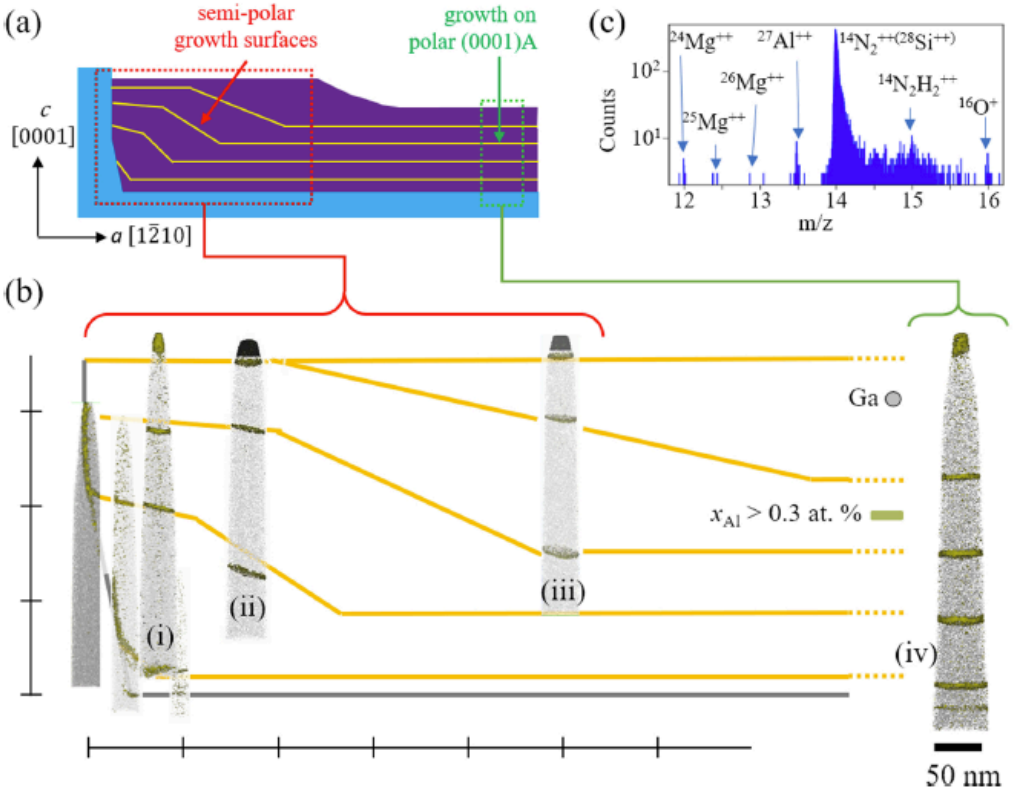

(a) *Schematic of regrowth regions.*
(b) *Atom probe tomographic reconstructions from different locations in (a). Yellow lines represent the shape of the regrowth interface at various growth times.*
(c) *Section of APT mass spectrum with peaks for Mg, Al, and O.*

Alexander S. Chang, Bingjun Li, Sizhen Wang, Sam Frisone, Rachel S. Goldman, Jung Han, Lincoln J. Lauhon, Work performed in part at SHyNE Resource.

Nano Energy 102 (2022) 107689.

National Research Priority: NSF–Growing Convergence Research

National Nanotechnology Coordinated Infrastructure

SHyNE Soft Hybrid Nanotechnology Experimental Resource

Compositional Gradient Thin Films for Material Selection

It is axiomatic that a materials properties will depend on the materials composition.

Even a system as simple as two metals can be quite complicated.[a]

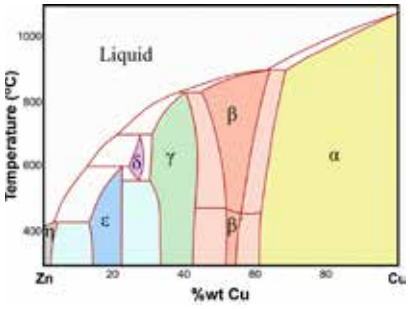

Thin film systems are further complicated by the influence of the substrate.

In such situations, a graded composition film is a powerful tool for materials discovery.

The Pulsed Laser Deposition Facility has implemented hardware and software such that alternating mono-layer wedges of two materials, A&B, can be deposited by PLD to form a graded composition film.

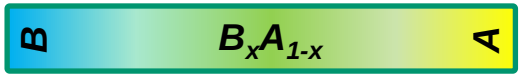

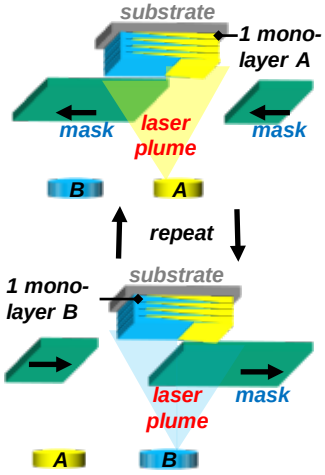

The X-Ray Diffraction Facility can configure instruments to achieve a sampling size as small as 400μm to allow the film to be analyzed as a function of location[b] *(i.e. composition).*

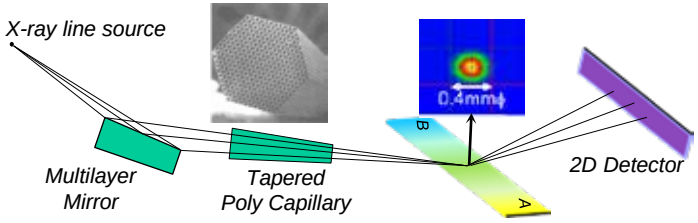

[a] E. Kapara, et al., Journal of Hazardous Materials 262 (2013) 606–613
[b] K. V. L. V. Narayanachari, et al., *ACS Applied Electronic Materials* 2, 11, (2020) 3571–3576

National Research Priority: NSF–Growing Convergence Research

National Nanotechnology Coordinated Infrastructure

SHyNE Soft Hybrid Nanotechnology Experimental Resource

Equipment Predictive Maintenance

Major equipment

Monitor status, predict future failure

Logfile data engineering → *ML* → *Dashboard & prediction*

Example: Deep RIE

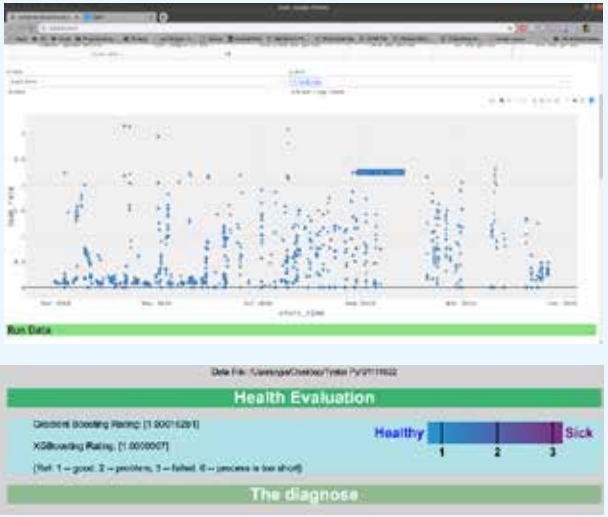

Dashboard for leak rate monitoring
Overall health evaluation and prediction

Small essential equipment

Real-time anomaly detection and alert

Inline sensors Micro processor → *ML* → *Dashboard & anomaly detection*

Example: Chiller

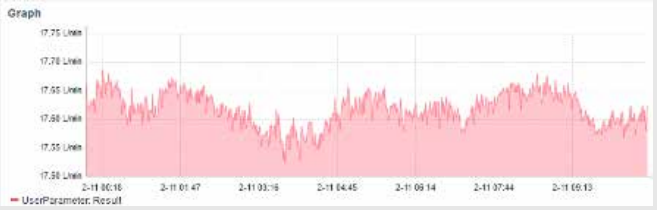

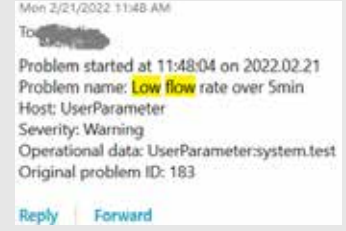

Real-time flow rate and email alert

Medium equipment

Reduce routine checkup workload

Camera & Edge device → *AI* → *Data record Dashboard*

Example: Parylene coater

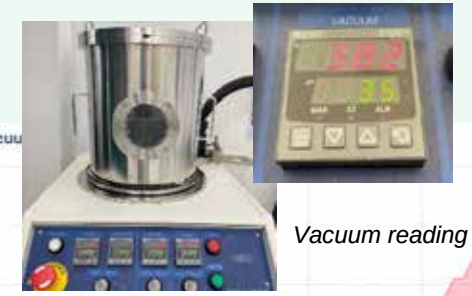

Real-time image-to-digit conversion and recording. Reduce in-person observation

National Research Priority: NSF–Harnessing the Data Revolution

National Nanotechnology Coordinated Infrastructure

SHyNE Soft Hybrid Nanotechnology Experimental Resource

Southeastern Nanotechnology Infrastructure Corridor (SENIC)

National Nanotechnology Coordinated Infrastructure

Formation of Paddle Interlocking System in the Mouse Eye Lens

The transparent eye lens permits incident light to pass through and help form a focused image on the retina. All lens fiber cells contain a high concentration of crystallin proteins for increasing the refractive index. The fiber cell membranes also undergo major specializations to develop an elaborate paddle interlocking system that is required for maintaining the structural order, stability, and lens transparency, especially during the deformation associated with visual accommodation. However, the timing and the regulatory factors for the paddle formation during lens development are not clear.

In this study, we used scanning EM to investigate the formation and changes of paddle interlocking system in the wild-type mice. The images were collected sequentially from the superficial region of the young fiber cells (left) toward the deeper region of the older fiber cells (right) during lens maturation and aging. In addition, we tested the effect of certain actin-regulatory proteins (e.g., Cap2) on the formation and maturation of the paddle system using the gene knock-out mice.

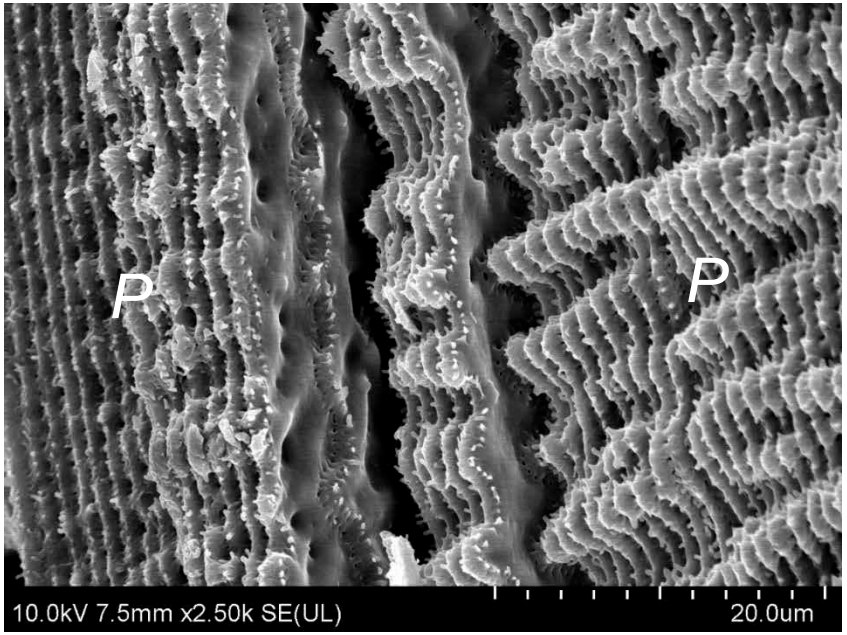

SEM of fiber cell membrane surface shows that paddle inter-locking structures (p) were first formed in the young cells (left), then elaborated into a complex system in the older cells (right).

W.K. Lo1, S.K. Biswas1, S. *Cheheltani2 and V. Fowler2, 1Neurobiology, Morehouse School of Medicine, Atlanta, GA; 2Biological Sciences, University of Delaware, Newark, DE.* Work performed at SENIC facility at Georgia Tech.

This work was supported by a SENIC Catalyst Grant through NSF Award # ECCS-2025462.

National Research Priority: NSF–Understanding the Rules of Life

National Nanotechnology Coordinated Infrastructure

SENIC Southeastern Nanotechnology Infrastructure Corridor

III-Nitride Triangular Microcantilevers for Multimodal Sensing Applications

This work presents the design, fabrication, and characterization of AlGaN/GaN triangular microcantilevers for UV, Volatile Organic Compounds (VOCs), and airflow detection. A portable IoT system was developed for this MEMS-based sensor for multimodal sensing applications.

The study utilizes a novel UV photodetector structure employing dual AlGaN/GaN heterostructure-based two-dimensional electron gas (2DEG) channels and a semi-insulating GaN layer in a triangular microcantilever shape. We demonstrated a technique for real-time detection of VOCs using AlGaN/GaN dual-channel triangular microcantilevers. These cantilevers were exposed to various VOCs, and corresponding changes in electrical characteristics were recorded and monitored. Additionally, this work showcases a single-channel triangular microcantilever-based airflow sensor.

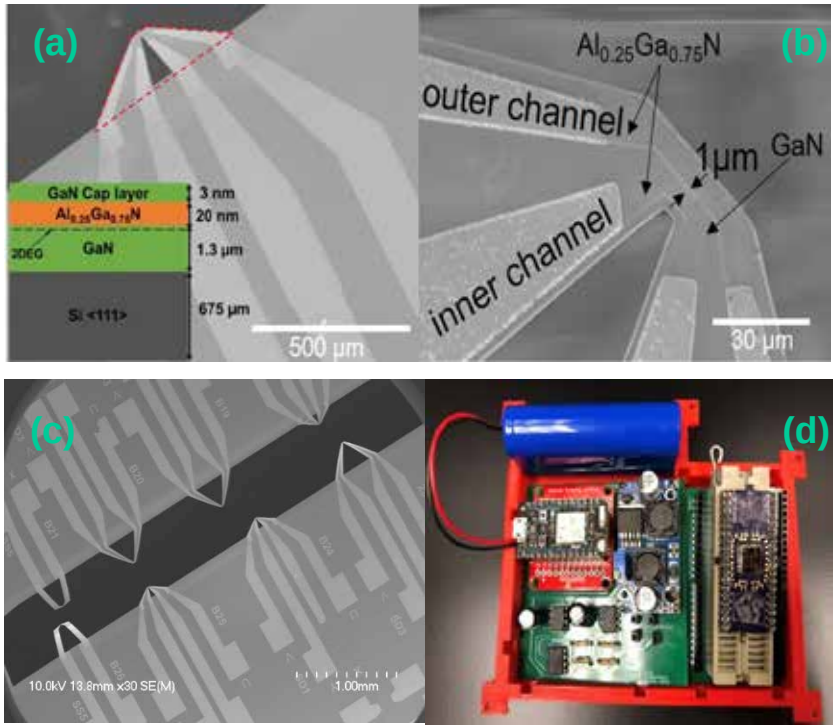

(a)-(c). SEM images of Triangular Microcantilever sensors, (d). Portable IOT system for multimodal sensing applications

Balaadithya Uppalapati, Durga Gajula, Goutam Koley, Holcombe Department of Electrical and Computer Engineering, Clemson University, Clemson, SC. Fabrication work performed at Georgia Tech's Institute for Electronics and Nanotechnology (SENIC).

This work was supported by NSF ECCS-1809891 and TI-2234512. *Sensors*, 23(17), p.7465.

BEOL Compatible Oxide Power Transistors for On-Chip Voltage Conversion

To support vertical power delivery network (PDN) in heterogeneous 3-dimensional (H3D) integrated circuits with multi-tier stacking, we demonstrated high-voltage back-end-of-line (BEOL) compatible devices: tungsten-doped indium oxide (IWO) power transistors and high-breakdown voltage (V_{BD}) superlattice MIM capacitors. Monolithic co-integration of enhancement(E)- and depletion(D)-mode transistors are demonstrated for high-side and low-side switches, respectively, to implement a switched-capacitor (SC) based DC-DC voltage converter. Using calibrated measurement data from fabricated devices, a BEOL compatible DC-DC converter was designed to demonstrate efficient voltage conversion in a multi-tier H3D transformer accelerator with multiple domains: logic (0.75 V), eDRAM (1.5 V), and ferroelectric transistor (FeFET) non-volatile memory (3 V).

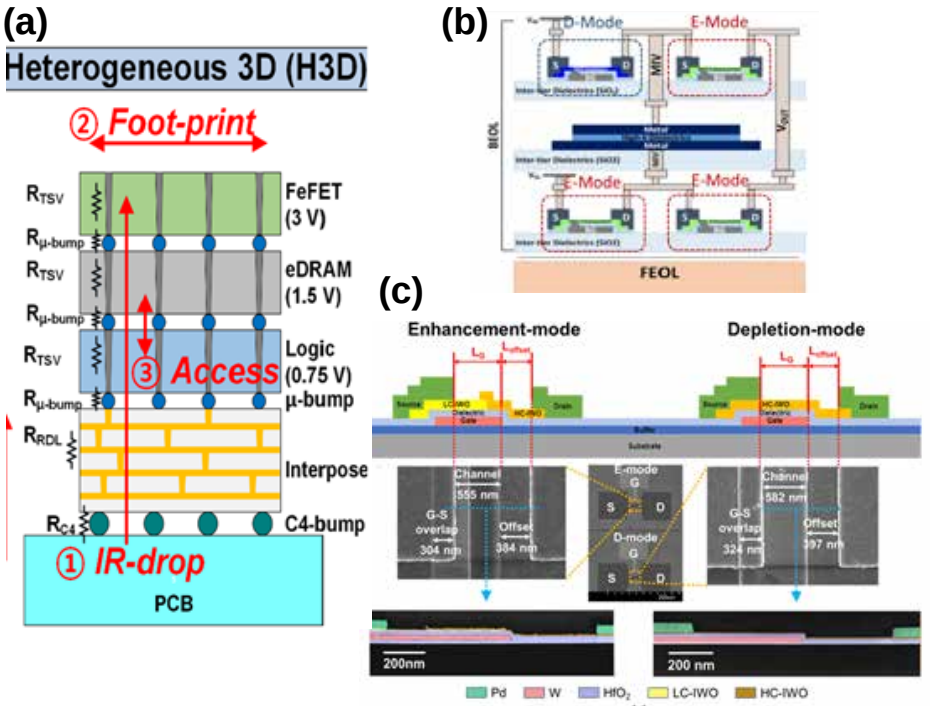

Schematic diagram of (a) H3D stacked transformer accelerator and (b) SC based DC-DC voltage converter. (c) SEM and TEM images of E- and D-mode IWO power transistors co-integrated on the same chip.

Sunbin Deng, Jungyoun Kwak, Junmo Lee, Shimeng Yu and Suman Datta, School of Electrical and Computer Engineering, Georgia Institute of Technology. Work performed at Georgia Tech's Institute for Electronics and Nanotechnology (SENIC).

This work was supported by SRC/DARPA JUMP 2.0 center CHIMES. *2023 IEEE International Electron Devices Meeting (IEDM).*

National Research Priority: DoD Critical Technology Area–Microelectronics

National Nanotechnology Coordinated Infrastructure

SENIC Southeastern Nanotechnology Infrastructure Corridor

Improved Reliability and Performance in BEOL Compatible W-doped In_2O_3 Dual-Gate Transistor

We investigate both hot carrier induced degradation (HCD) and positive bias stress instability (PBTI) in back-end-of-the-line (BEOL) compatible tungsten-doped In2O3 (IWO) dual-gate field effect transistor (DG-FET) with scaled-EOT (1.18 nm) gate stack. The DG-FET shows simultaneous improvement in threshold voltage (V_T) stability and enhancement in device performance. The DG-FET exhibits 11mV V_T-shift under 4.24 MV/cm oxide field (E_{ox}=$V_{overdrive}$/EOT) stress for 1Ks, while exhibiting drive current gain of 3x over the back-gate (BG) FET. This makes the IWO DG-FET a viable BEOL transistor candidate for enabling next generation monolithic 3D (M3D) integrated circuits.

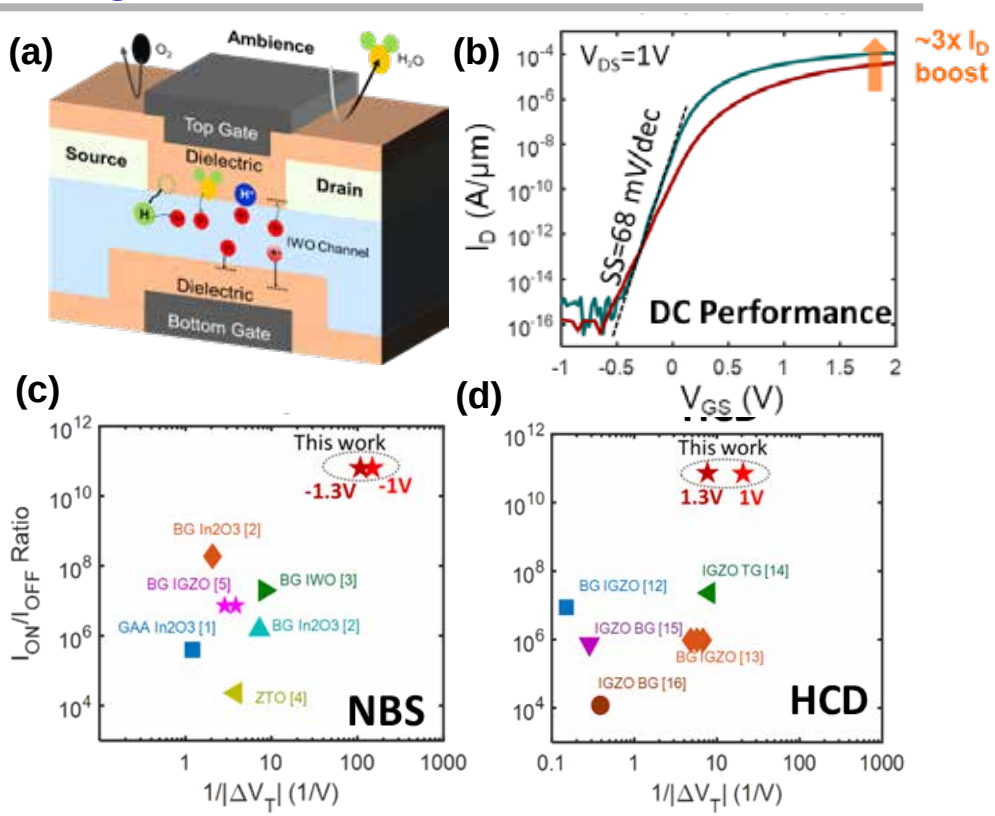

(a) Schematic diagram and (b) transfer characteristics of dual-gate IWO FETs. Benchmark of dual-gate IWO FETs on (c) NBS and (d) HCD reliability compared to other BEOL compatible oxide FETs.

Khandker Akif Aabrar, Sharadindu Gopal Kirtania, Sunbin Deng and Suman Datta, School of Electrical and Computer Engineering, Georgia Institute of Technology. Work performed at Georgia Tech's Institute for Electronics and Nanotechnology (SENIC)..

This work was supported by the SRC/DARPA JUMP 2.0 center PRISM. *2023 IEEE International Electron Devices Meeting (IEDM).*

National Research Priority: DoD Critical Technology Area–Microelectronics

National Nanotechnology Coordinated Infrastructure

SENIC Southeastern Nanotechnology Infrastructure Corridor

Ferroelectric gate stack with a tunnel dielectric insert for NAND applications

To overcome the limits of the FE gate stack in NAND applications, our work demonstrates the ability to surpass current barriers by inserting a tunnel dielectric layer. We experimentally show that the insertion of an Al_2O_3 layer in the middle of the ferroelectric $Hf_{0.5}Zr_{0.5}O_2$ (HZO) stack significantly enhances the memory window (MW). For instance, the MW increases from 3 V in a reference HZO gate stack without the Al_2O_3 insert to as high as 7.3 V, representing a more than 2x improvement, in the engineered HZO-Al_2O_3-HZO stack with the same total thickness and a write voltage ≤15 V. A comprehensive design space exploration of the gate stack of FEFETs, based on the model, reveals a pathway to achieving a 12 V MW.

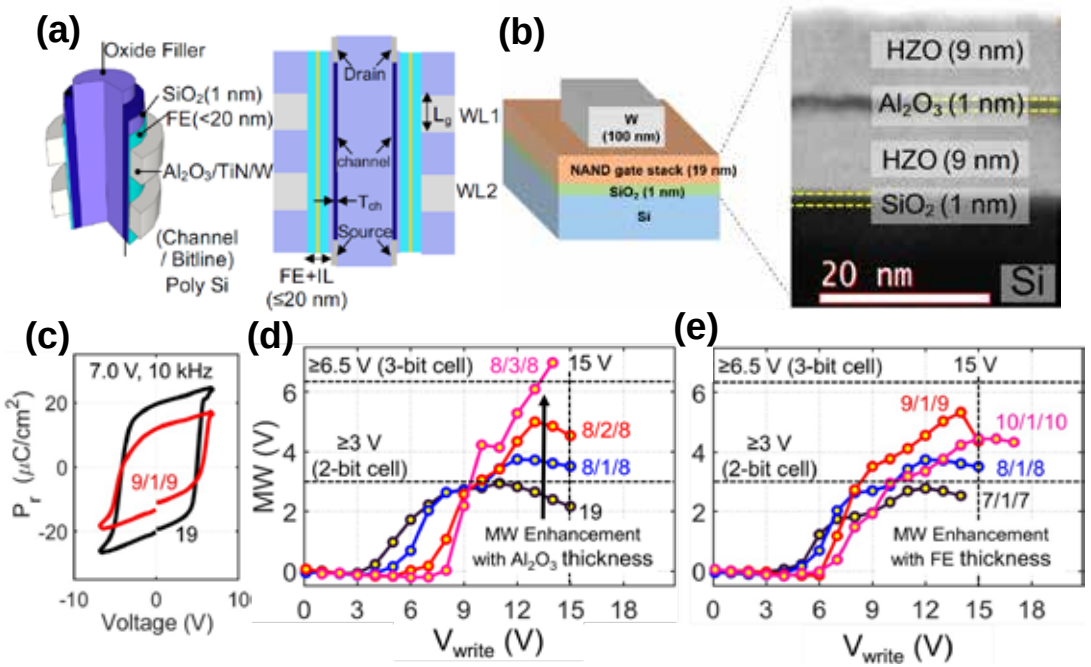

Schematic diagram of (a) Proposed gate stack with FE/Al_2O_3/FE, (b) HR-TEM of gate stack HZO(9)/Al_2O_3(1)/HZO(9), (c) PV hysteresis, (d~e) MW Enhancements with Al_2O_3 thickness (d) and FE thickness (e).

Dipjyoti Das, Lance Fernandes, Chinsung Park, Winston Chern, Asif Khan, School of Electrical and Computer Engineering, Georgia Institute of Technology. Work performed at Georgia Tech's Institute for Electronics and Nanotechnology (SENIC).

This work was supported by Samsung and SRC/DARPA JUMP 2.0 center CHIMES. *2023 IEEE International Electron Devices Meeting (IEDM).*

National Research Priority: DoD Critical Technology Area–Microelectronics

Developing Ferroelectric AlScN for Efficient Memory

Intro: AlxSc1-xN, which has recently been shown to be ferroelectric with a large polarization, has the potential for memory applications because it can be integrated with current semiconductor nanofabrication processes. The energy it takes to switch a ferroelectric material's state/memory is significantly less than the traditional devices – these energy savings span across thousands of devices.

Problem: The electric field needed for switching the polarization (Ec) in AlxSc1-xN is near the electrical breakdown (Ebd) of the material. AlxSc1-xN also has a propensity to exhibit faceting – which increases the likelihood of breakdown.

Approach: This work investigates the impact of deposition temperature on faceting as a route to decrease the likelihood of breakdown. We propose that increasing temperature should reduce faceting by increasing adatom mobilities during deposition.

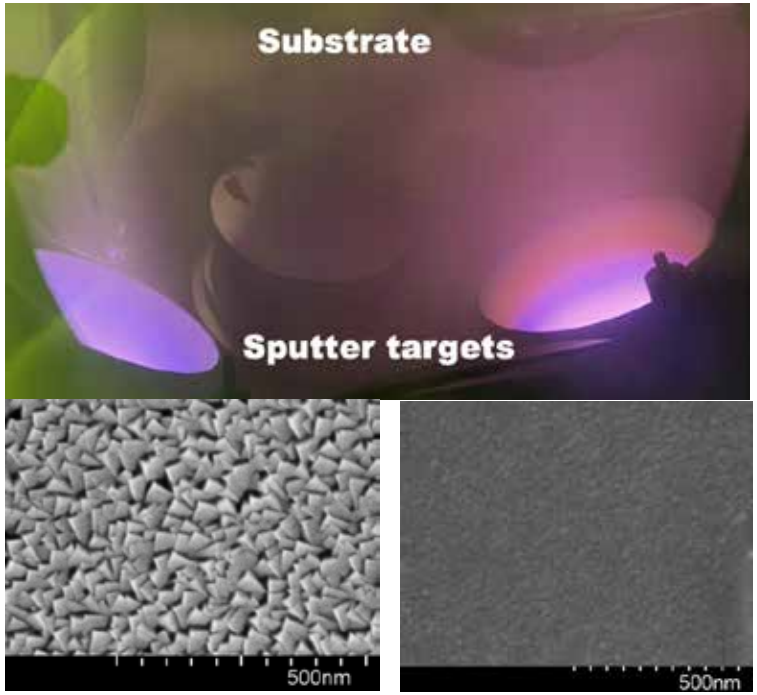

Top: AJA Chamber with Al and Sc plasma lit from DC & RF targets
Bottom: SEM images showing faceted sample (left) and then the non-faceted sample (right). The left is grown at 350C and DC only; the right is grown at 450C RF/DC; growths at 5mTorr.

John Allen Wellington-Johnson, Lauren M. Garten, School of Materials Science & Engineering, Georgia Institute of Technology. Work performed at Georgia Tech's Institute for Electronics and Nanotechnology (SENIC).

This work was supported by a GT IEN Facility Seed Grant.

National Research Priority: DoD Critical Technology Area–Microelectronics

Phage Discovery and Genomics

During the Fall 2023 semester at Spelman College, seven undergraduate students took Phage Discovery (BIO350), a 4-credit elective course in the Biology curriculum. This course was the first part of a two-semester, course-based undergraduate research (CURE) program that is based on a model developed by the Howard Hughes Medical Institute (HHMI) in collaboration with colleges and universities around the United States. *Arthrobacter globiformis* and *Gordonia rubripertincta* were used as bacterial hosts. Each of these students isolated a phage from soil and imaged their sample on a transmission electron microscope (TEM).This was the students first experience seeing how a TEM works.

For Spring 2024 these seven students are enrolled to take Phage Genomics (BIO351). DNA from each sample was sequenced on a Nanopore MinION at Spelman College. Students will assemble and annotate their phage genome and hopefully publish their research.

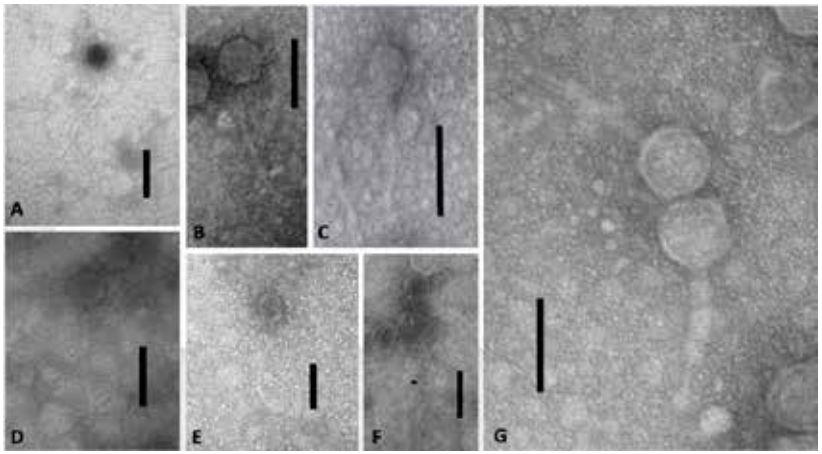

Figure1A-G. Phages isolated from soil. These phages represent members of the Siphoviridae (A-F) and Myovirdae (G). *Arthrobacter globiformis* (B, C, E, F) and *Gordonia rubripertincta* (A, D, G) were used as bacterial hosts. Scale bar is 100 nm.

James T. Melton III, Spelman College. Work performed at SENIC at Georgia Tech.

This work was supported by a SENIC Catalyst Grant through NSF Award # ECCS-2025462.

National Research Priority: NSF–INCLUDES

National Nanotechnology Coordinated Infrastructure

SENIC Southeastern Nanotechnology Infrastructure Corridor

Novel Bismuth Oxyhalides (BiOX) Nanomaterials for Energy Storage Applications

A collaborative team of STEM faculty and undergraduate researchers is actively involved in synthesizing and characterizing chemically modified bismuth oxyhalide solid electrolyte nanomaterials. Their primary goal is to advance the development of a stable bismuth oxyhalide lithium-ion conducting electrolyte, particularly resilient in ambient air and when interacting with standard anodes and cathodes, emphasizing compatibility with lithium metal. The Joint School of Nanoscience and Nanoengineering (JSNN) serves as a crucial hub, offering essential infrastructure, including the use of the JEOL JSM-IT800 Schottky FESEM for imaging and characterization, contributing to a comprehensive understanding of the synthesized Bismuth Oxyhalide Nanomaterials.

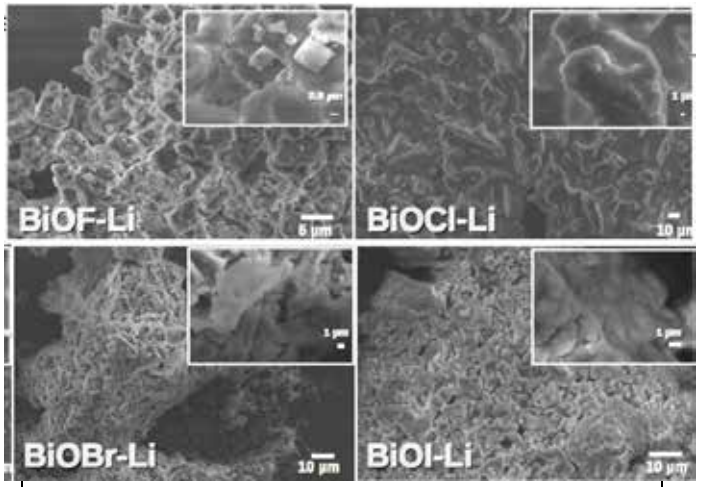

The JEOL JSM-IT800 Schottky FESEM at JSNN is used for imaging and characterization, playing a crucial role in enhancing the overall understanding of the synthesized Bismuth Oxyhalide Nanomaterials.

Darkeyah G. Reuven, Natural and Behavioral Sciences Department, Johnson C. Smith University. Work was performed at SENIC at Georgia Tech.

This work was supported by a SENIC Catalyst Grant through NSF Award # ECCS-2025462.

National Research Priority: NSF–INCLUDES

National Nanotechnology Coordinated Infrastructure

SENIC Southeastern Nanotechnology Infrastructure Corridor

Digital data storage on DNA tape using CRISPR base editors

While the archival digital memory industry approaches its physical limits, the demand is significantly increasing, therefore alternatives emerge. Recent efforts have demonstrated DNA's enormous potential as a digital storage medium with superior information durability, capacity, and energy consumption. This work created a molecular digital data storage system called "DNA Mutational Overwriting Storage" (DMOS) that stores information by leveraging combinatorial, addressable, orthogonal, and independent in vitro CRISPR base-editing reactions to write data on a blank pool of greenly synthesized DNA tapes. As a proof of concept, a bitmap representation of JSNN logo and the title of this study was written on DNA tapes, and accurately recovered later.

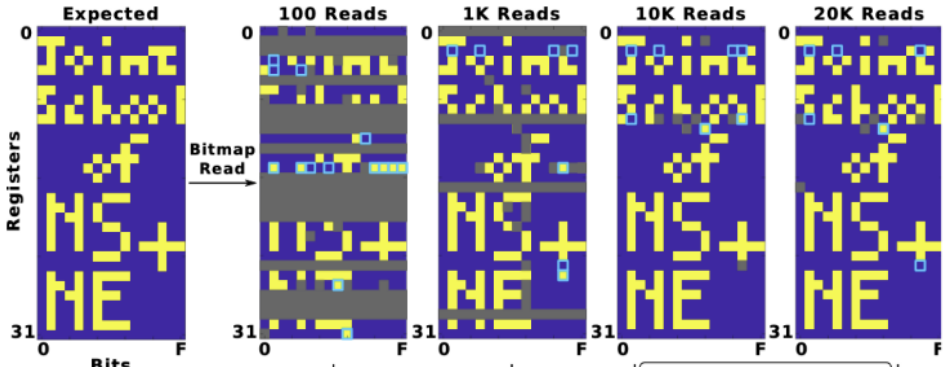

Bitmap representation of the logo of our school (the Joint School of Nanoscience (NS) and Nanoengineering (NE)) written on DMOS tap

Reza Zadegan, Dennis LaJeunesse, Eric Josephs, Departments of Nanoengineering and Nanoscience, North Carolina A&T State University and UNCG. Work performed at Joint School of Nanoscience and Nanotechnology (SENIC).

This work was supported by NSF MCB 2027738, NIH award # R35GM133483. *Nat Commun* 14, 6472 (2023)

National Research Priority: NSF–Understanding the Rules of Life

National Nanotechnology Coordinated Infrastructure

SENIC Southeastern Nanotechnology Infrastructure Corridor

Impacts of Forest Fire Ash on Aquatic Mercury Cycling

Mercury (Hg) is a ubiquitous contaminant in the environment and its methylated form, methylmercury (MeHg), poses a worldwide concern for humans and wildlife, primarily through fish consumption. Global production of forest fire ash, derived from wildfires and prescribed burns, is rapidly increasing due to a warming climate, Herein, we compared the differences of wildfire ash with activated carbon and biochar on the sorption of aqueous inorganic Hg and sedimentary Hg methylation. Sorption of aqueous inorganic Hg was greatest for wildfire ash materials among all of the solid sorbents evaluated. Overall, our study indicates that while wildfire ash can sequester aqueous Hg, the leaching of its labile organic matter may promote production of toxic MeHg in anoxic sediments, which has an important implication for potential MeHg contamination in downstream aquatic ecosystems after wildfires.

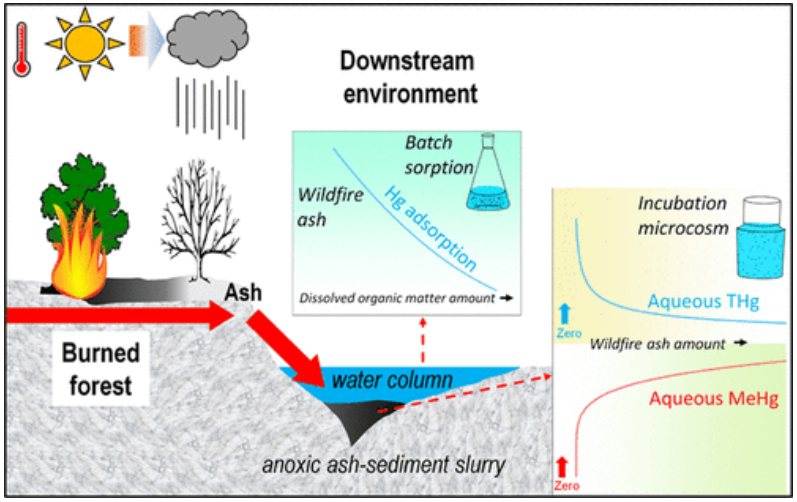

Global production of forest fire ash, derived from wildfires and prescribed burns, is rapidly increasing due to a warming climate, but their interactions with aqueous and sedimentary Hg are poorly understood.

H. H. Li, R. A. Dahlgren, T. C. Hoang, and A. T. Chow, UNCG, UC Davis, Auburn U and Clemson U, Partial work performed in part at Joint School of Nanoscience and Nanoengineering (SENIC).

This work was supported by NSF EAR-1711642, NSF CBET-1917156 and NIFA # 2018-67019-27795. *Environ Sci Technol.* 2022 Aug 16;56(16):11835.

National Research Priority: NSF–Growing Convergence Research

National Nanotechnology Coordinated Infrastructure

SENIC Southeastern Nanotechnology Infrastructure Corridor

GaAs/GaAsSb Core–Shell Configured Nanowire-Based Avalanche Photodiodes up to 1.3 μm Light Detection

This work presents the first study on a GaAs/GaAsSb core–shell (CS)-configured nanowire (NW)-based separate absorption, charge control, and multiplication region avalanche photodiode (APD) operating in the near-infrared (NIR) region. Heterostructure NWs consisted of GaAs and tunable band gap GaAs1–xSbx serving as the multiplication and absorption layers, respectively. A doping compensation of absorber material to boost material absorption, segment-wise annealing to suppress trap-assisted tunneling, and an intrinsic i-type and n-type combination of the hybrid axial core to suppress axial electric field are successfully adopted in this work to realize a room-temperature (RT) avalanche photodetection extending up to 1.3 μm. Thus, this work provides a foundation and prospects for exploiting greater freedom in NW photodiode design using hybrid axial and CS heterostructures.

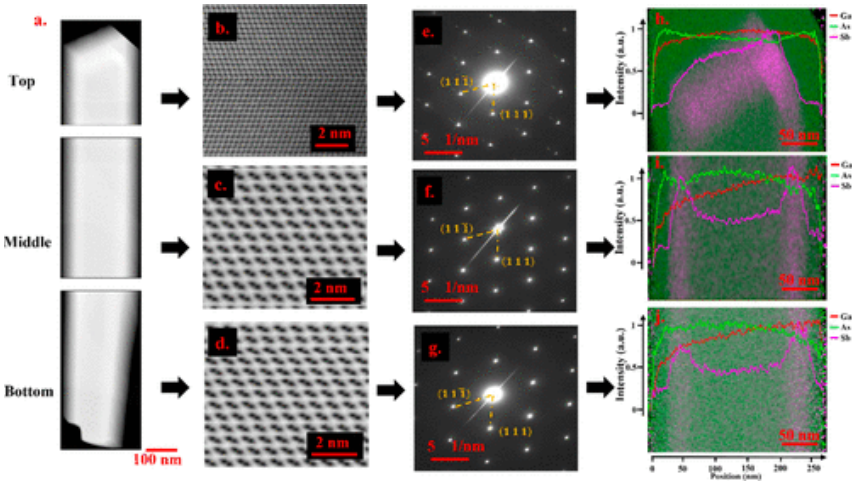

Top, middle, and bottom of S10 APD NW segments: (a) TEM images, (b–d) HRTEM images, (e–g) SAED patterns, and (h–j) HAADF STEM with false-color EDS mapping superimposed and EDS elemental line scans.

Rabin Pokharel, Hirandeep Kuchoor, Jia Li, Christopher Winkler, Lew Reynolds and Shanthi Iyer North Carolina A&T State University and North Carolina State University (SENIC).

This work was funded by NSF EECS-18322117. And U.S. Army Grant# W911NF-19-1-0002 and Air Force Office of Scientific Research. *ACS Applied Nano Materials*, 6(7), 5093-5105.

National Research Priority: NSF–Quantum Leap

National Nanotechnology Coordinated Infrastructure

SENIC Southeastern Nanotechnology Infrastructure Corridor

Impact of TiO2 nanoparticles during early life on cardiac and neurobehavioral performance

Nanoparticles (NPs) are increasingly incorporated in everyday products. This study investigated the effects of early life exposure to orally ingested TiO2 NP. Oral administration of TiO2 NP to rat pups impacted basic cardiac and neurobehavioral performance, neurotransmitters and related metabolites concentrations in brain tissue, and the biochemical profiles of plasma. The findings suggested that female pups were more likely to experience adverse outcome following early life exposure to oral TiO2 NP than male pups. Collectively the data from this study suggest oral administration of TiO2 NP cause adverse biological effects in an age- and sex-related manner, emphasizing the need to understand the short- and long-term effects of early life exposure to TiO2 NP.

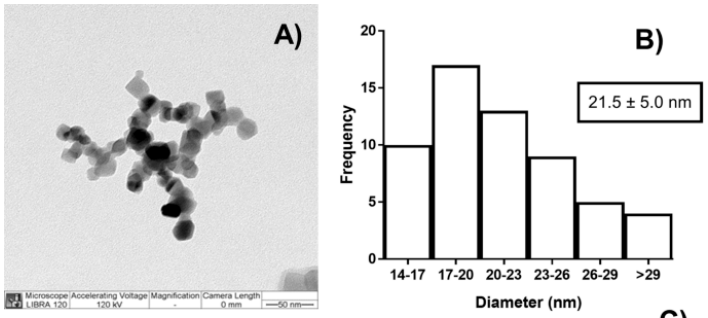

C)

Time (h)	Dynamic Light Scattering (DLS)		Nanoparticle Tracker (NTA)	
	Hydrodynamic Diameter (nm)	Polydispersity index (PdI)	Mean diameter (nm)	Mode (nm)
0	477 ± 23	0.534	114 ± 76	46
4	504 ± 32	0.561	123 ± 54	85

TEM of TiO2 NP and B histogram of size distribution. C Characterization of the 2 mg/mL dosing solutions was conducted by DLS and NTA at 0 and 4 h after preparation

Ninell Mortensen, Susan Sumner 2, Timothy Fennell, RTI International and UNC Chapel Hill; Part of work performed at Joint School of Nanoscience and Nanotechnology (SENIC).

This work was supported by NIH Grant # U01ES027254 as part of Nanotechnology Health Implications Research Consortium. *Part Fibre Toxicol* 19, 3 (2022).

National Research Priority: Environmental Health and Safety

Texas Nanofabrication Facility (TNF)

National Nanotechnology Coordinated Infrastructure

TNF TEXAS

Power FETs with low subthreshold slope and ON resistance

A new class of Si power MOSFET technology (ANDFET) with sub-30um substrate (Fig. 1) has been developed by AND with some of the development work carried out at the NNCI facility in UT-Austin. ANDFET has 2x lower Qoss and superior specific on-resistance at gate drive as low as 2.5V compared to state-of-the-art low-voltage (<60V) MOSFETs. ANDFET also has near-zero reverse-recovery charge/losses for all voltage applications. ANDFET is manufactured with self-aligned and low-complexity process in a high-volume 8-inch Si foundry. Thin-Crystalline Technology is utilized to yield mechanically handleable sub-30um substrate. Finally, the ANDFET architecture is well-suited for SiC and GaN-like wide-bandgap (WBG) devices as it inherently yields enhancement-mode WBG MOSFETs.

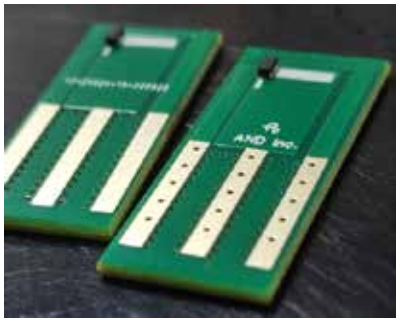

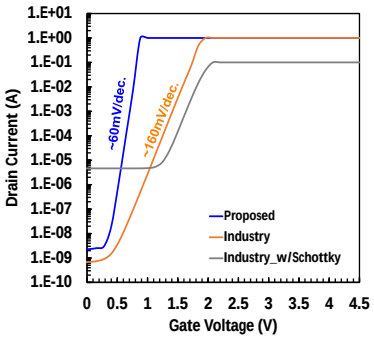

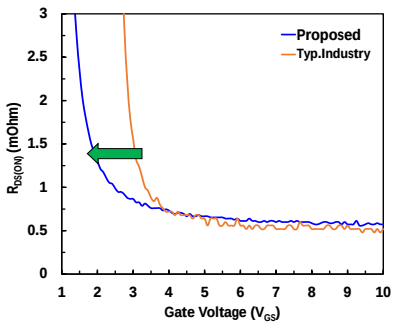

Power FETs on sub-30 micron Si

Leo Mathew, Rajesh Rao, Dan Fine, AND. Work performed at Texas Nanofabrication Facility.

This work led to productization at Skywater Foundry.

National Research Priority: NSF–Growing Convergence Research

National Nanotechnology Coordinated Infrastructure

TNF TEXAS

Compact Hyperspectral Imager Using Tunable Metasurfaces

Nanohmics, Inc. is developing a battery-operated, low-SWaP HSI system by combining a metasurface tunable spectral filter with a COTS LWIR camera. This system will fit aboard small mobile platforms, achieve full focal plane array (FPA) resolution and be capable of detecting targets in cluttered environments.

Nanohmics' compact LWIR HSI will be electronically switchable between two image collection modes: (1) high-frame rate broadband imaging, and (2) hyperspectral imaging. The key enabling technology is an electronically tunable spectral notch filter based on a microfabricated ultrathin patterned graphene optical metasurface. The tunable IR filter is a nanofabricated graphene metasurface with engineered features smaller than the optical wavelength. Portions of the fabrication is carried out in The University of Texas at Austin Microelectronics Research Center facilities. The tunable filter is thin enough to be integrated into the objective lens of a LWIR camera, converting it to a dual-mode HSI camera, enabled by custom software for spectral reconstruction.

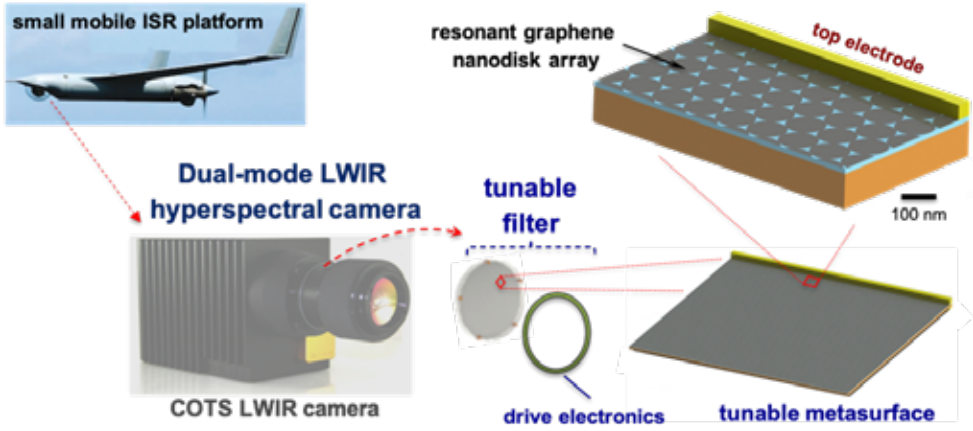

Mark Lucente, Nanohmics. Work performed at Texas Nanofabrication Facility.

This work was supported by Navy SBIR Phase II, N6893622C0002

National Research Priority: NSF–Quantum Leap

Chip-scale Hyperspectral Imaging MISSE Payload (CHIMP) for the International Space Station

Through a User Agreement with the ISS National Lab, Nanohmics built and launched a low-SWaP video-rate spectral imager that was installed on the ram-facing side of the MISSE flight facility on the exterior of the International Space Station. The spectral imager was manufactured by Nanohmics by microfabricating and bonding a custom micro-optical chip to a commercial-off-the-shelf camera core. Two out of the three micro-optical chips were manufactured at The University of Texas at Austin Microelectronics Research Center facilities and included extensive dual-side processing and characterization on each chip.

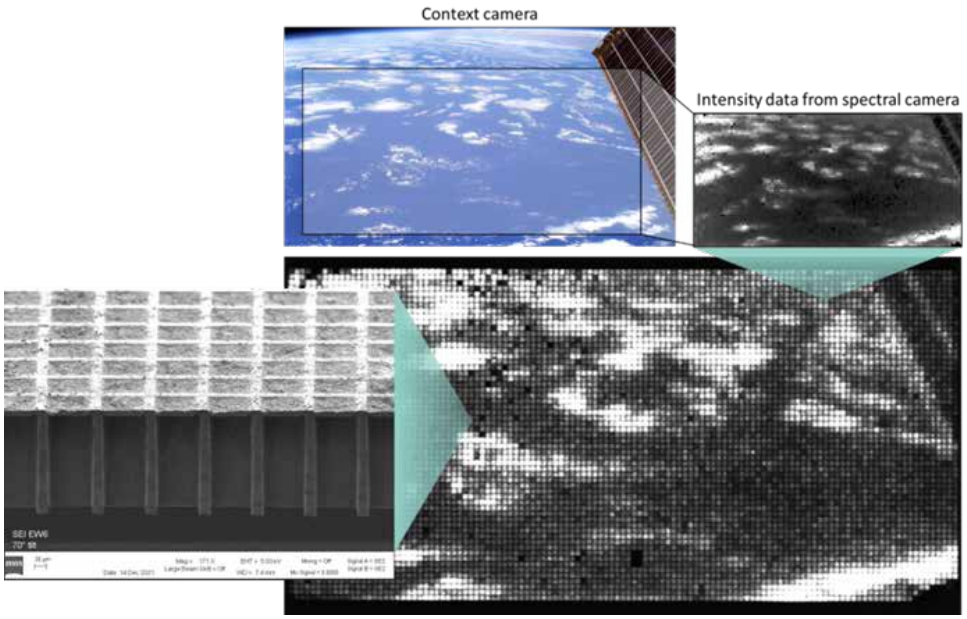

Chris Mann, Nanohmics. Work performed at Texas Nanofabrication Facility.

This work was supported by a Nanohmics IRAD program and a cooperative agreement with the International Space Station National Lab, Agreement No. 80JSC018M0005.

National Research Priority: NSF–Quantum Leap

Nonreciprocal optical metasurfaces for photonic systems

The overall goal of this program is to develop passive, solid-state, magnet-free optical isolators in the near-infrared spectrum (120 – 300 THz). The devices are designed on the principles of metasurface 'flat optics' in which the optical properties of light can be manipulated by sub-wavelength scaled patterns on a wafer. The isolators are designed using novel Fano-metasurface technology and the goal is to demonstrate better optical isolation performance per size, weight, power and cost than Ferrite-based devices employed in applications such as directed energy laser systems or photonic integrated circuits.

Ferrite isolators

25mm x 12.5 mm x 16 mm
$1000

Proposed 'flat optic' isolator

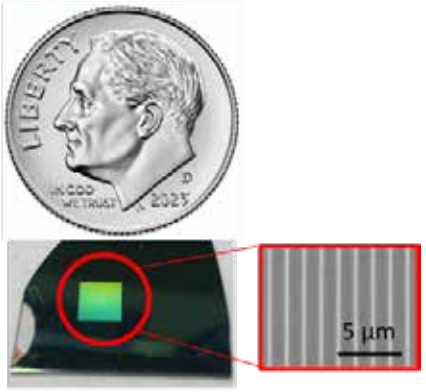

1 mm x 1 mm x 0.3 mm
<$100

Karun Vijayraghavan, Nanohmics. Work performed at Texas Nanofabrication Facility.

This work was supported by OSD STTR Phase I grant W911NF22P0025

National Research Priority: NSF–Quantum Leap

Efficient Integrated Thermoelectric Devices

We report the development of efficient device structures for monolithically integrated thin-film Bi-Sb-Te-Se thermoelectric technology on Si and SiC substrates. The device structures exploit non-equilibrium transport of electron/phonon systems in nanostructured thin films. The thermoelements operate at high fields ~10^5 V/m resulting in local cooling flux exceeding 7kW/cm^2 , and exhibit figure-of-merit ZT ~1.5, that is 2✕ better than commercial thermoelectric coolers. The integrated chips are solder-free, hermetic, with densities >1000 couples/cm^2, making it a compelling proposition for optoelectronics, 5G wireless, thermal cyclers in genomics, wearables, and battery-free IoT. Sheetak fabricates structured Si substrates at the UT MER. The SEM image shown here was obtained using Scios 2HiVac Dual beam FIB/SEM at TMI@EERC.

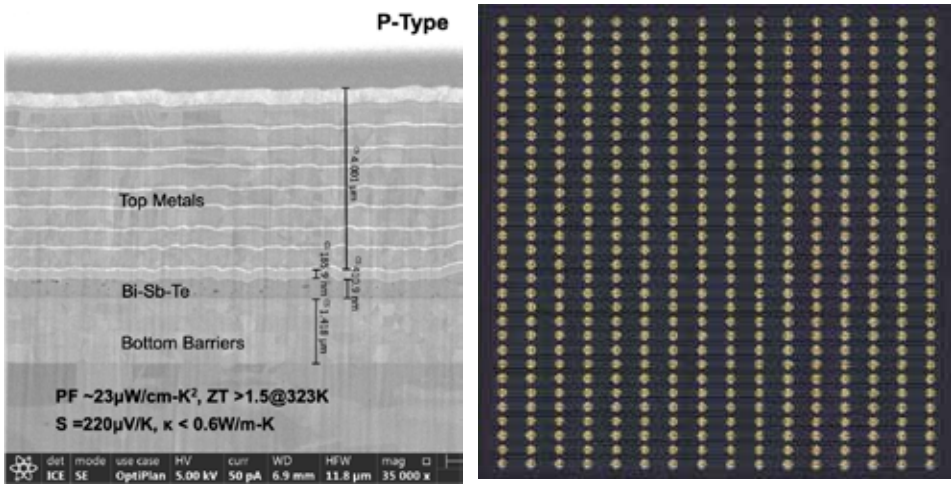

High-zT Integrated Thermoelectric Coolers and Harvesters (EON®)

S. Majumder, A. Sridharan, A. Stautzenberger, R. Warren, K. Kolle, and U. Ghoshal, Sheetak Inc. Work performed at Texas Nanofabrication Facility.

National Research Priority: NSF–Growing Convergence Research

National Nanotechnology Coordinated Infrastructure

TNF TEXAS

Domain Wall – Magnetic Tunnel Junction

In neuromorphic computing, artificial synapses provide a multi-weight (MW) conductance state that is set based on inputs from neurons, analogous to the brain. Herein, artificial synapses based on magnetic materials that use a magnetic tunnel junction (MTJ) and a magnetic domain wall (DW) are explored. By fabricating lithographic notches in a DW track underneath a single MTJ, 3-5 stable resistance states that can be repeatably controlled electrically using spin-orbit torque are achieved. The effect of geometry on the synapse behavior is explored, showing that a trapezoidal device has asymmetric weight updates with high controllability, while a rectangular device has higher stochasticity, but with stable resistance levels. The device data is input into neuromorphic computing simulators to show the usefulness of application-specific synaptic functions. Implementing an artificial neural network (NN) applied to streamed Fashion-MNIST data, the trapezoidal magnetic synapse can be used as a metaplastic function for efficient online learning. Implementing a convolutional NN for CIFAR-100 image recognition, the rectangular magnetic synapse achieves near-ideal inference accuracy, due to the stability of its resistance levels. This work shows MW magnetic synapses are a feasible technology for neuromorphic computing and provides design guidelines for emerging artificial synapse technologies.

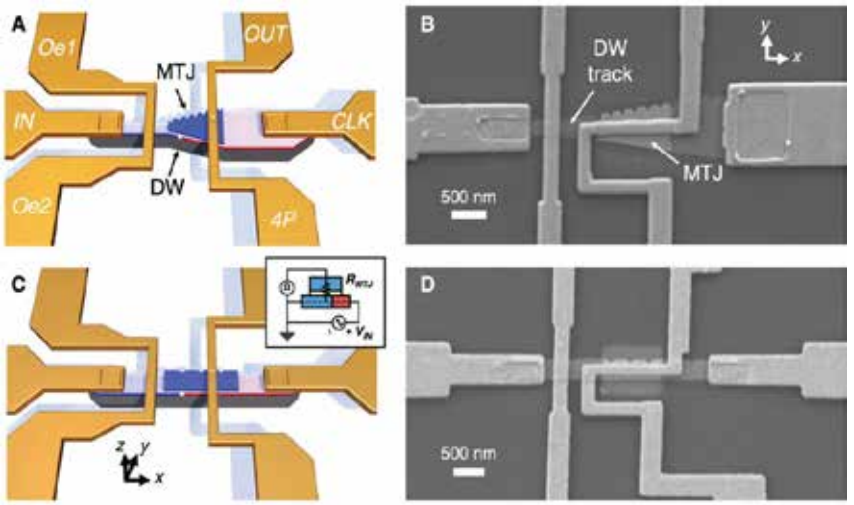

DW-MTJ synapse device structure.

C.Bennett, Sandia with Prof. Incorvia (UT). Work performed at Texas Nanofabrication Facility.

This work was supported by NSF MRSEC grant DMR-1720595. Sandia supported by DOE grant DE-NA0003525.

National Research Priority: NSF–Growing Convergence Research

National Nanotechnology Coordinated Infrastructure

TNF TEXAS

High-speed mid-wave infrared holey photodetectors

A high-speed mid-wave infrared detection using InSb photoconductive material was developed. InSb pixels were patterned with nano-scale hole arrays, integrated into a coplanar waveguide structure. The addition of the hole arrays provides a significant additional surface area for surface recombination, reducing the average lifetime of photoexcited carriers in the detector. The hole-array samples show a dramatic improvement in the photoconductor time response, with approximately a 10×10× decrease in the detector impulse response time and a similar increase in the bandwidth when compared to the control, unpatterned pixels. With a hole diameter of D=480nm and an array period of 600nm, a ~10×~10× improvement in detector temporal performance is achieved, resulting in a detector bandwidth of ~7GHz~7GHz. This drastic improvement in bandwidth is achieved with a commensurate penalty in the signal amplitude of 3×3×, when compared to the unpatterned pixel, primarily a result of the decrease in the absorber material fill factor.

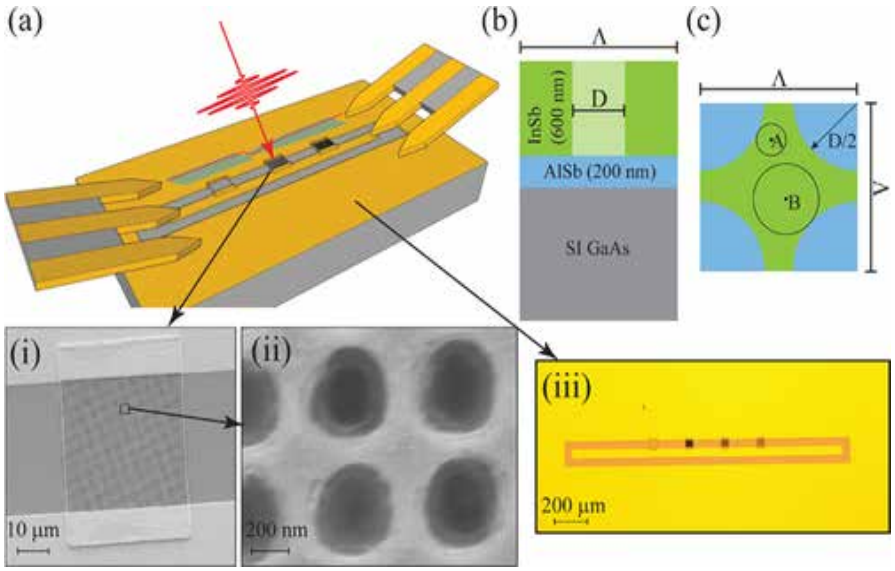

Schematic of a photoconducting infrared detector with a coplanar waveguide read-out mechanism.

Yinan Wang, Prof Dan Wasserman. UT and Prof. Monica Allen, UCSD. Work was performed at TNF.

This work was funded by AFOSR. *J.Appl. Phys.* 133, 104501 (2023).

National Research Priority: NSF–Growing Convergence Research

Memristors using Transition Metal Dischalcogenides

Molybdenum was sulfurized under different temperatures using e-beam evaporated Mo metal and MoO_3 on Si/SiO_2 substrates. As-grown samples showed relatively high-quality growth with thicknesses ranging from a few layers to monolayers based on spectroscopic and AFM characterizations. XRD and XPS depicted the 2H-MoS_2 structure along with the successful sulfurization of MoO_3. Electrical measurements revealed p-type behavior featuring an Ohmic contact to Au source and drain electrodes, with mobilities in the range of 21–41 $cm^2 V^{-1} s^{-1}$. Furthermore, the switching phenomenon showed that sulfurized thin films successfully behaved as an active material for bipolar resistive switching with an on/off ratio of 10^4 at an operating voltage of ±1 V. The successful sulfurization using the reported CVD route can further be implemented on different substrates for scalable growth and device realization

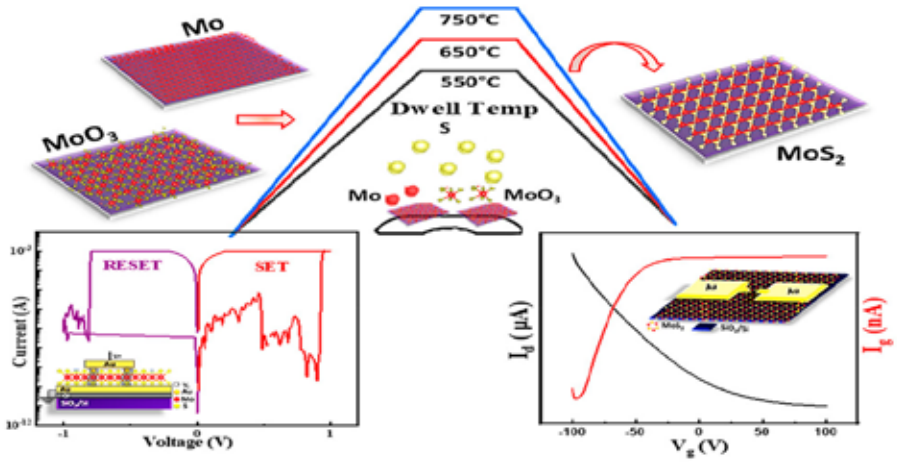

Memristors in MoS_2.

S. Fatima, Prof. Deji Akinwande, UT Austin.

This work was supported by IRSIP program, Pakistan.

National Research Priority: NSF–Quantum Leap

National Nanotechnology Coordinated Infrastructure

TNF TEXAS

Virginia Tech National Center for Earth and Environmental Nanotechnology Infrastructure (NanoEarth)

National Nanotechnology Coordinated Infrastructure

Significance of pH and iron-sulfur chemistry for molybdenum sequestration under sulfidic conditions

- Molybdenum (Mo) records ancient changes in Earth's redox conditions
- Mobility and reactivity of Mo closely tied to the chemistry of reduced sulfur and iron species
- Not clear what external conditions control formation of Fe-Mo sulfides in past environments

NanoEarth scientists are collaborating with researchers at Arizona State University and University of Texas at El Paso to characterize the (nano)mineralogy of samples containing nanosized and amorphous Fe-Mo sulfides. The findings suggest that changes in pH and Fe^{2+} concentrations may be responsible for the sulfide-independent variations in Mo behavior observed in euxinic basins.

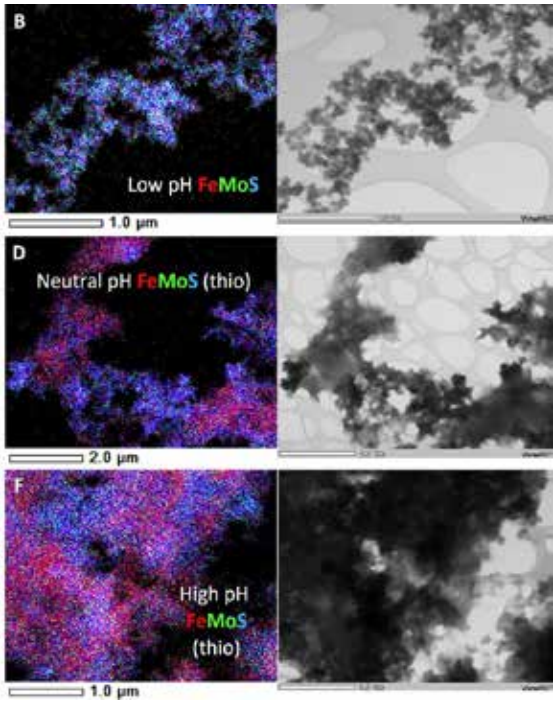

EDS composite X-ray maps of representative MoS and FeMoS precipitates showing distribution of Fe, Mo, and S.

Phillips, R., Singerling, S., Leng, W., & Xu, J., University of Texas at El Paso and Arizona State University. Work performed in part at NanoEarth.

Funding provided by DOE award DE-SC0023251, NSF/Geological Society of America (NSF/GSA) grant 13124-21, and NSF-NNCI NanoEarth awards ECCS-1542100 & ECCS 2025151. Chemical Geology, 638(2023), 121702.

National Research Priority: NSF–Understanding the Rules of Life

National Nanotechnology Coordinated Infrastructure

NanoEarth

Investigating graphene content in commercial gloves using Raman spectroscopy and scanning electron microscopy

NanoSafe Inc. is a small local start-up focused on managing emerging nanotechnology environmental health and safety (EHS) risks. The study aimed to determine if the graphene content in commercial gloves was consistent with the manufacturer's claims. The study found that Raman spectroscopy is the most effective tool for identifying the presence of graphene in gloves. We concluded that some commercial gloves did contain graphene oxides, but most of the time the manufacturer's claims were false. Carbon materials are extremely allotropic materials used in industry, however, graphene is a specific family of carbon materials. Some false claims can be made intentionally to profit from the popularity of "graphene" as an additive, and some can be made unintentionally when material provided from a supplier is a non-graphene material or when the material is ambiguous (i.e. similar but not within the accepted definition of graphene). This study suggests that a rigorous independent test is needed to ensure integrity of the "graphene-enabled" market.

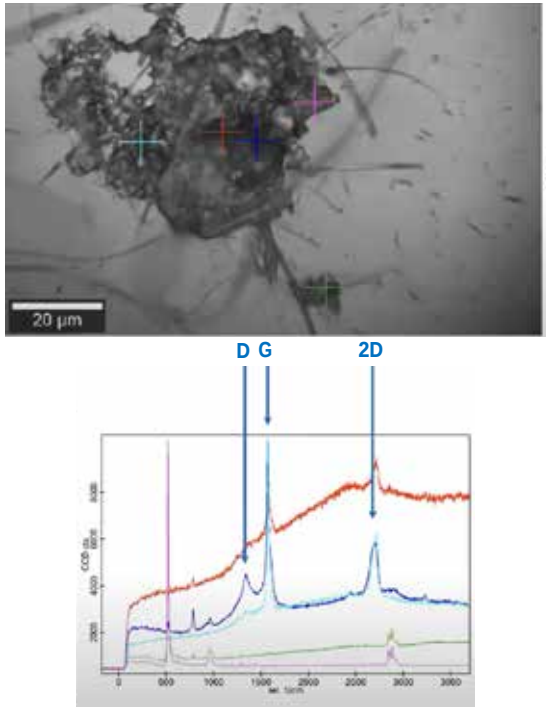

Single Raman spectra reveal different carbon materials are contained in the glove sample.

Cary Hill, NanoSafe Inc. This work was completed at Virginia Tech's Nanoscale Characterization and Fabrication Laboratory (NCFL).

These results were shared via "The Graphene Council" online webinar and published on YouTube: https://www.youtube.com/watch?v=Qw7vn8SjxPA

National Research Priority: Environmental Health and Safety

Size-resolved elemental composition of respiratory particles

The chemical composition of respiratory particles is of interest because the viability of any viruses and bacteria in the particles has been shown to depend on this factor. Moreover, the distribution of viruses and bacteria in respiratory particles as a function of size is a longstanding question in the field of airborne transmission of infectious disease. In this project, we applied computer controlled scanning electron microscopy/energy dispersive X-ray spectroscopy (CCSEM/EDX), and analyzed the size-resolved chemical composition of greater than 35,000 individual respiratory particles collected from three healthy human subjects, quantitatively at nanometer-scale spatial resolution.

We observed substantial differences in the chemical composition of respiratory particles as a function of size and large intrapersonal and interpersonal variability. These data are useful for advancing our understanding of the fate and transport of pathogens carried in respiratory particles, an important step in human-to-human transmission of certain infectious diseases.

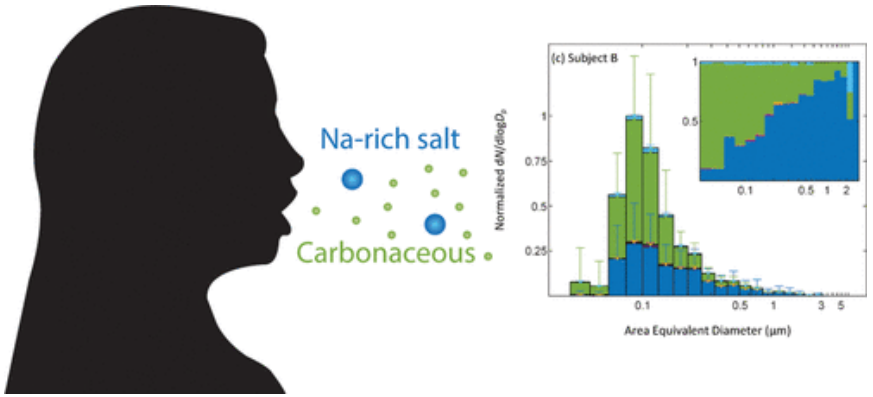

Size-dependent differences in the chemical composition of respiratory particles

Prussin, A. J., Cheng, Z., Leng, W., China, S., & Marr, L. C. Work performed in part at NanoEarth.

Research supported by project award 10.46936/ltds.proj.2021.60174/60000948 of the Environmental Molecular Sciences Library (EMSL) operated under DOE DE-AC05-76RL01830, the Flu Lab, and NSF-NNCI NanoEarth awards ECCS-1542100 & ECCS 2025151. *Environmental Science & Technology Letters*, 10(4), 356-362.

National Research Priority: American Health

National Nanotechnology Coordinated Infrastructure

NanoEarth

High-Resolution Transmission Electron Microscopy Study of a Powder River Basin Coal-Derived Fly Ash

Examination of a fly ash derived from the combustion of a low-S, subbituminous Powder River Basin coal by Scanning Electron Microscopy (SEM) and High-resolution Transmission Electron Microscopy (HRTEM), both supplemented by Energy-dispersive X-ray spectroscopy (EDS), showed that the fly ashes were dominated by amorphous phases, Ca-rich plagioclase feldspars, Mg-rich phases, complex Ca-Mg-Al-Si-Ti-Fe grains, and trace amounts of REE-rich particles. Many of the particles were rimmed by a Ca-S, possibly a sulfate. HRTEM-EDS examination of a REE-rich particle proved it to be a mix of light- and heavy-rare earth minerals mixed with amorphous phases.

DS for area 1 within area 1213. The full counts for the 0 to 10,000 eV range are shown on the (left) and a restricted count range for the 4000–7500 eV range is shown on (right) (dashed box on full-range figure indicates the area of the right figure). The Dy, Ho, and Er "peaks" do not represent significant concentrations of those elements. The Cu peak belongs to the grid holder, not the sample.

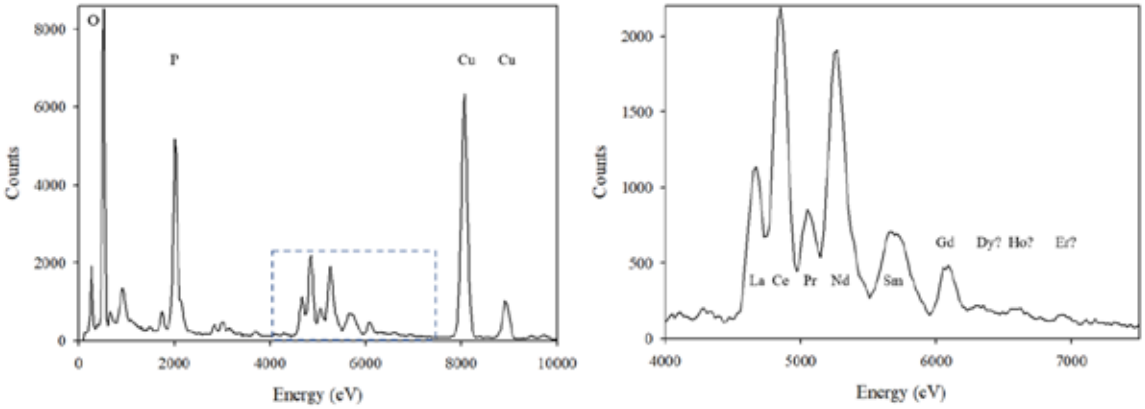

Hower, J.C., Berti, D., Winkler, C. R., Qian, D., and Briot, N. J. Work performed in part at NanoEarth.

Research supported by DOE contracts DE-FE0026952, DE-FE0027167, and DE-FE0032053; NSF CBET-1510861; NSF EPSCoR OIA-1355438 and the Commonwealth of Kentucky; and NSF-NNCI NanoEarth awards ECCS-1542100 & ECCS 2025151. . *Minerals*, 12(8), 975.

National Research Priority: Sustainable Use of Natural Resources

National Nanotechnology Coordinated Infrastructure

NanoEarth

From the Earth Surface to Atmospheric Aerosols: Understanding Dust Mineralogy and Geochemistry

NanoEarth scientists are collaborating with engineers in Civil Engineering and biologists from the Universidad de La Laguna to characterize the (nano)mineralogy of aerosols released from the arid deserts of northern Africa. The results will inform large-scale Earth Systems Models that use NASA satellite data to understand and predict climate change.

- Current models do not account for variability in mineralogy
- Iron oxides, especially nanosized particles, are considered critical components
- Preliminary analyses of samples collected from Tenerife (Canary Islands, Spain) demonstrate characterization results

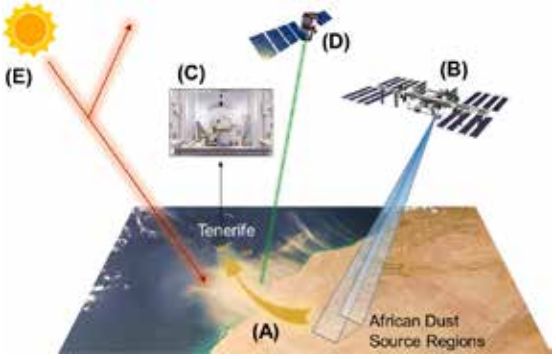

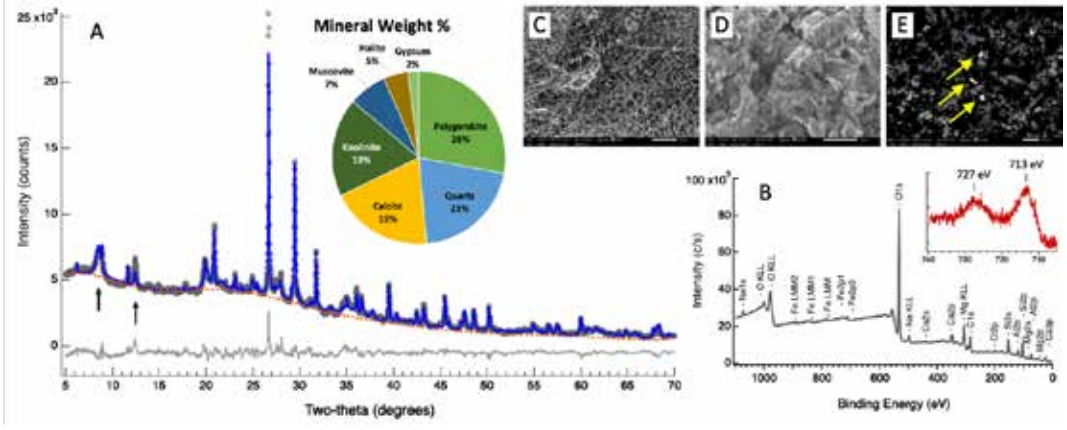

Foroutan, H. (VT CEE), Mardi, A. H. (VT CEE), González Martín, C. (ULL), and Michel, F. M. (VT GEOS). This work was completed at Virginia Tech's Nanoscale Characterization and Fabrication Laboratory (NCFL) supported by NSF-NNCI NanoEarth awards ECCS-1542100 & ECCS 2025151.

National Research Priority: Climate Change

National Nanotechnology Coordinated Infrastructure

NanoEarth

Education and Outreach Highlight: REU

NSF OPP-2244212 & 2244213

NanoEarth participated in the Arctic REU Greenland lead by Concord University in partnership with Montana State University. The REU is focused on developing skills in arctic geoscience research by integrating studies of bedrock geology with records of environmental change in a remote, international setting. The 4 REU students spent a week at NanoEarth analyzing their samples with our team. Students finished the REU at MSU and attended the NNCI REU Convocation.

REU students and mentors at NanoEarth

All students completed the NNCI REU Assessment survey.

NNCI REU Convocation

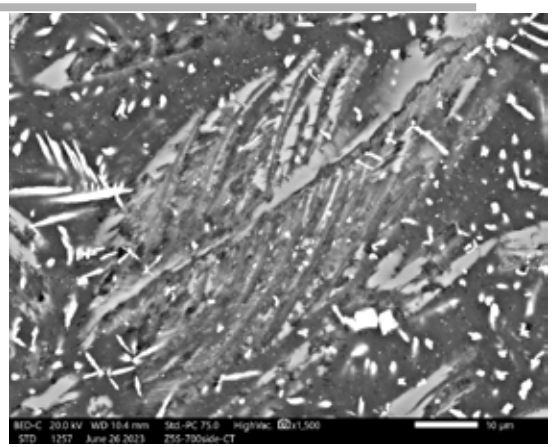

FESEM image of a feathered crystal of amphibole that grew in pseudotachylyte from Greenland

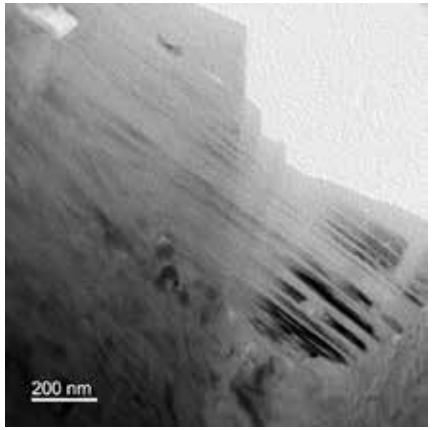

TEM image of a plagioclase feldspar crystal twins (TEM sample made by FIB lift-out)

National Nanotechnology Coordinated Infrastructure

MONT

NanoEarth

NTEC Path – Create "Translational" Momentum for Users

Aditya Garg
PhD Student
Virginia Tech

NanoEarth

2021 NTEC Project Lead **$2,000**

2022 NTEC Project Lead **$2,000**

2022 Participant, LAUNCH Start-up Labs at VT

2023 Project Lead LAUNCH Concept Grant **$50,000**

2023 Regional I-Corps

2023 Activate Fellowship application

NNCI

Local

Regional

National

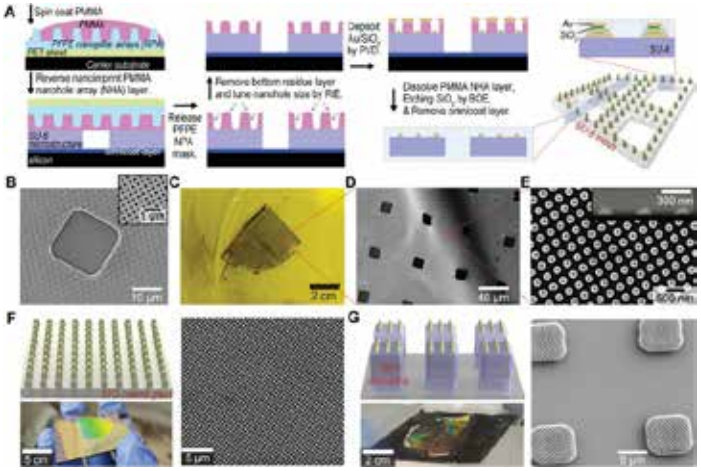

Nanoplasmonic SERS Meshes for environmental monitoring

National Nanotechnology Coordinated Infrastructure

NanoEarth